Molecular Adsorption at Solid/Liquid Interfaces Using Self-Assembled Monolayer Films

by

Seok-Won Lee

B.S., Chemical Engineering (1993)
Seoul National University

Submitted to the Department of Chemical Engineering
in partial fulfillment of the requirements for the degree of

Doctor of Philosophy in Chemical Engineering

at the

MASSACHUSETTS INTITUTE OF TECHNOLOGY

July 1999

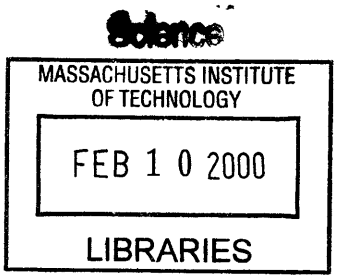

Author .....
Department of Chemical Engineering
July 9, 1999

Certified by .....
Paul E. Laibinis
Associate Professor of Chemical Engineering
Thesis Supervisor

Accepted by .....
Robert E. Cohen
St. Laurent Professor of Chemical Engineering
Chairman, Committee on Graduate Students

Molecular Adsorption at Solid/Liquid Interfaces Using Self-Assembled Monolayer Films

by

Seok-Won Lee

Submitted to the Department of Chemical Engineering
on July 9 1999, in partial fulfillment
of the requirements for the degree of
Doctor of Philosophy in Chemical Engineering

Abstract

Many areas of technology rely on interfacial events that are controlled by nanometer-level interactions present at solid/liquid interfaces. Properties of wetting, corrosion inhibition, and molecular recognition provide convenient examples. To investigate such interactions at the molecular level, self-assembled monolayers (SAMs) have been employed as a model system as they offer the ability to produce well-defined organic surfaces of controlled composition. This thesis addresses the development and characterization of such films for controlling the adsorptive properties of surfaces toward various surfactant-like molecules and for proteins. Adsorption is controlled to facilitate the organized assembly of molecular precursors, retard the non-specific adsorption of proteins, provide a specificity for the adsorption of select proteins, and the use of molecular adsorption to generate local surface energy gradients useful for directing self-propelled drop movement. A common theme in these studies is the importance of controlling the energetics and compositions of surfaces at the molecular level to influence microscopic events that translate into macroscopically observable changes in behavior.

The first part of this thesis details the formation of monolayer films by the solution-phase adsorption of n-alkyl-chained adsorbates [$CH_3(CH_2)_{n-1}Y$] onto the polar surfaces of terminally substituted SAMs [$Au/S(CH_2)_mX$]. The polar tail groups (X and Y) of the adsorbate and SAM included amine, carboxylic acid, and amide groups, and the formation of the adsorbed monomolecular films on the SAMs relied on non-covalent interactions between X and Y. Highly organized monomolecular adlayers could be produced that were as densely packed as the alkanethiolate SAMs on gold comprising the first layer. This thesis also used this molecular adsorption process to cause liquid drops to move spontaneously on surfaces by creating local changes in surface energy. The drops

could be directed to move along specified paths using patterned substrates that contained inner tracks of polar functionality and exterior domains of oleophobic methyl groups. The adsorption process allowed sequential transport of two drops on a common track and also regeneration of the initial high energy surface for reuse. The developed system provides an experimental platform for examining reactive flow and offers a novel "pumpless" method for sequentially delivering multiple drops along surfaces and within microfluidic devices.

The second part of this thesis discusses various oligo(ethylene glycol)-terminated alkyltrichlorosilanes [$Cl_3Si(CH_2)_{11}(OCH_2CH_2)_nX$; X = $-OCH_3$ or $-O_2CCH_3$, n = 2 - 4] that can form robust films on glass and metal oxide surfaces and control the adsorption of proteins. The adsorption of the methyl-capped trichlorosilanes produces densely packed, oriented monolayer films that are 2-3 nm in thickness. The trichlorosilyl group anchors the molecules to the surface, and the resulting film exposes the ethylene glycol units at its surface, as noted by its moderate hydrophilicity. The films are robust with stabilities similar to those of other alkylsiloxane coatings. These oligo(ethylene glycol)-terminated silane reagents produce films that exhibit resistances against the non-specific adsorption of proteins and that are better than for films prepared from octadecyltrichlorosilane. These oligo(ethylene glycol)-siloxane coatings offer performance advantages and could easily provide a direct and superior replacement for protocols that presently use silane reagents to generate hydrophobic, "inert" surfaces. This thesis also discusses the development of an acetate-capped oligo(ethylene glycol)-terminated silane to produce a HO-terminated oligo(ethylene glycol)-based coating on glass and metal oxide surfaces. The HO-termini of these films provide sites for covalently grafting biomolecules to the parent surface. As a demonstration, biotin and mannose moieties were covalently attached to the HO-surfaces to provide a means to induce the specific adsorption of proteins. For these surfaces, the presence of oligo(ethylene glycol) groups reduces the nonspecific adsorption of other competing proteins. The results indicate that the developed systems could offer a strategy to arrange biomolecules selectively on glass and metal oxide surfaces.

Thesis Supervisor : Paul E. Laibinis

Title : Associate Professor

To my wife, Jin-Ok, who has been through the journey at MIT with me

Acknowledgments

In 1967, my father, **Ki-Son Lee**, flew from Korea to the United States to participate in a one-year training program sponsored by the U.S. Agency for International Development (USAID), an independent government agency of the United States. During his stay, he developed a dream of receiving an advanced degree in the States, but he returned to Korea since he couldn't leave his elderly parents (my father was born when my grandfather and grandmother were 50 and 43 years old) and family behind. Two years later, he married my mother, **Kyoung-sook Lee**, and I was born in the following year. In retrospect, I still cannot forget my father's study full of school brochures and application forms he collected during his stay in the States and I have always felt that I studied here at MIT "in the name of my father" (he also majored in an engineering discipline). I also cannot be more grateful to my wonderful mother for her undying support. She was a bright young student with a major in English literature and worked in a national bank until she met my father. She would tell my brothers and me that she regretted quitting her career after marriage, but I think she instead made one of the greatest mothers. She allowed me to foster interests in reading books, playing the piano, playing sports at the YMCA, and joining a boy-scout troop for my personal growth , instead of being a high GPA nerd. Therefore, I dedicate this thesis first to my parents. Without their support and love, this couldn't happen. Also I have to thank **Seok-Woo** and **Seok-Min**, my wonderful brothers, for being my good friends, and so many thanks to my only matermal aunt, **Kyoung-Oh Lee** for being such a nice aunt for me since I was a baby.

Prior to coming to MIT, I didn't know much about Boston (I cheered for the Lakers over the Celtics in the '80s) but I remember my mother telling me that Boston is the city of education. Several years later, however, Boston became my Seoul in the States. I am sure that I will miss this city and area so much. When I close my eyes, a lot of things that happened here are surfacing in my mind, and among them, the time I shared with my advisor and mentor, **Prof. Laibinis**, comes first. He indeed taught me how to write, speak, think, and do research with his patience, enthusiasm, and healthy criticism. Especially the first year in the lab, when I learned every detail of experiments directly from him, is still unforgettable and I am pretty sure that I would be the last lucky person who enjoyed that prerogative. I sincerely thank him.

I also would like to thank the members of my thesis committee, **Profs. Blankschtein**, **Merrill**, and **Rubner** for their insightful comments and support. Prof. Blankschtein's 10.40 lectureship in my first semester at MIT was one of my best experiences at MIT and I thank him for his continued advice and encouragement. I also thank Prof. Merrill for his advice on my protein adsorption work and I hope I reminded him of his old Korean student, Tae-sup Lee. I also would like to express my sincere gratitude to Prof. Rubner for his consistent support and advice on my thesis work.

I thank **Dr. Atul N. Parikh** (Los Alamos Laboratory), **Prof. Ralph G. Nuzzo** (University of Illinois at Urbana-Champaign), and **Prof. David L. Allara** (Penn State) for their help with the IR analysis, **Dr. Susan Sofia** for her advice on my protein adsorption work, **Gillian L. Brown** for her help with my biotin-streptavidin work, **Insung Choi** of the Whitesides group at Harvard for his help with my concanavalin A-mannose work, **Dr. Noo Li Jeon** of the Whitesides group at Harvard for his help with patterning substrates that moved my moving drop work to another level , and **Gregg M. Duthaler** and **Prof.**

Ain A. Sonin (Mechanical Engineering, MIT) for insightful discussions on my moving drop work. I also thank **Felice Frankel** (Edgerton Center) for her advice on capturing nice images of my moving drops.

Thanks to the Laibinis research group: **Namyong, Mark, Ivan, Daniel, Vikas, Jiehyun, Lifen, Tim, Richard,** and **Chen.** I also would like to thank former Laibinis group members: **Kane, Jianfeng, Ben, Inge, Seichi,** and **Prof. Murray Baker** in Australia. Especially I thank Kane for being such a wonderful senior student and resource for me. I am sure that he will make a great professor at Vanderbilt University.

Special thanks to **Dr. Tae-sup Lee,** who called me personally and encouraged me to choose MIT over other outstanding graduate schools. I am honored to be the first recipient of the fellowship he endowed at MIT.

I would like to thank the professors in the **chemical engineering department of Seoul National University (SNU)** for establishing an excellent program that helped me continue my studies in the States. Especially I'd like to mention **Profs. Kookheon Char, Hwayong Kim, Sangheup Moon,** and **Hyun-ku Rhee** for their advice and support that made my graduate studies at MIT come true.

Thanks to all my friends and colleagues I met at MIT, Harvard, and the Boston area. First, thanks to **Taejung,** who is my high school, SNU, and MIT alum, for guiding (?) me to MIT (and picking me up at the Logan airport on my historic arrival in Boston in 1994!). Thanks to my ChemE family: **Taeshin** (thanks for always being my big brother at MIT!), **Chonghun, Sung Min, Yongpil, Heeyeop** (my godfather), **Sang Jun,** and **Sungjoon.** I will miss our post-lunchen discussion. Also, thanks to **Byeonghyuk, Dongsik, Jinkyu, Joon, Yongki, Jinwook, Jeongyoon, Jae bum, Jinsang,** and **Bo Won** for their friendship and fun. My fellow **Korean Graduate Student Association board members: Gukhyun, Jun Beom, Tae-soon, Jin-woo, Min-ha, Seonghwan, Donghyun, Cheolmin, Songyee, Edward, Hyunjong, Rena, Sang Hoon,** and **Junhee.** Thanks to **Gwangpyo, Michelle, Sung Moon,** and **Hyun-Seung** of **Harvard Korean Society.** Thanks to **Soon Kyu Lee** at Samsung Advanced Institute of Technology, **Semi Cho** at McKinsey and Co., **Hyung Jun Choi** at Samsung Life, **Jay Lee** and **Andrew Kim** at LG, and **In-Sup Jung** at Daewoo for helping me to broad en my eyes beyond technology. Thanks to my wonderful ChemE classmates including **Matheos, Lesley, Cathy, Isabela, Chen-Chi, Aaron,** and **John.** I wish all of you the best success and luck, and I also wish all of us make a huge contribution to our society by using what we learned and experienced. **If I have missed anybody here, please accept my apologies**

I also have to thank my wonderful and talented friends in Korea: **Jehwan, Youngsuk, Seongmoon, Jeongwon,** and **school news board fellows at Chamsil Middle School; Jaegyun, Sanghoon, Seongho, Sanghyun, Soo-cheol, Youngkyu, Sangwoo, Yooyeon, Han-Seung,** and other **Chungdong High School alums; fellow Barcelona International Youth Camp Korean delegation members; Ilsoon, Kwangkyu, Byeongwoo,** and other **SNU ChemE classmates;** colleagues I met in the **SNU Philharmonic Orchestra** and **SNU Computer Science Club.** In retrospect, I think that I couldn't step forward and aim high without their being around me.

Finally, I would like to thank my best friend and lovely wife, **Jin-Ok Cho,** for her love, patience, and support throughout all my years at MIT. I also thank her parents for raising her into a wonderful lady. Therefore, I also dedicate this thesis to her and wish we always live the way we have been.

This work was funded by the **Office of Naval Research** and the **Whitaker Foundation.**

Table of Contents

List of Figures

List of Tables

Chapter 1

Introduction

1.1. Historical Perspective

Molecular films with dimensions of a few nanometers have shown considerable technological promise across a wide range of areas and have provided useful platforms for investigating a variety of interfacial phenomena.[1] One of the most flexible of these systems is that of self-assembled monolayers (SAMs) due to their ease of use, wide tailorability, and well-defined structure.[2,3] These SAMs form by the spontaneous adsorption of surface-active molecules onto a solid substrate and often produce highly ordered molecular assemblies (Figure 1-1). Numerous studies have been conducted using SAMs and have demonstrated their potential in technological areas such as corrosion prevention,[4,5] lubrication,[6] adhesion promotion,[7,8] passivation of prosthetic devices,[9,10] and molecular recognition.[11-14]

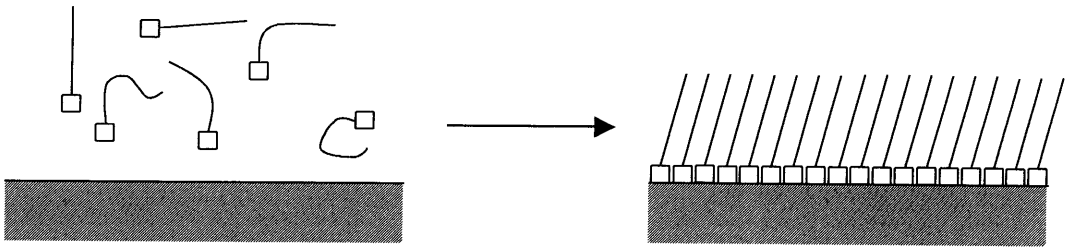

Figure 1-1. Schematic illustration of the formation of a self-assembled monolayer

The earliest formation of a molecular film by a self-assembly process can be traced to the seminal papers of Zisman and his coworkers over fifty years ago.[15-21] By exposing glass surfaces to dilute solutions of a long-chained alcohol in hexadecane, these researchers formed oriented monomolecular films that were not wet by the solvent medium and exhibited wetting properties similar to those of oriented Langmuir-Blodgett monolayers. They extended this generic approach to include a range of metal and metal oxide surfaces and various amphiphilic molecules including long-chained amines, carboxylic acids, and primary amides. The driving force for the assembly was the large interfacial free energy between the solid surface and the hydrocarbon solvent phase and its reduction upon adsorption of the amphiphilic molecules. In these cases, the polar head groups adsorbed to the solid substrates and the nonpolar alkyl tails oriented away from the substrate to expose a low energy surface of CH_3 groups to the solvent.[15] Shafrin and Zisman also demonstrated that specific chemical interactions between the head group of a molecule and a metal surface could drive the formation of an oriented monolayer film by adsorbing alkylamines onto platinum from water.[17] However, the films developed by Zisman and coworkers had low energies of adsorption (5 - 15 kcal/mol),[16] exhibited only modest stabilities, and therefore were limited in that they could only generate low-energy surfaces.

Sagiv extended Zisman's work to prepare organized monolayers that were covalently-attached to solid substrates.[22] He reported the formation of SAMs derived from octadecyltrichlorosilane ($CH_3(CH_2)_{17}SiCl_3$, or OTS) onto glass slides and demonstrated the superior stability of the silane-based monolayers to other systems (such as that of fatty acid monolayers on glass). The reactivity of the trichlorosilane reagents makes them useful for coating a broad class of substrates (glass and metal oxides)[2] and they have become widely used in a variety of practical applications. These films exhibit dramatically superior levels of stability to those of another SAM films reported to date.[7]

Nuzzo, Allara, and coworkers reported an alternative adsorption process in the early '80s to form oriented organic films that relied on the specific interactions between gold and sulfur. These films were notable in that they could produce both high- and low-energy surfaces, simply by changing the tail group present in the adsorbing organic disulfide,[23] sulfide,[24] or thiol.[25,26] The general inertness of gold toward many chemical species allowed the adsorption of organosulfur compounds to occur exclusively through the sulfur atom(s) and without concurrent adsorption by any non-sulfur-based moieties included in the adsorbates. The specific interaction between sulfur and gold—the "soft-soft" chemical ligation between the soft ligand (sulfur) and a soft late transition element (gold)[27]—allowed adsorbates to contain the wide range of "hard" polar groups that are typically encountered in organic and biological systems. This tolerance allowed formation of two-dimensional assemblies expressing these types of functional groups at their active surfaces for the first time by a single adsorption step. This difference for the thiol-based films contrasts that for the ultrathin organic films made by other methods such as spin coating and Langmuir-Blodgett transfer.[2]

1.2. Self-Assembled Monolayers

The first part of this thesis employed various thiol-based SAMs for studies of molecular adsorption onto well-defined polar organic surfaces since the thiol-based SAMs provided the best strategy for arranging polar groups at a surface. The second part of this thesis focused on the development of new silane-based SAMs for controlling protein adsorption on glass and metal oxide surfaces. Silanes were selected in order to generate SAMs with long-term stability to biological conditions. The following sections of this chapter provide background about these thiol- and silane-based systems.[28]

1.2.1. SAMs of Organosulfur Compounds

Sulfur has a strong affinity for many late transition metal surfaces. The reported surface-active organosulfur compounds that can form SAMs include thiols,[25,26] sulfides,[24] disulfides,[23] xanthates,[29] and thiocarbamates[30] (Figure 1-2).[31] SAMs derived from organosulfur compounds (mostly alkanethiols) have been prepared on substrates including gold,[3,25] silver,[32-36] copper,[5,34] mercury,[37] platinum,[38] iron,[39] GaAs,[40] and YBa_2CuO_x.[41]

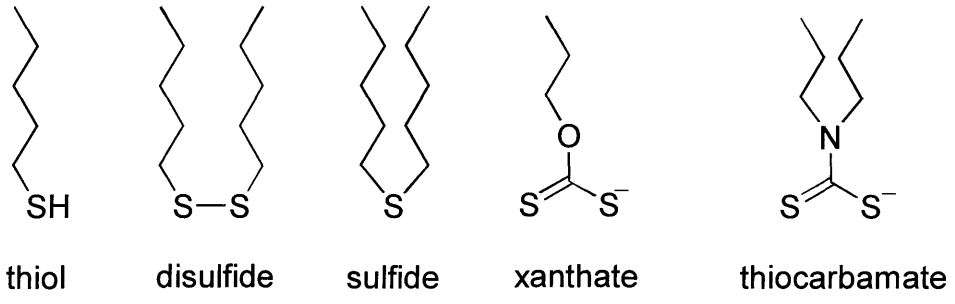

Figure 1-2. Organosulfur compounds used to form SAMs[31]

Among these sulfur-based systems, the most studied is that based on the adsorption of alkanethiols onto gold surfaces. These thiol-based SAMs have been characterized by a variety of techniques including ellipsometry, contact angle measurements, various scanning probe microscopies, infrared and Raman spectroscopies, X-ray photoelectron spectroscopy (XPS), and electrochemical measurements.[25,42-45] The collective experimental results from these studies confirm that the adsorption produces monolayer films that are strongly anchored to the gold surface through the sulfur atom and contain a densely packed array of trans-extended hydrocarbon chains that are tilted approximately 30° from the surface normal.[45,46] This tilt is a result of a sulfur-to-sulfur distance (~5.0 Å) in the assembly that is larger than the distance (~4.6 Å) between perpendicularly oriented alkyl chains in a densely-packed arrangement. The alkyl chains thereby tilt to maximize the van der Waals contact between the chains in the assembly. A wide range of nonpolar and polar functional groups (including CH_3, CF_3, CO_2H, NH_2, $CONH_2$, and OH) has been incorporated within these alkanethiolate SAMs.[3] With these tail groups, the monolayer films express a two-dimensional homogeneous sheet of organic functionality at their exposed surface. The resulting SAMs have provided useful models for fundamental studies in organic surface chemistry.

1.2.2. SAMs of Organosilane Compounds

Hydroxylated surfaces are required for generating organized SAMs from chloro- and alkoxy-organosilane compounds as their assembly forms a polysiloxane network that connects silanol groups (-SiOH) to the substrate via Si–O–Si bonds (Figure 1-3).

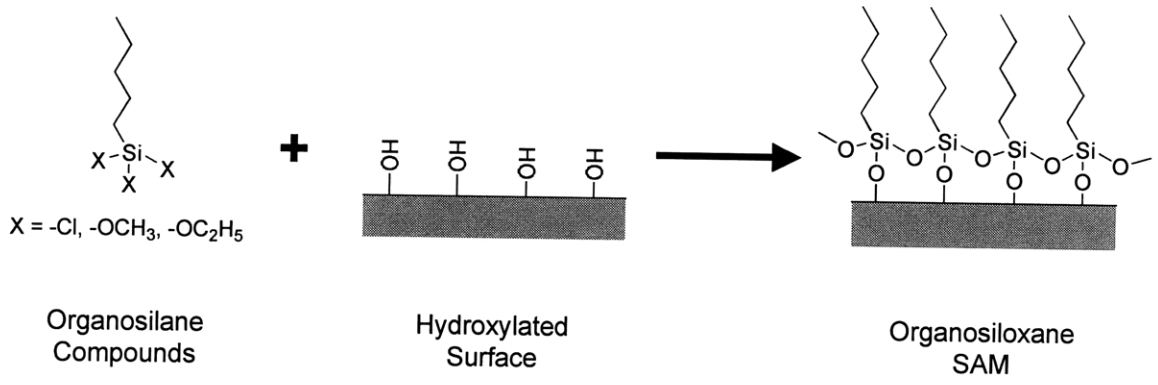

Figure 1-3. Formation of an organosiloxane SAM

By this procedure, organosiloxane SAMs have been prepared on silicon oxide,[22,47-50] aluminum oxide,[51,52] mica,[53,54] zinc selenide,[50,51] germanium oxide,[50] and gold.[55] The parent silane agents have been extensively used to coat silica particles for chromatography[56] and to promote adhesion at various organic/inorganic interfaces.[7] The derivatization of surfaces with silane reagents has recently shown promise in the areas of tribology,[57] chemical sensing,[58] biocompatibility,[10] and microdevices.[59]

Experimental results from characterization methods including ellipsometry,[47-49] wetting measurements,[47-49] infrared spectroscopy,[52] and sum frequency generation (SFG) spectroscopy[60,61] have demonstrated a high degree of structural order in SAMs derived from OTS and determined a chain tilt of less than 18° for n-alkyltrichlorosilane-based SAMs. These organosiloxane SAMs can be produced using ω-substituted alkyltrichloro- and trialkoxy-silanes that incorporate terminal functional groups such as Br, CN, thioacetyl, and vinyl groups;[2,31] however, silane-based SAMs are limited to include these functionalities that are unreactive toward the trichlorosilyl or trialkoxysilyl group in the adsorbate. This limitation can be contrasted with the thiol-based SAMs that can incorporate a wide range of hydrophilic groups. The superior stability of the

organosiloxane SAMs,[10,62,63] however, makes them more widely used in technology.[7] Subsequent surface reactions have been used for these SAMs to incorporate hydrophilic groups into these films.[64-66]

1.3. Motivation

Numerous technological involve interfacial events that occur at solid/liquid interfaces. Self-assembled monolayers (SAMs) have been employed as model systems to manipulate and investigate these and other types of interfacial phenomena at a molecular level. This thesis addresses the development and characterization of such systems and their use to investigate the adsorption of various molecules at solid (SAM)/liquid interfaces.

The first part of this thesis (Chapters 2 – 5) investigates the self-assembly of amphiphilic molecules onto chemically well-defined polar organic surfaces by non-covalent interactions and demonstrates their use for the controlled delivery of fluids. The formation of self-assembled films on organic surfaces by non-covalent interactions has not received much attention in contrast with the large body of work on inorganic surfaces. This thesis discusses the formation of organized monolayer films by the solution-phase adsorption of n-alkyl-chained adsorbates [$CH_3(CH_2)_{n-1}Y$] onto the polar surfaces of terminally substituted SAMs [$Au/S(CH_2)_mX$] using various polar tail groups (X and Y) that include amine, carboxylic acid, and amide groups. Chapter 5 discusses the use of this solution-phase adsorption process to cause the directed movement of liquid drops on surfaces and demonstrates the unique properties that can be obtained from this system due to its reliance on non-covalent interactions for adsorption.

The controlled adsorption of proteins onto glass and metal oxide surfaces remains an important issue in the development of biomaterials, biodevices, and biosensors. The second part of this thesis (Chapters 6 – 7) focuses on the development of new methods for controlling protein adsorption using silane-based SAMs that incorporate oligo(ethylene glycol) units. Chapter 6 details an approach for reducing and often eliminating the non-specific adsorption of proteins on glass and metal oxide surfaces, and Chapter 7 discusses a strategy for inducing the selective adsorption of proteins onto these substrates for potential application in biosensor construction.

1.4. References

(1) Swalen, J. D.; Allara, D. L.; Andrade, J. D.; Chandross, E. A.; Garoff, S.; Israelachvili, J.; McCarthy, T. J.; Murray, R.; Pease, R. F.; Rabolt, J. F.; Wynne, K. J.; Yu, H. *Langmuir* **1987**, *3*, 932-950.

(2) Ulman, A. *An Introduction to Ultrathin Organic Films: From Langmuir-Blodgett to Self-Assembly*; Academic Press: Boston, 1991.

(3) Laibinis, P. E.; Palmer, B. J.; Lee, S.-W.; Jenning, G. K. In *Thin Films*; Ulman, A., Ed.; Academic Press: New York, 1998; Vol. 24.

(4) Jennings, G. K.; Laibinis, P. E. *J. Am. Chem. Soc.* **1997**, *119*, 5208-5214.

(5) Haneda, R.; Aramaki, K. *J. Electrochem. Soc.* **1998**, *145*, 1856-1861.

(6) Srinivasan, U.; Houston, M. R.; Howe, R. T.; Maboudian, R. *J. Microelectromechanic. Sys.* **1998**, *7*, 252-260.

(7) Plueddemann, E. P. *Silane Coupling Agents*; Plenum Press: New York, 1982.

(8) Turyan, I.; Mandler, D. *J. Am. Chem. Soc.* **1998**, *120*, 10733-10742.

(9) Prime, K. L.; Whitesides, G. M. *J. Am. Chem. Soc.* **1993**, *115*, 10714-10721.

(10) Lee, S.-W.; Laibinis, P. E. *Biomaterials* **1998**, *19*, 1669-1975.

(11) Schmitt, F.-J.; Knoll, W. *Biophys. J.* **1991**, *60*, 716-720.

(12) Spinke, J.; Liley, M.; Schmitt, F.-J.; Guder, H.-J.; Angermaier, L.; Knoll, W. *J. Chem. Phys.* **1993**, *99*, 7012-7019.

(13) Bamdad, C. *Biophys. J.* **1998**, *75*, 1997-2003.

(14) Disley, D. M.; Cullen, D. C.; You, H. X.; Lowe, C. R. *Biosen. & Bioelec.* **1998**, *13*, 1213-1225.

(15) Bigelow, W. C.; Pickett, D. L.; Zisman, W. A. *J. Colloid Sci.* **1946**, *1*, 513-538.

(16) Bigelow, W. C.; Glass, E.; Zisman, W. A. *J. Colloid Sci.* **1947**, *2*, 563-591.

(17) Shafrin, E. G.; Zisman, W. A. *J. Colloid Sci.* **1949**, *4*, 571-590.

(18) Schulman, F.; Zisman, W. A. *J. Colloid Sci.* **1952**, *7*, 465-481.

(19) Baker, H. R.; Shafrin, E. G.; Zisman, W. A. *J. Phys. Chem.* **1952**, *56*, 405-411.

(20) Bewig, K. W.; Zisman, W. A. *J. Phys. Chem.* **1963**, *67*, 130-135.

(21) Hare, E. F.; Zisman, W. A. *J. Phys. Chem.* **1955**, *59*, 335-340.

(22) Sagiv, J. *J. Am. Chem. Soc.* **1980**, *102*, 92-98.

(23) Nuzzo, R. G.; Allara, D. L. *J. Am. Chem. Soc.* **1983**, *105*, 4481-4483.

(24) Troughton, E. B.; Bain, C. D.; Whitesides, G. M.; Nuzzo, R. G.; Allara, D. L.; Porter, M. D. *Langmuir* **1988**, *4*, 365-385.

(25) Bain, C. D.; Troughton, E. B.; Tao, Y.-T.; Evall, J.; Whitesides, G. M.; Nuzzo, R. G. *J. Am. Chem. Soc.* **1989**, *111*, 321-335.

(26) Nuzzo, R. G.; Fusco, F. A.; A llara, D. L. *J. Am. Chem. Soc.* **1987**, *109*, 2358-2368.

(27) Pearson, R. G. *J. Am. Chem. Soc.* **1963**, *85*, 3533-3539.

(28) Dubois, L. H.; Nuzzo, R. G. *Annu. Rev. Phys. Chem.* **1992**, *43*, 437-463.

(29) Ihs, A.; Uvdal, K.; Liedberg, B. *Langmuir* **1993**, *9*, 733-739.

(30) Mielczarski, J. A.; Yoon, R. H. *Langmuir* **1991**, *7*, 101-108.

(31) Ulman, A. *Chem. Rev.* **1996**, *96*, 1533-1554.

(32) Keller, H.; Schrepp, W.; Fuchs, H. *Thin Solid Films* **1992**, *210/211*, 799-802.

(33) Chang, S.-C.; Chao, I.; Tao, Y.-T. *J. Am. Chem. Soc.* **1994**, *116*, 6792-6805.

(34) Laibinis, P. E.; Whitesides, G. M. *J. Am. Chem. Soc.* **1992**, *114*, 1990-1995.

(35) Sellers, H.; Ulman, A.; Shnidman, Y.; Eilers, J. E. *J. Am. Chem. Soc.* **1993**, *115*, 9389-9401.

(36) Walzcak, M. M.; Chung, C.; Stole, S. M.; Widrig, C. A.; Porter , M. D. *J. Am. Chem. Soc.* **1991**, *113*, 2370-2378.

(37) Demoz, A.; Harrison, D. J. *Langmuir* **1993**, *9*, 1046-1050.

(38) Shimazu, K.; Sato, Y.; Yagi, I.; Uosaki, K. *B. Chem. Soc. Jpn.* **1994**, *67*, 863-865.

(39) Volmer, M.; Stratmann, M.; Viefhaus, H. *Surf. Interface Anal.* **1990**, *16*, 278-282.

(40) Sheen, C. W.; Shi, J.-X.; Mårtensson, J.; Parikh, A. N.; Allara, D. L. *J. Am. Chem. Soc.* **1992**, *114*, 1514-1515.

(41) Mirkin, C. R.; Chen, K.; Lo, R. K.; Zhao, J.; McDevitt, J. T. *J. Am. Chem. Soc.* **1995**, *117*, 6374-6375.

(42) Porter, M. D.; Bright, T. B.; Allara, D. L.; Chidsey, C. E. D. *J. Am. Chem. Soc.* **1987**, *109*, 3559-3568.

(43) Chidsey, C. E. D.; Loiacono, D. N. *Langmuir* **1990**, *6*, 682-691.

(44) Dubois, L. H.; Zegarski, B. R.; Nuzzo, R. G. *J. Am. Chem. Soc.* **1990**, *112*, 570-579.

(45) Nuzzo, R. G.; Dubois, L. H.; Allara, D. L. *J. Am. Chem. Soc.* **1990**, *112*, 558-569.

(46) Laibinis, P. E.; Whitesides, G. M.; Allara, D. L.; Tao, Y.-T.; Parikh, A. N.; Nuzzo, R. G. *J. Am. Chem. Soc.* **1991**, *113*, 7152-7167.

(47) Silberzan, P.; Léger, L.; Aus serré, D.; Benattar, J. J. *Langmuir* **1991**, *7*, 1647-1651.

(48) Wasserman, S. R.; Tao, Y.-T.; Whitesides, G. M. *Langmuir* **1989**, *5*, 1074-1087.

(49) Maoz, R.; Sagiv, J. *J. Colloid Interface Sci.* **1984**, *100*, 465-496.

(50) Gun, J.; Sagiv, J. *J. Colloid Interface Sci.* **1986**, *112*, 457-472.

(51) Gun, J.; Iscovici, R.; Sagiv, J. *J. Colloid Interface Sci.* **1984**, *101*, 201-213.

(52) Tillman, N.; Ulman, A.; Schildkraut, J. S.; Penner, T. L. *J. Am. Chem. Soc.* **1988**, *111*, 6136-6144.

(53) Carson, G.; Granick, S. *J. Appl. Polym. Sci.* **1989**, *37*, 2767-2772.

(54) Kessel, C. R.; Granick, S. *Langmuir* **1991**, *7*, 532-538.

(55) Finklea, H. O.; Robinson, L. R.; Blackburn, A.; Richter, B.; Allara, D.; Bright, T. *Langmuir* **1986**, *2*, 239-244.

(56) Nashabeh, W.; Elrassi, Z. *J. Chromatog.* **1991**, *559*, 367-383.

(57) DePalma, V.; Tillman, N. *Langmuir* **1989**, *5*, 868-872.

(58) Lee, Y. W.; Reed-Mundell, J.; Sukenik, C. N.; Zull, J. E. *Langmuir* **1993**, *9*, 3009-3014.

(59) Dulcey, C. S.; Georger, J. H.; Krauthamer, V.; Stenger, D. A.; Fare, T. L.; Calvert, J. M. *Science* **1991**, *252*, 551-554.

(60) Guyot-Sionnest, P.; Superfine, R.; Hunt, J. H.; Shen, Y. R. *Chem. Phys. Lett.* **1988**, *144*, 1-5.

(61) Watanabe, N.; Yamamoto, H.; Wada, A.; Domen, K.; Hirose, C. *Spectrochim. Acta* **1994**, *50A*, 1529-1537.

(62) Cohen, S. R.; Naaman, R.; Sagiv, J. *J. Phys. Chem.* **1986**, *90*, 3054-3056.

(63) Calistri-Yeh, M.; Kramer, E. J.; Sharma, R.; Zhao, W.; Rafailovich, M. H.; Sokolov, J.; Brock, J. D. *Langmuir* **1996**, *12*, 2747-2755.

(64) Rabke-Clemmer, C. E.; Leavitt, A. J.; Beebe Jr., T. P. *Langmuir* **1994**, *10*, 1796-1800.

(65) Wenzler, L. A.; Moyes, G. L.; Oslon, L. G.; Harris, J. M.; Beebe Jr., T. P. *Anal. Chem.* **1997**, *69*, 2855-2861.

(66) Wenzler, L. A.; Moyes, G. L.; Raikar, G. N.; Hansen, R. L.; Harris, J. M.; Beebe Jr., T. P. *Langmuir* **1997**, *13*, 3761-3768.

Chapter 2

Molecular Adsorption of Amphiphilic Molecules onto Well-Defined, Polar Organic Surfaces

2.1. Introduction

Monomolecular organic thin films have been the focus of numerous investigations for their application in areas of wetting,[1-3] adhesion,[4,5] lubrication,[6] and corrosion inhibition.[7,8] In such studies, self-assembled monolayers (SAMs) formed by the spontaneous chemisorption of specific long-chained adsorbates onto reactive metal or metal oxide surfaces have provided useful model systems due to their ability to generate chemically tailored organic surfaces.[9] Among the reported systems of SAMs, the best characterized and synthetically most flexible is that based on the adsorption of alkanethiols onto gold.[10] Notably, the assembly accommodates a wide variety of tail groups and can generate both polar and nonpolar surfaces. For example, polar groups such as $-CO_2H$, $-NH_2$, $-CONH_2$, and -OH can be localized at the exposed surface of these SAMs, and these moieties have been used as sites for further modification, often by metal ligation or covalent attachment. On homogeneous surfaces of these organic functional groups, non-covalent interactions can also direct the localization of molecular species on their surface. The interactions that drive formation of these films at a solid/liquid interface are often weak and insufficient to

allow their isolation from the liquid phase. The formation of such an adlayer has been limited to recent studies using the gas-phase adsorption of short-chained compounds of low molecular weight on the SAMs.[11,12] The formation of highly organized structures within the plane of the adlayer (as for alkanethiolate SAMs on gold) by this method is unlikely. In addition, the procedure places restrictions on the adsorbates, as it cannot accommodate molecules of high molecular weight or longer chain length due to their low vapor pressure.

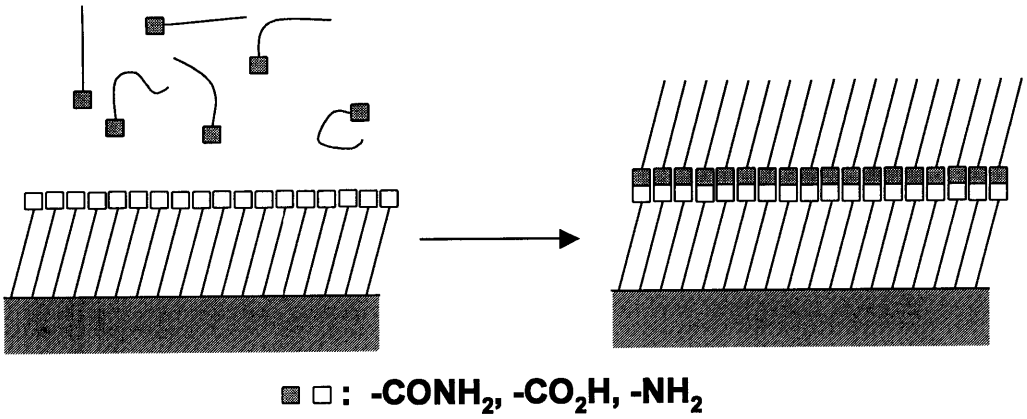

Figure 2-1. Formation of an adlayer on a terminally substituted SAM

This chapter discusses the ability of various surface-active molecules to form organized adlayers on the surface of terminally substituted SAMs ($Au/S(CH_2)_mX$) by non-covalent (i.e., ionic or hydrogen bonding) interactions from solution (Figure 2-1). These experiments were performed in a nonpolar organic solvent (decahydronaphthalene, DHN) to lessen competing adsorption processes by the solvent molecules. We used long-chained adsorbates ($CH_3(CH_2)_nY$; n = 15 - 17) and examined various X···Y interaction pairs for their ability to produce stable, organized adlayer films that could be isolated from the adsorbate solution. Among the various combinations of 'Y on X' that were examined, only 'NH_2 on CO_2H,' '$CONH_2$ on $CONH_2$,' and '$CONH_2$ on CO_2H' formed oriented monomolecular adlayers that could be isolated from the adsorption solution and

exhibited as densely-packed an organized layer as the underlying thiol-based SAM. Reflectance-adsorption infrared spectroscopy (RAIRS) provided direct spectroscopic information regarding the extent of interactions between the terminal X and Y groups and the level of organization within the films.

2.2. Results

2.2.1. Monomolecular Films: $Au/S(CH_2)_mX$

SAMs terminating in CO_2H, $CONH_2$, and NH_2 groups were prepared by immersing freshly evaporated gold-coated silicon slides (ca. 1×3 cm^2) in 0.1 - 1 mM ethanolic solutions of the corresponding alkanethiol overnight at room temperature. The strong interaction between the sulfur atom and the gold surface induces the spontaneous assembly of an oriented monolayer on the gold surfaces. The films prepared from the CO_2H- and $CONH_2$-terminated thiols exposed highly polar surfaces that were wet by liquids such as water and hexadecane (i.e. contact angles of water were less then 15°).[10,13] In contrast, the NH_2-terminated SAMs were less hydrophilic and exhibited contact angles of water of ~56°.[14] This difference in wetting is possibly due to the high reactivity of amine groups and their ability to adsorb CO_2 and other atmospheric species on the SAM surface.[10,15] In the RAIRS spectra of the SAMs, the asymmetric C-H stretching mode (d^-) appeared at ~2928 cm^{-1} for the NH_2-terminated SAMs and at ~2919 cm^{-1} for the CO_2H and $CONH_2$-terminated SAMs. These values indicate a more dense packing and superior level of organization for the hydrocarbon chains within the CO_2H- and $CONH_2$-terminated SAMs. From these results, we conclude that the exposed NH_2 groups were not as densely arranged at the surface as for the CO_2H and $CONH_2$ SAMs.

2.2.2. Bilayer Films: $Au/S(CH_2)_mX\cdots Y(CH_2)_nCH_3$

The terminally substituted SAMs ($Au/S(CH_2)_mX$; X = CO_2H, $CONH_2$, NH_2) were each immersed into DHN solutions of the various long-chained adsorbates ($CH_3(CH_2)_nY$; Y = CO_2H, $CONH_2$, NH_2) to examine their ability to produce adlayers through non-covalent interactions between X and Y. DHN was selected as solvent for these experiments based on its general inertness, its high surface tension, and its nonpolar nature—this combination of attributes should minimize any effects that could hinder the formation and isolation of a non-covalently linked adlayer. In particular, the high surface tension of DHN allowed some of the SAMs to emerge dry from the DHN solution. The dewetting of samples upon removal from solution provided a visual indication of the formation of a CH_3-terminated adlayer on the oriented SAM and also allowed the omission of any rinsing procedures that could disrupt the assembled adlayers. The dewetting of the slides did not occur with every combination of X and Y, and this oleophobic behavior was observed only for the adsorption of $C_{18}NH_2$ onto CO_2H-terminated SAMs and of $C_{17}CONH_2$ onto $CONH_2$- and CO_2H-terminated SAMs. While the amine and amide adsorbed onto the CO_2H-surface and produced oleophobic surfaces, the dewetting process did not occur for the related cases where amine and amide-terminated SAMs were exposed to heptadecanoic acid ($CH_3(CH_2)_{15}CO_2H$).

Table 2-1 shows the ellipsometric thicknesses and wetting properties of adlayer-SAM combinations that yielded oleophobic surfaces. The thicknesses of the resulting adlayers from adsorbates of similar chain lengths (n = 15 - 17) were similar (about 21 Å) and roughly the same as the thickness of a SAM derived from an alkanethiol of similar chain length on gold. The wetting behaviors of the adlayers were also similar to those for a densely-packed, CH_3-terminated SAM on gold.

Table 2-1. Physical properties of various SAM/adlayer combinations

Underlying SAM	Adlayer	Adlayer Thickness (Å)	$\theta_a(H_2O)$	θ_a(BN[a])	θ_a(DHN)	θ_a(HD[b])
$Au/S(CH_2)_{15}CO_2H$	$CH_3(CH_2)_{17}NH_2$	19	105	61	44	42
$Au/S(CH_2)_{15}CO_2H$	$CH_3(CH_2)_{16}CONH_2$	19	93	66	46	45
$Au/S(CH_2)_{11}CONH_2$	$CH_3(CH_2)_{16}CONH_2$	22	105	67	48	46
$Au/S(CH_2)_{17}CH_3$		22	115	67	51	46

[a]BN = α-bromonaphthalene
[b]HD = hexadecane

2.2.3. Examination of the Non-Covalent Interactions within Bilayers by Infrared Spectroscopy

Figures 2-2 and 2-3 show infrared spectra for the various systems that yielded bilayer films as well as spectra for the parent SAMs. In Figure 2-2, the d^- and d^+ CH_2 C–H stretching modes for the $CONH_2$ and CO_2H-terminated SAMs appear at ~2919 and ~2851 cm^{-1}, respectively, indicating an all-trans conformation for the alkyl chains and the presence of few gauche defects within the SAMs. After formation of the adlayers, the positions of the d^- and d^+ modes remain unchanged and new peaks appear at ~2965 and ~2879 cm^{-1} for the r^- and r^+ CH_3 C-H stretching modes, respectively, indicating the adsorption of methyl-containing species on the SAM. This spectral region also displays the bands for the N-H stretching modes. In the spectrum of the native $CONH_2$-terminated SAMs, a peak appears at ~3498 cm^{-1} that is assigned as a free N-H stretching mode for the amide.[16] After the formation of an adlayer from stearamide ($C_{17}CONH_2$) onto both the CO_2H- and $CONH_2$-SAMs, two bands at ~3400 and ~3200 cm^{-1} (assigned as asymmetric and symmetric hydrogen-bonded N-H stretching vibrations, respectively)[16] appear suggesting that the adsorption of the amides onto these surfaces leads to hydrogen bonding between the amide of the adsorbate and tail group of the SAM—for these systems, the adsorption of the long-chained amides onto the two SAM surfaces is not the result of simple physisorption.

Figure 2-3 shows the lower frequency region of the spectra and contains the absorptions for the C=O stretching and N-H deformation modes. The positions of these modes provide specific information about the chemical environment around the C=O and N-H bonds. For example, the C=O stretching bands for the native CO_2H-terminated SAMs appeared at 1742 and 1719 cm^{-1} and are due to non H-bonded and H-bonded C=O stretching modes, respectively.

Changes in these spectral modes that occurred after adlayer formation were influenced by the head group of adsorbate and its interaction with the CO_2H-terminated surfaces. For example, upon adsorption of $C_{17}CONH_2$ onto the CO_2H-surface, the peak for the non-H-bonded C=O stretching mode disappeared and a new peak at ~1592 cm^{-1} appeared corresponding to the N-H deformation mode. Meanwhile, the formation of an adlayer of $C_{18}NH_2$ on the CO_2H-surface resulted in the complete disappearance of the two C=O stretching modes for the native CO_2H-terminated SAMs and the appearance of a new band at ~1583 cm^{-1} corresponding to a combination of the C=O stretching mode for a carboxylate ($-CO_2^-$) and the N-H deformation mode for an NH_3^+ species. The transformation of the C=O absorptions upon amine adsorption suggests that most of the terminal carboxylic acids are deprotonated by the adsorbing amines. The completeness of conversion suggests that a stoichiometric correspondence between the carboxylic acids and amines and that the amine adlayer should have a similar coverage (and thus surface density) to the alkanethiols comprising the underlying SAM.

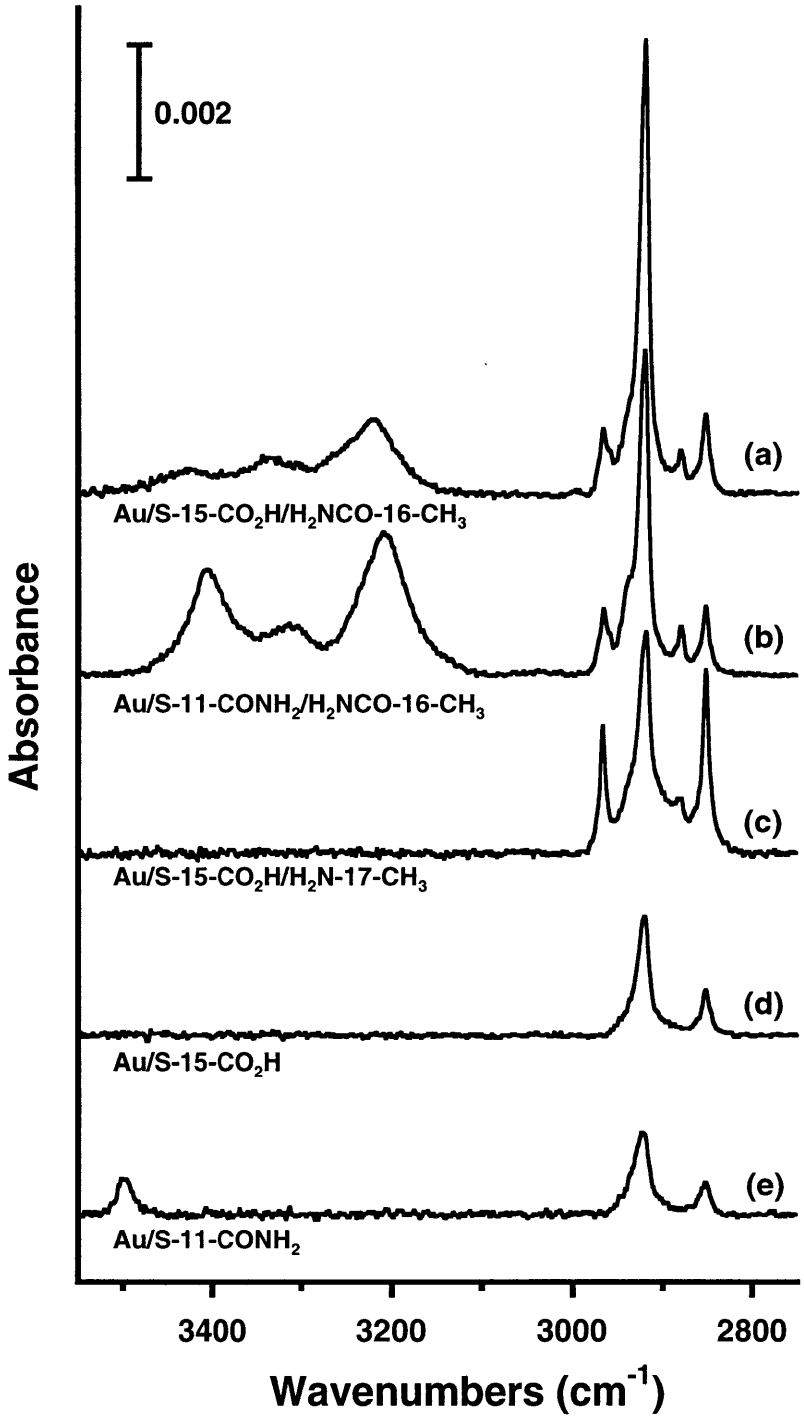

Figure 2-2. RAIRS spectra of bilayers and terminally-substituted SAMs on gold. The numbers in the molecular structure represent the number of methylene units comprising each hydrocarbon chain.

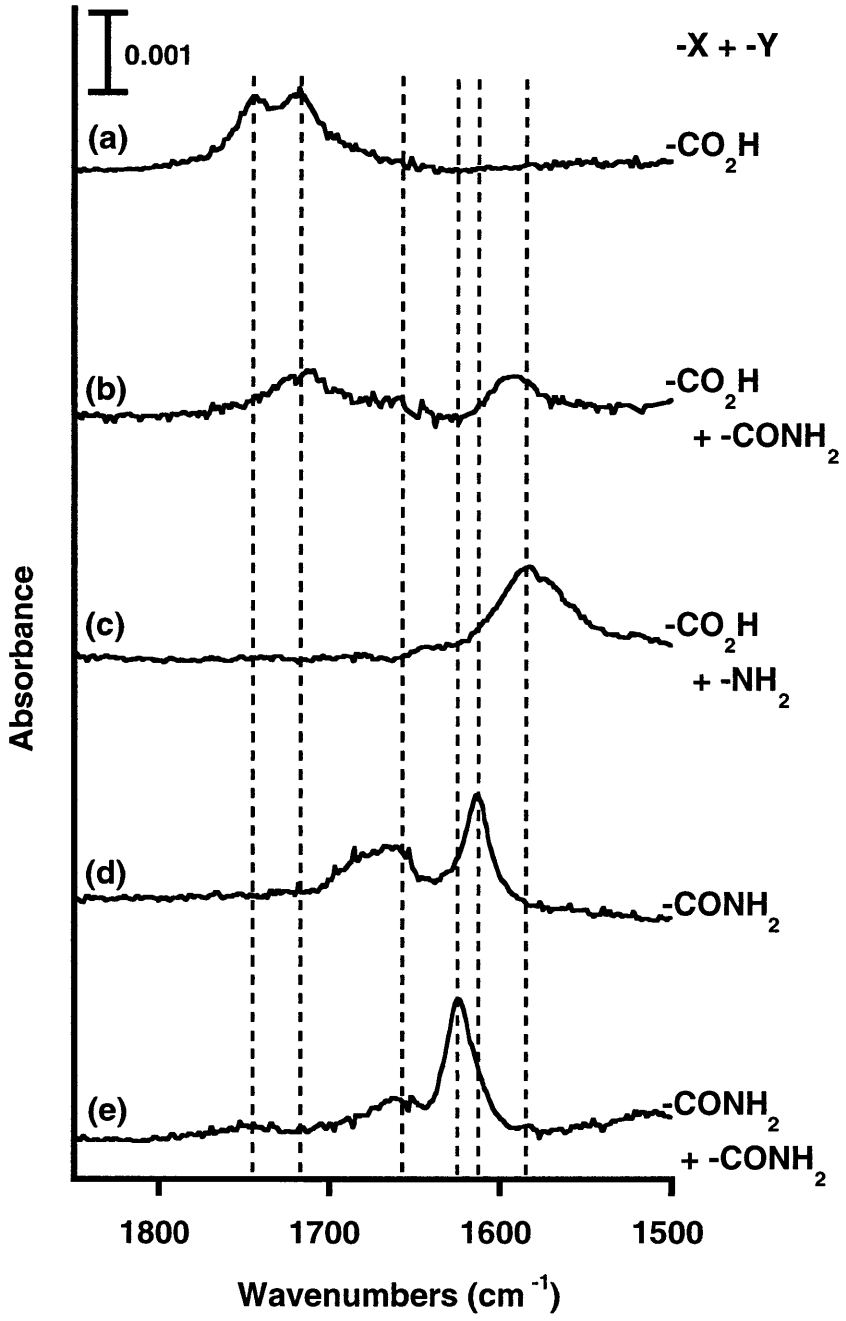

Figure 2-3. Low frequency region of the RAIRS spectra in Figure 2-2. X and Y represent the terminal groups of the SAMs and adsorbates, respectively.

The $CONH_2$-terminated SAM exhibited a broad C=O stretching peak (amide I band) at ~1663 cm^{-1} and a sharp N-H deformation peak (amide II band) at ~1613 cm^{-1}. For a primary amide in a dilute solution, its amide I band typically appears between 1680 and 1700 cm^{-1}.[17] The broadness of the C=O stretching peak in Figure 2-3d indicate that the native amide-terminated SAMs does not appear to form a strong H-bonding network within the SAM. This assignment is supported by the sharp band at 3500 cm^{-1} for the free N-H stretching mode.[2] Upon formation of an adlayer of $C_{17}CONH_2$ on the $CONH_2$-surface, the free N-H stretching mode at 3500 cm^{-1} disappears and H-bonded asymmetric and symmetric N-H stretching modes appear at 3400 and 3200 cm^{-1}, respectively. The latter peaks are characteristic features in the solution-phase IR spectra of head-to-head H-bonded amide dimers and also appeared upon formation of the $C_{17}CONH_2$ adlayer on a CO_2H-surface (Figure 2-2a). The N-H stretching peaks were less intense than for the adlayer of $C_{17}CONH_2$ on the $CONH_2$-surface primarily due to the lower surface density of amides.

2.3. Discussion

Among the various combinations of 'Y on X' (X and Y = NH_2, CO_2H, and $CONH_2$), only 'NH_2 on CO_2H,' '$CONH_2$ on $CONH_2$,' and '$CONH_2$ on CO_2H' formed oriented monomolecular adlayers that could be isolated from the adsorption solution and exhibited as densely-packed an organized layer as the underlying thiol-based SAM. One of the interesting observations with these experiments is that 'CO_2H on NH_2' and 'CO_2H on $CONH_2$' did not form oriented films, while related systems of 'NH_2 on CO_2H' and '$CONH_2$ on CO_2H' did. These differences could be ascribed to differences in the surface characteristics of the SAMs and the level of intermolecular H-bonding.

On the NH_2-terminated SAMs, none of the investigated long-chained adsorbates ($CH_3(CH_2)_nY$; Y = CO_2H, $CONH_2$, NH_2) formed a stable adlayer. The poor packing within the parent NH_2-terminated SAM and the possible contamination of its surface by adventitious species may explain our inability to form an organized adlayer from these adsorbates on this surface. NH_2-terminated SAMs have been used to deposit particles covered with CO_2H-terminated SAMs onto them.[18] Because of their large size (on the order of 10 μm) and their multiple points of attachment, the particles are less likely to be sensitive to the poor organization of NH_2-terminated SAMs. The adsorption of individual molecules on the NH_2-SAMs to form an assembled adlayer is more sensitive to the organization of a poorly structured SAM since the stability of the adlayer also relies on van der Waals contact that results from dense packing between hydrocarbon chains. In contrast, the CO_2H and $CONH_2$-terminated SAMs exhibit a better-defined structure and their hydrocarbon chains are more densely packed, thereby producing a two-dimensional sheet of polar functionality at their surface that can better allow adlayer formation.

The strength of intermolecular H-bonds can be influenced by several factors including the electronegativities of the proton acceptor and donor, charges on the donor and acceptor, steric effects, and the number of H-bonds per molecule.[19] The order of decreasing H-bonding strength is suggested to be O–H N > O–H O=C ~ N–H N > N–H O=C.[19] According to this order of H-bonding strength, a stable monolayer from heptadecanoic acid would be expected to readily form on the CO_2H-terminated SAM since O–H O=C is rated stronger than N–H O=C (Figure 2-4); however, a stable film was not assembled with the combination of 'CO_2H on CO_2H.' This observation can be unraveled with a couple of explanations. First, each adsorbed amide is capable of forming a greater number of H-bonds to stabilize an adlayer than each adsorbed carboxylic acid: the primary amide has two proton donors and one proton acceptor, which allow formation of intermolecular H-bonds between adsorbed amides (Figure 2-4a). Meanwhile, each carboxylic

acid has only one proton acceptor and one donor; therefore, the intermolecular H-bonding between adjacent adsorbed acids within a layer will be weak or absent for the formation of head-to-head dimers (Figure 2-4b). The difference in physical properties clearly manifest the outcome of multiple H-bonds; for example, the melting point of hexanoic acid is ~3 °C, while that of hexanoamide is ~101 °C. Therefore, these results may generally explain the superior stability of amide adlayers to acid adlayers. In addition, the terminal CO_2H groups of SAMs can participate in H-bonding with their adjacent CO_2H groups (Figure 2-4b), possibly contributing to the poor stability of adlayers of heptadecanoic acid on CO_2H-SAMs. The influence of the intralayer H-bonding within CO_2H-SAMs may also be observed in the adlayers of stearamide onto CO_2H-SAMs. As shown in Figure 2-2a, the relative intensity of the asymmetric N-H stretching band at 3400 cm^{-1} to that of the symmetric N-H stretching band at 3200 cm^{-1} is apparently weaker than for the adlayers of stearamide onto $CONH_2$-SAMs (Figure 2-2b). This observation indicates that the N-H bonds of adsorbing amides are at a different orientation possibly to maximize the stability of adlayers in response to the chemical environments of CO_2H-surfaces that are different from those of $CONH_2$-surfaces. The spectrum suggests that most of the N-H bonds of adsorbing amides may form H-bonds with the carbonyl group of their adjacent adsorbing amides rather than that of CO_2H-SAMs, as the carbonyl group of the SAMs may have already been H-bonded with enough number of adjacent CO_2H groups through the intralayer H-bonding. Therefore, the two N-H bonds of each adsorbing amide may have to be oriented more toward its adjacent adsorbing amides leading the C-N bond of each amide to rotate for the new configuration and causing the weak intensity of the asymmetric N-H stretching mode due to the dipole moment of the mode being less normal to the surface.

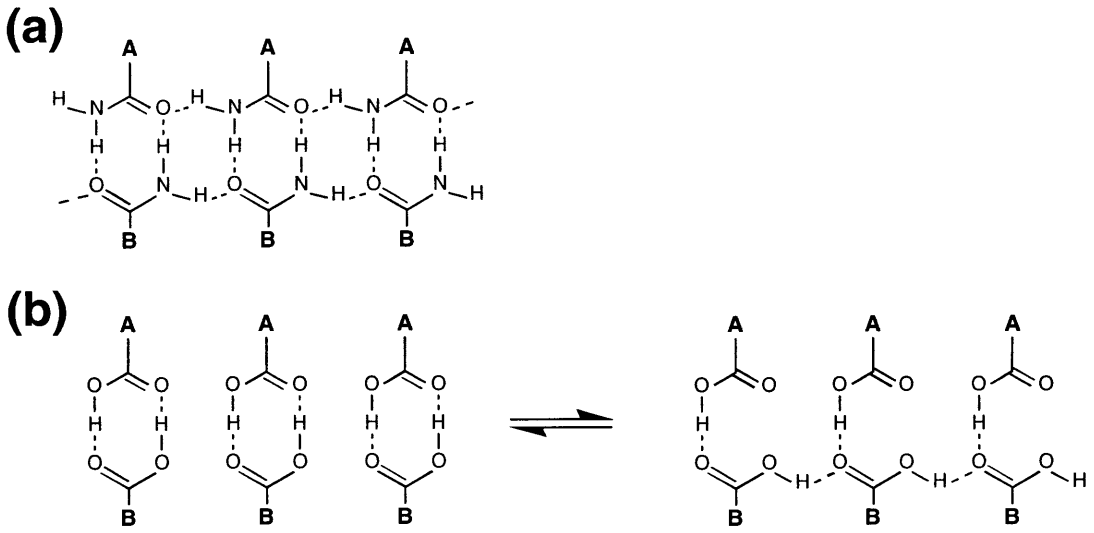

Figure 2-4. Hydrogen bonding interactions between the polar end groups of adsorbates and SAMs within the bilayer assemblies. "A-" and "B-" represent "$CH_3(CH_2)_m$-" and "$Au/S(CH_2)_n$-," respectively.

2.4. Conclusions

We have demonstrated the formation and isolation of oriented adlayers derived from the assembly of n-alkyl-chained adsorbates ($CH_3(CH_2)_{n-1}Y$; Y = CO_2H, NH_2, $CONH_2$) onto SAMs ($Au/S(CH_2)_mX$; X = CO_2H, NH_2, $CONH_2$) terminated with various polar groups. The identities of X and Y are an important factor that affects the quality of the resulting adlayers. On the NH_2-terminated SAMs, none of the investigated long-chained adsorbates formed a stable adlayer due to the poor packing within the parent NH_2-terminated SAM and the possible contamination of its surface by adventitious species. Three systems ($C_{18}NH_2$ on CO_2H-terminated SAMs and $C_{17}CONH_2$ on $CONH_2$- and CO_2H-terminated SAMs) have shown the physical properties of organized films similar to those of alkanethiolate SAMs on gold with our experimental conditions. In the formation of an adlayer employing H-bonding between $CONH_2$ and CO_2H groups, only the adsorption of amides onto acid-surfaces resulted in the formation of a stable adlayer

suggesting that not only the strength of bonding interactions but also the capability of the adsorbing molecules to form multiple intermolecular bonds is an important factor in the assembly process.

2.5. Experimental

2.5.1. Materials

Octadecanamide ($CH_3(CH_2)_{16}CONH_2$), heptadecanoic acid ($CH_3(CH_2)_{15}CO_2H$), and octadecylamine ($CH_3(CH_2)_{17}NH_2$) were obtained from Fluka (Ronkonkoma, NY) or Aldrich (Milwaukee, WI) and used without further purification. 16-Mercaptohexadecanoic acid ($HS(CH_2)_{15}CO_2H$),[2,13] 12-mercaptododecamide ($HS(CH_2)_{11}CONH_2$),[2,13] and 11-mercaptoundecyl amine ($HS(CH_2)_{11}NH_2$)[18] were synthesized by literature procedures. n-Octadecanethiol was obtained from Aldrich and recrystallized before use. Silicon wafers were test grade and obtained from Silicon Sense (Nashua, NH). Gold shot (99.99 %) and chromium-coated tungsten filaments were obtained from Americana Precious Metals (East Rutherford, NJ) and R. D. Mathis Co. (Long Beach, CA), respectively.

2.5.2. Sample Preparation and Treatment

Gold substrates were prepared by the sequential thermal evaporation of 100 Å of Cr (99%) and 1000-2000 Å of Au onto Si(100) test wafers. The evaporation was conducted in a vacuum chamber at less than 10^{-5} torr. The SAMs were prepared by immersing the substrates into 0.1-1 mM thiol solutions in ethanol for at least 10 h. The terminally-substituted SAMs ($Au/S(CH_2)_nX$; $X = CO_2H$, $CONH_2$, NH_2) were rinsed with ethanol and deionized water (Milli-Q, Millipore) and blown dry in a stream of N_2 prior to use, while the SAMs from octadecanethiol were rinsed only

with ethanol before being blown dry with N_2. Adlayers of the alkyl-chained adsorbates ($CH_3(CH_2)_nY$; Y = CO_2H, $CONH_2$, NH_2) were formed on the terminally-substituted SAMs by soaking the SAMs in dilute solutions of the amine or acid (1 to 10 mM) or supersaturated solutions of the amide (less than 1 mM) in anhydrous decahydronaphthalene (DHN) for at least 8 h. Substrates that formed stable adlayers emerged dry from the DHN solution and were blown dry with nitrogen to remove any remaining drops from the edges of substrates.

2.5.3. Film Thickness Measurements

The thicknesses of the films were determined using a Gaertner L116A ellipsometer (Gaertner Scientific Corporation, Chicago, IL) at a wavelength of 6328 Å. For each substrate, measurements were made before and after derivatization with the thiols and after exposure to the other adsorbates. The thicknesses of the films were calculated using a real refractive index of 1.45.[20]

2.5.4. Wetting Measurements

Contact angles were measured using a Ramé-Hart goniometer (Mountain Lakes, NJ) equipped with a videoimaging system. Measurements were made on both sides of the drop under ambient condition. Drops were advanced and receded at ~1 μL/s with an Electrapipette (Matrix Technologies Corporation, Lowell, MA). Contact angles were reproducible from sample to sample within ±2°, and reported data are the averages of at least three drops.

2.5.5. Reflection Absorption Infrared Spectroscopy (RAIRS)

IR data were obtained using a Digilab FTS 175 spectrometer (Bio-Rad, Cambridge, MA) equipped with a Universal Reflectance Accessory and wire grid polarizer. The p-polarized light

was focused onto the Au surface at an 80° angle of incidence, and the reflected beam was detected by a liquid N_2-cooled MCT detector. After 256 to 1024 scans at 2 cm^{-1} resolution, triangular apodization was applied and the final absorption spectra were baseline-corrected. Reference spectra were obtained from an octadecanethiol-d_{37} SAM on gold. Spectra are reported as $-\log R/R_0$ where R is the reflectivity of the substrate with the monolayer and R_0 is the reflectivity of the reference.

2.6. References

(1) Whitesides, G. M.; Laibinis, P. E. *Langmuir* **1990**, *6*, 87-96.

(2) Nuzzo, R. G.; Dubois, L. H.; Allara, D. L. *J. Am. Chem. Soc.* **1990**, *112*, 558-569.

(3) Allara, D. L.; Nuzzo, R. G. *Langmuir* **1985**, *1*, 45-52.

(4) Plueddemann, E. P. *Silane Coupling Agents*; Plenum Press: New York, 1982.

(5) Turyan, I.; Mandler, D. *J. Am. Chem. Soc.* **1998**, *120*, 10733-10742.

(6) Srinivasan, U.; Houston, M. R.; Howe, R. T.; Maboudian, R. *J. Microelectromechanic. Sys.* **1998**, *7*, 252-260.

(7) Jennings, G. K.; Laibinis, P. E. *J. Am. Chem. Soc.* **1997**, *119*, 5208-5214.

(8) Haneda, R.; Aramaki, K. *J. Electrochem. Soc.* **1998**, *145*, 1856-1861.

(9) Ulman, A. *An Introduction to Ultrathin Organic Films: From Langmuir-Blodgett to Self-Assembly*; Academic Press: Boston, 1991.

(10) Laibinis, P. E.; Palmer, B. J.; Lee, S.-W.; Jenning, G. K. In *Thin Films*; Ulman, A., Ed.; Academic Press: New York, 1998; Vol. 24.

(11) Matsuura, K.; Ebara, Y.; Okahata, Y. *Langmuir* **1997**, *13*, 814-820.

(12) Crooks, R. M.; Ricco, A. J. *Acc. Chem. Res.* **1998**, *31*, 219-227.

(13) Laibinis, P. E.; Whitesides, G. M. *J. Am. Chem. Soc.* **1992**, *114*, 1990-1995.

(14) Bain, C. D.; Troughton, E. B.; Tao, Y.-T.; Evall, J.; Whitesides, G. M.; Nuzzo, R. G. *J. Am. Chem. Soc.* **1989**, *111*, 321-335.

(15) Whitesides, G. M. *CHIMIA* **1990**, *44*, 310-311.

(16) Bellamy, L. J. *The Infrared Spectra of Complex Molecules*; 3rd ed.; Chapman & Hall: London, 1975.

(17) Silverstein, R. M.; Bassler, G. C.; Morrill, T. C. *Spectrometric Identification of Organic Compounds, 5th Ed.*; John Wiley & Sons: New York, 1991.

(18) Tien, J.; Terfort, A.; Whitesides, G. M. *Langmuir* **1997**, *13*, 5349-5355.

(19) Vinogradov, S. N.; Linnell, R. H. *Hydrogen Bonding*; Van Nostrand Reinhold Company: New York, 1971.

(20) Allara, D. L.; Nuzzo, R. G. *Langmuir* **1985**, *1*, 52-66.

Chapter 3

Adsorption of n-Alkylamine Monolayers onto Carboxylic Acid-Terminated Self-Assembled Monolayers from Solution

3.1. Introduction

The Adsorption of long-chained amphiphilic molecules at surfaces to form localized supramolecular assemblies has been a topic of ongoing interest. These studies have been directed at understanding the factors that influence aggregation, identifying their assembled structures, and developing means to generate well-defined supported films often by the Langmuir-Blodgett (LB) or self-assembly methods.[1] The primary difference in these techniques is that they produce physisorbed and chemisorbed monolayers, respectively. The interest in these films has resulted from their potential in areas of corrosion prevention, lubrication, adhesion, and molecular recognition.

The spontaneous adsorption of amphiphilic molecules was first reported by Zisman and coworkers almost fifty years ago.[2] By exposing glass surfaces to dilute solutions of various long-chained alcohols in hexadecane as solvent, these researchers formed monomolecular films that were not wet by the solvent medium and exhibited wetting properties similar to those of oriented LB monolayers formed by a more tedious process. Zisman and coworkers extended this approach

to include a range of metal and metal oxide surfaces and a variety of surfactant-like molecules including long-chained amines, carboxylic acids, and primary amides. The adsorption of these and related amphiphilic molecules has been further studied more recently on other solid substrates.[3,4]

Alkanethiolate SAMs on gold have attracted much attention than any other organic thin film systems in the last decade. The preparation of these SAMs is extremely straightforward, as gold (unlike other metals) does not form a stable oxide and can be handled in air with few precautions. A notable aspect of this system is that the assembly onto gold can accommodate a wide variety of tail groups and can generate both polar and nonpolar surfaces. Polar groups such as $-CO_2H$ and $-CONH_2$ can be localized at the exposed surface of the SAM and have been used as sites for molecular recognition and attachment to the surface. These SAMs can also serve as chemically well-defined model surfaces for investigating fundamental aspects of adsorption by a variety of species.

The previous chapter demonstrated the ability of specific surface-active molecules ($CH_3(CH_2)_nY$) to form organized adlayers on the surface of terminally substituted SAMs ($Au/S(CH_2)_mX$) as a result of non-covalent (i.e., ionic or hydrogen bonding) interaction Of the examined bilayer systems in Chapter 2 that produced densely-packed organized adlayers that could be isolated from the adsorption solution, the formation of oriented monolayers of n-alkylamines on carboxylic acid-terminated SAMs provided a case that resulted from an acid-base interaction. The previous chapter showed that a strong ionic interaction between the polar head groups of the adsorbates and the SAMs were responsible for the formation of a stable, organized adlayer of the long-chained amines on the CO_2H-surface. In addition to the head group interactions, factors due to the chain length of the adsorbate and the orientation of the tail group of the SAM may influence the quality and formation of the adsorbed film. This chapter investigates the effects of

such structural factors on the physical properties and structure of adlayers formed by the self-assembly of n-alkylamine adlayers onto carboxylic acid-terminated SAMs.

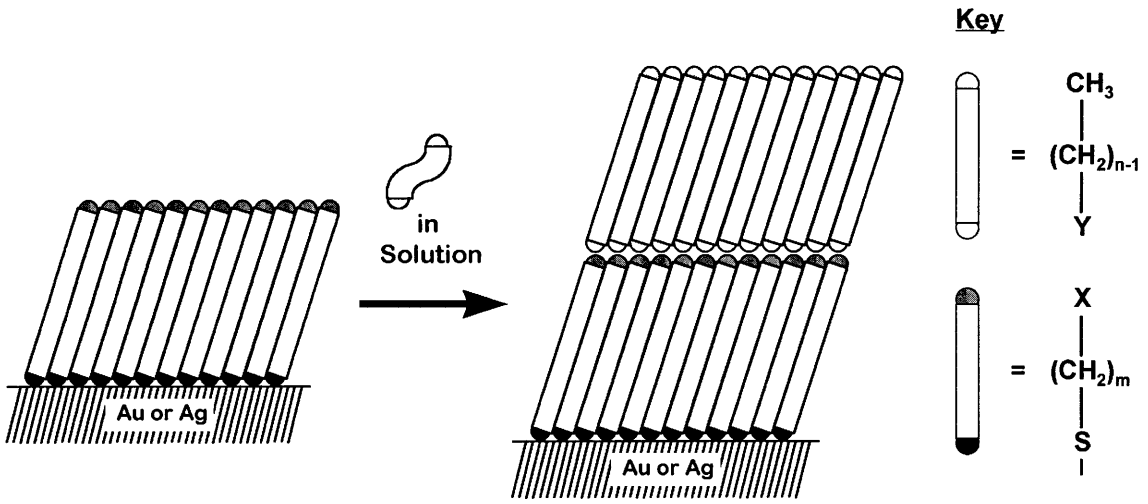

Figure 3-1. Schematic illustration of a non-covalently-bonded bilayer formed by self-assembly; specific chemical interactions between the functional groups X and Y are responsible for formation of the second layer.

3.2. Results and Discussion

3.2.1. Formation of Bilayers

The bilayer assemblies were formed on gold and silver surfaces by a two-step process. The mercaptoalkanoic acids ($HS(CH_2)_mCO_2H$; m = 10, 11, 15) were first adsorbed onto freshly evaporated films of gold or silver from ethanol. This adsorption produces an oriented monolayer that expresses carboxylic acid groups at the monolayer/air(liquid) interface. The resulting SAMs are wet by water ($\theta_a(H_2O) < 15°$), indicating formation of a high-energy organic surface. The CO_2H-terminated SAMs were then immersed in a solution of an n-alkylamine ($CH_3(CH_2)_nNH_2$) to complete formation of a bilayer assembly (Figure 3-1). In preparing these films, various properties

of the solvent such as polarity and surface tension played a critical role in our ability to produce high quality bilayer films. Solvent polarity is an important factor in producing SAMs with high-energy surfaces that are readily wet by water. For the primary layer, we formed the CO_2H-terminated SAMs from 1 mM solutions in ethanol and used adsorption times of 6 to 24 h with no apparent change in the properties of the SAMs. Non-polar solvents (isooctane, for example) yielded bilayers that were less wet by water and proved to be useful for the formation of bilayer assemblies. On silver, the CO_2H-terminated SAMs were prepared by minimizing exposure of the freshly evaporated silver films to the atmosphere before their derivatization, and only SAMs that were wet by water ($\theta_a(H_2O) < 15°$) were used for the preparation of bilayers.

The adsorption of alkylamines onto the carboxylic acid surfaces from the liquid phase proved to be more sensitive to experimental conditions than the assembly of thiols onto gold or silver. For example, exposure of $Au/S(CH_2)_{10}CO_2H$ to 1 mM $CH_3(CH_2)_{17}NH_2$ in ethanol for 24 h followed by a solvent rinse yielded the initially formed CO_2H-terminated SAM. As polar solvents such as ethanol would be expected to disrupt interactions between the carboxylic acid and amine functional groups, we performed similar experiments in isooctane and could form adsorbed amine layers; however, the properties of these assemblies (by ellipsometry, infrared spectroscopy, and wetting) were highly variant and appeared to depend on the rinsing conditions performed after the assembling process. For example, assemblies that exhibited ellipsometric thicknesses and infrared spectra consistent with the formation of an adsorbed monolayer of the alkylamine were transformed by subsequent rinsing with isooctane back to the original CO_2H-terminated monolayer.

To avoid the variations in composition that resulted from the rinsing process, we took advantage of the low-energy methyl surface that forms upon adsorption of the alkylamines onto the CO_2H-terminated SAMs. By using non-polar solvents with increasingly higher surface

tensions, it was possible to produce bilayer assemblies that emerged dry from the alkylamine solution and required no rinsing to remove residual material. For example, in contrast with the poor reproducibility for assemblies formed from isooctane (γ_{LV} = 19 mN/m), high quality bilayer films were regularly formed when the solvent was replaced with decahydronaphthalene (DHN; γ_{LV} = 31 mN/m). Similar reproducible formation of such bilayers was accomplished from alkylamine solutions in n-hexadecane (HD; γ_{LV} = 26.7 mN/m) and benzene (γ_{LV} = 28.9 mN/m) as the slides also emerged dry from these solutions and required only the use of a stream of nitrogen to remove any droplets of solution that collected near the edges of the slides. Although we did not conduct an extensive study of solvent selection on the properties of the bilayer films, we were able to infer that non-polar solvents with surface tensions greater than ~25 mN/m provided the required non-polar environment for formation of the bilayer and the requisite ability to dewet the assembled film (i.e., $\theta_{receding}$(solution) > 0°). The use of conditions where the contacting solution was autophobic to the resulting assembly simplified our ability to reproducibly produce and isolate films from solution that had a high level of structural organization.

Based on these results, we used DHN as solvent to form adlayers for most of our experiments. We immersed the CO_2H-terminated SAMs in 1-10 mM solutions of the alkylamines in DHN at room temperature to form the bilayer assemblies. We observed that the assembly of the amine layer under these conditions was rapid as samples immersed in the DHN solutions for times ranging from ~1 s to 24 h exhibited no significant difference in properties by our methods of characterization. For consistency, we immersed samples in the amine solutions for 6-24 h.

3.2.2. Ellipsometric Thicknesses of the Bilayers on Gold as a Function of the Chain Length of the n-Alkylamine Adsorbate

Ellipsometry was used to measure the thicknesses of bilayer assemblies on gold ($Au/S(CH_2)_mCO_2H/H_2N(CH_2)_{n-1}CH_3$) formed from various mercaptoalkanoic acids (m = 10, 11, and 15) and a variety of *n*-alkylamines (Figure 3-2a). The data on each SAM for the different alkylamine were fit by lines with slopes of 1.5 Å per methylene unit and intercepts of 12 and 17 Å for m = 11 and 15, respectively; data for m = 10 (not shown) exhibited a similar slope and an intercept of 11 Å. The differences between the intercepts for the three SAMs and the measured ellipsometric thicknesses for the parent CO_2H-terminated SAMs ($Au/S(CH_2)_mCO_2H$; m = 10, 11, 15) were the same; however, the intercepts for the three SAMs were ~4 Å less than the measured values for the CO_2H-terminated SAMs (thicknesses of 15, 16, and 21 Å for m = 10, 11, and 15, respectively). This disparity may reflect a difference in the amount of adsorbed adventitious materials by these two systems at atmospheric conditions. For example, the higher energy CO_2H surface is likely to adsorb a greater amount of material from the atmosphere than the lower energy CH_3 surface that is produced after adsorption of the alkylamine. For direct interaction between the amine and carboxylic acid groups, these contaminants would have to be displaced by the adsorbing amines, and could thereby result in effective thicknesses for the primary SAMs from the intercepts that are lower than their originally measured ellipsometric thicknesses.

The consistency and strong linearity of the data in Figure 3-2a strongly suggest that the alkylamines adsorb and form organized monolayer films with a common structure as the chain length of the amine is varied. The slopes for the data sets of three bilayers are similar to those obtained by Porter et al.[5] and Bain et al.[6] by ellipsometry for the adsorption of *n*-alkanethiols on gold to form SAMs. The similarity suggests that the amine layers may have a structure related to those for the underlying *n*-alkanethiolate SAMs on gold.

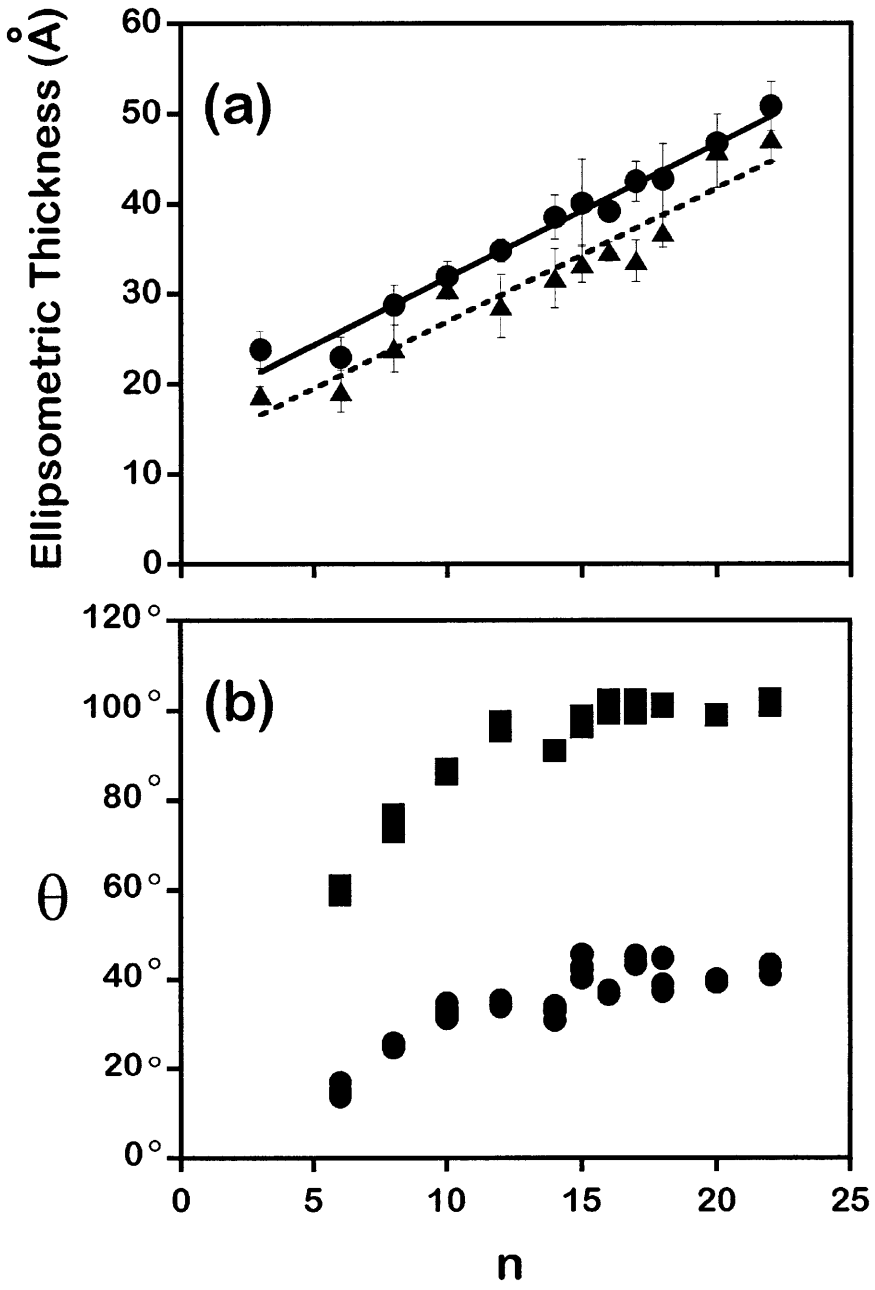

Figure 3-2. Properties of bilayers formed by assembly of n-alkylamines ($CH_3(CH_2)_{n-1}NH_2$) onto SAMs derived from CO_2H-terminated alkanethiols ($HS(CH_2)_mCO_2H$; ▲, ● for m = 11 and 15, respectively) on gold. (a) Ellipsometric thicknesses of the bilayer assemblies. The lines are least-squares fits to the data. (b) Contact angles of water (■) and hexadecane (●) on $Au/S(CH_2)_{15}CO_2H/H_2N(CH_2)_{n-1}CH_3$.

3.2.3. Wetting Properties of the Bilayer Assemblies

The wetting properties of the bilayer assemblies were examined using sessile drops of water and n-hexadecane (HD). Figure 3-2b displays the wetting properties of $Au/S(CH_2)_{15}CO_2H$ substrates after exposure to various n-alkylamine solutions in DHN. The data exhibit an increase in contact angle with increasing chain length of the alkylamine for $n < 12$ and an asymptotic value for $n \geq 12$. The wetting properties of these samples are consistent with the formation of a methyl surface.[3,7] The plateau in wetting at $n = 12$ is similar to that observed by others for the adsorption of alkylamines on platinum,[7] alkanoic acids on oxidized aluminum,[3] and alkanethiols on gold[5,6]. We also measured the contact angles of water and HD on the other CO_2H-teminated SAMs ($Au/S(CH_2)_mCO_2H$; $m = 10$ and 11) after exposure to the various alkylamines and observed no significant difference in wetting behavior from Figure 3-2b. This result indicates that the odd-even variation of hydrocarbon chains of the CO_2H-terminated SAMs does not affect the wetting properties of adlayers.

The contact angles of HD, a nonpolar liquid, on the bilayer assemblies were slightly lower than those on alkanethiolate SAMs when the hydrocarbon chain of alkylamines is short ($n < 12$). One possibility was that the shorter-chained alkylamines might desorb more readily into the liquid phase than the more strongly chemisorbed alkanethiol-based SAMs. As a test, we applied drops of DHN that contained various amounts of the alkylamines onto the bilayer to see whether any change in contact angle occurs since the presence of alkylamines within liquid droplets would prevent or retard the desorption of alkylamines from the bilayer assemblies depending on the concentration of the amines within the drops. We used DHN for this experiment instead of HD not only because DHN was used for the formation of bilayer assemblies but also because HD molecules composed of a long-alkyl chain can replace the adsorbed alkylamine molecules and the

inclusion of the HD molecules in the assemblies can complicate analysis of the wetting results. The experiment was performed over a concentration regime where the addition of alkylamines does not alter the surface tension of DHN as evidenced in the observation that the wetting properties of DHN drops with 1-40 mM hexylamine ($CH_3(CH_2)_5NH_2$) on an octadecanethiolate SAM on gold showed no change (Figure 3-3). As shown in Figure 3-3, the contact angles of DHN droplets on octadecanethiolate SAMs in the 1- 40 mM regime are the same as that of pure DHN, which indicates that the concentration of n-hexylamine in that regime does not influence the interfacial tension (γ_{LV}) at liquid/air interfaces. This result allows us to infer that any changes in contact angle that may occur on bilayer assemblies result from the coverage of adlayers on solid surfaces. In contrast, the contact angle on the bilayer assemblies ($Au/S(CH_2)_{15}CO_2H/H_2N(CH_2)_5CH_3$) increases as the concentration of n-hexylamine in DHN droplets increases, and saturates at ~5 mM (Figure 3-3) possibly by preventing desorption of adsorbed alkylamines from the adlayer. The further study on this topic will be discussed in Chapter 5.

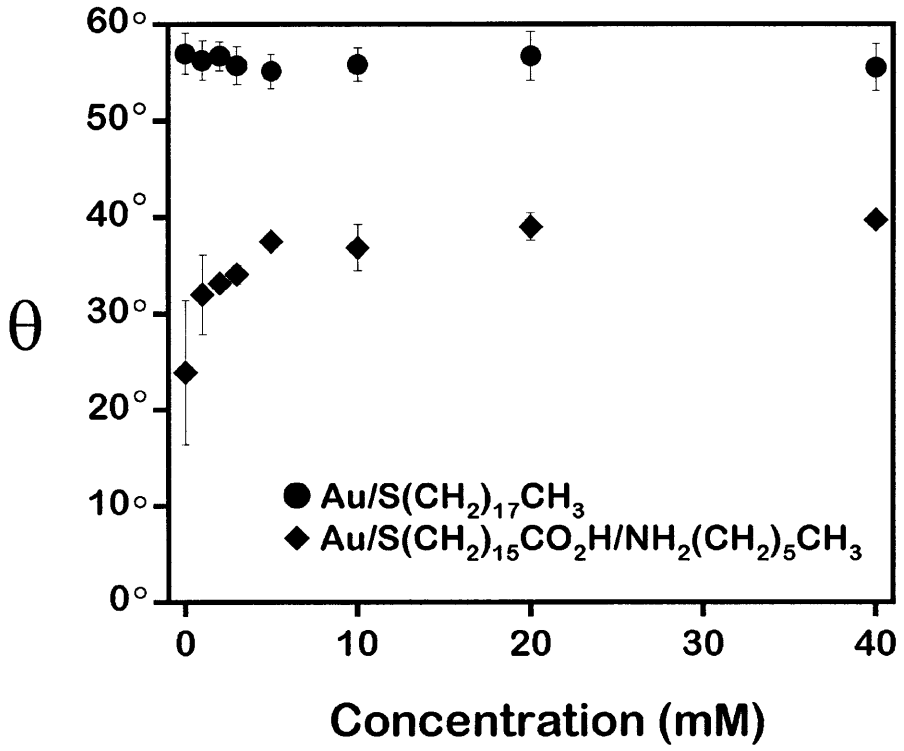

Figure 3-3. Wetting properties of DHN containing various concentrations of $CH_3(CH_2)_5NH_2$ on $Au/S(CH_2)_{17}CH_3$ (●) and an adsorbed layer of $CH_3(CH_2)_5NH_2$ on $Au/S(CH_2)_{15}CO_2H$

3.2.4. Characterization by Infrared Spectroscopy

Figure 3-4 shows spectra of carboxylic acid-terminated SAMs ($HS(CH_2)_mCO_2H$; m = 10, 11, and 15) before and after their exposure to 2-4 mM n-octadecylamine ($CH_3(CH_2)_{17}NH_2$) solutions. For all spectra reported here the units of intensity are $-\log(R/R_0)$ where R and R_0 are the reflectivities of the sample and reference, respectively and the assignments for the bands in the spectra are shown in Table 4-1.[8-10]

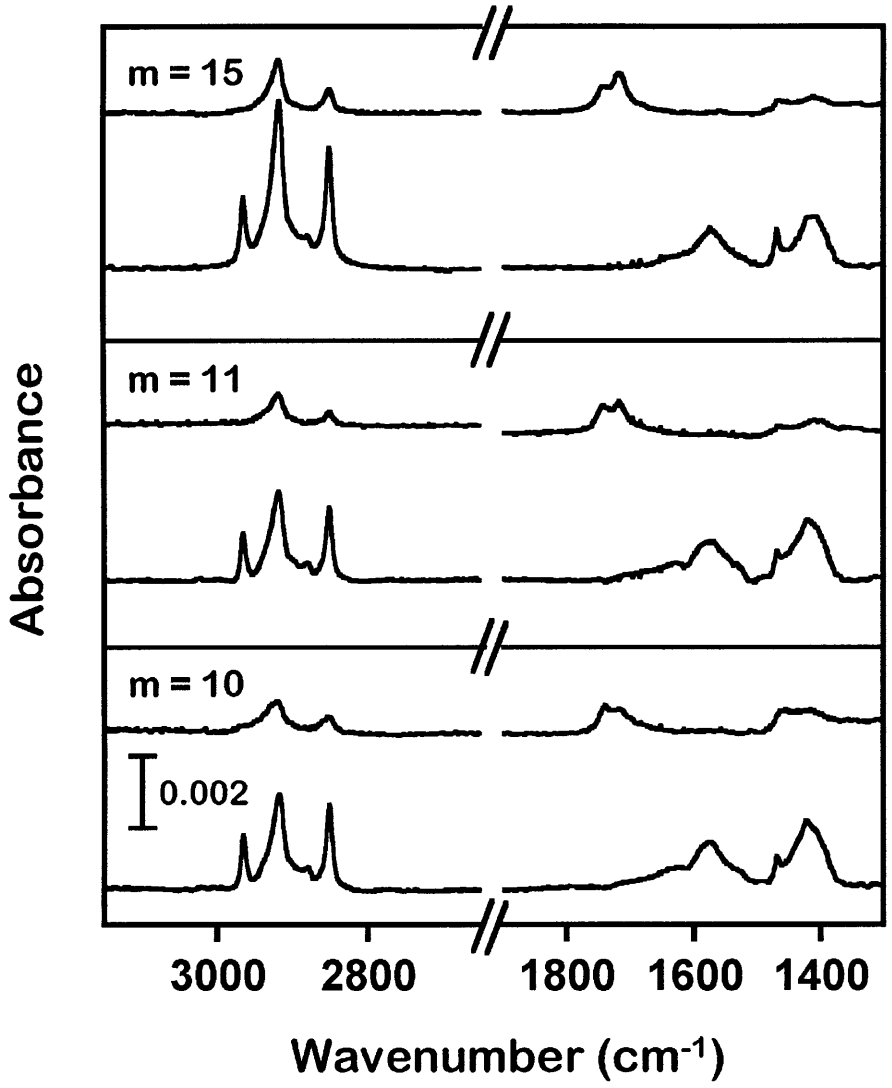

Figure 3-4. RAIRS spectra of Au/S$(CH_2)_mCO_2H$ (m = 10, 11, 15) before (upper spectra in each panel) and after (lower spectra in each panel) exposure to a n-octadecylamine solution.

Before exposure (upper spectra in each panel), the asymmetric and symmetric C-H stretching vibrations for the methylene groups of the SAMs are present at ~2919 and ~2851 cm^{-1} for m = 15, respectively. These results suggest the methylene chains are mostly ordered and closely packed in a solid-like environment, considering that disordered methylene chains usually exhibit stretching vibrations 5-10 cm^{-1} higher in frequency.[11,12] The bands at ~1740 and ~1719

cm^{-1} are due to the C=O stretching vibrations of non-hydrogen bonded and laterally hydrogen-bonded CO_2H terminal groups, respectively.[12]

After immersion of the CO_2H-terminated SAMs into a $CH_3(CH_2)_{17}NH_2$ solution, the intensities of the methylene stretching bands at 2919 and 2851 cm^{-1} increased and new peaks at 2966 and 2879 cm^{-1} appeared for the asymmetric and symmetric methyl stretching modes, respectively (lower spectra in each panel of Figure 3-4). These changes in the C-H stretching bands are consistent on any of the CO_2H-terminated SAMs suggesting that the quality of the adsorbed monolayer was not influenced by the odd-even variation of underlying monolayer when $m \geq 10$. This similarity parallels their similar wetting properties.

Table 3-1. Spectral mode assignments for monolayers of $HS(CH_2)_mCO_2H$ (m = 10, 11, 15) on gold before and after solution-phase adsorption of n-octadecylamine.

mode[a]	before	after
CH_3 C-H asym str		~2966
CH_2 C-H asym str	~2919	~2919
CH_3 C-H sym str		~2879
CH_2 C-Hsym str	~2851	~2852
CO_2H C=O str, non-H bonded	~1740	
CO_2H C=O str, H-bonded	~1719	
CO_2^- C=O asym str + NH_3^+ def		~1575
CH_2 scissor def	~1471	~1471
α-CH_2 scissor def + sym CO_2^- C=O str	~1412	~1412

[a]Abbreviations used: str = stretching, def = deformation, asym = asymmetric, sym = symmetric, and α = CH_2 groups located at either end of the alkyl chain.

Another notable change shown in the spectra is the position shift for C=O stretching bands. After exposure to the amine solution, the peaks for C=O stretching vibration modes of -CO_2H disappear and a new band at ~1575 cm^{-1} appears. This band is assigned as a combination of the asymmetric C=O stretching vibration mode of CO_2^- and the N-H symmetric bending mode, which results from the acid-base reaction between -CO_2H and -NH_2 groups.[13] The intensities of the bands in the 1410 - 1470 cm^{-1} region, which contains information about the C-O

and C=O stretching modes as well as the CH_2 scissors modes, apparently increases after exposure to the alkylamine solution, indicating that the collective orientation of the C=O or C-O bond becomes more normal to the surface after the acid-base reaction with NH_2 groups.[14] If you assume that most of the terminal carboxylic acid groups are laterally hydrogen-bonded prior to their reaction with amines, the C-O and C=O bonds of carboxylic acids have to be directed parallel to the surface to share the hydrogen atoms of terminal carboxylic acid groups via the lateral hydrogen bonding; therefore, once their reaction with amines occurs, the conversion of carboxylic acids to carboxylates will break the laterally hydrogen-bonded network causing C=O or C-O bonds to possess a more normal orientation.

Figure 3-5 shows the IR spectra of bilayer assemblies (Figure 3-5a) in the CH stretching region for n = 6, 8, 10, 12, 14 - 18, 20, and 22 and their corresponding difference spectra. The difference spectra were obtained from subtracting the spectra of underlying CO_2H-terminated SAMs from those of the bilayers (Figure 3-5b) to examine the chain conformation and orientation of the alkylamine adlayers. While the peak frequencies of the asymmetric and symmetric CH_2 stretching modes of the bilayer spectra correspond to or near those for trans-extended crystalline phase, the peak frequencies and their shape of those modes in the difference spectra are quite different from those of bilayer spectra at $n \leq 12$. In other words, the peak for the asymmetric CH_2 stretching mode appears at a higher wavenumber and its shape is broader than that of bilayer spectra, indicating liquid-like or disordered phase within the adlayers. In contrast, we observed no significant change in the peak positions at $n \geq 14$. Though the experimental errors and the overlap of absorption bands can affect the peak positions, these results serve as a good probe for the structure of alkylamine adlayers. The intensities of the asymmetric and symmetric methylene modes increase as n increases and increase quite linearly with $n \geq 14$, indicating that the films have a defined structure. In contrast to the linearly increasing trend of the CH_2 mode intensities with

respect to hydrocarbon chain length, the CH_3 modes display odd-even fluctuations in their peak intensities. These odd-even trends result from the orientation of the terminal C-CH_3 bond of adlayers relative to the surface normal.[15]

Figure 3-6 displays the intensity ratios between the asymmetric and symmetric methylene modes, I (d^-, CH_2)/I (d^+, CH_2). The ratio for the original CO_2H and CH_3-terminated SAMs was ~2.5. In contrast, the ratio decreased to ~1 upon adsorption of alkylamines on CO_2H-terminated SAMs at $n \geq 14$. These observations suggest that the adlayers may possess a different structure from the structure of the underlying SAMs. The structure of adlayers will be further discussed in a later section.

Figure 3-7 displays the intensity ratios between the asymmetric and symmetric methyl modes, I (r^-, CH_3)/I (r^+, CH_3), for the bilayer and the alkanethiolate SAMs on gold as functions of n. Both show odd-even variations, and the odd-even variation of the bilayer assemblies is offset by one methylene unit from that of the alkanethiolate SAMs on gold. The ranges of fluctuations of both systems are almost the same. These results allow us to infer that the orientation of the terminal N-C bond in the alkylamine adlayers is approximately normal to the surface under assumption that the canted polymethylene chains are trans-zig-zag extended.[15] The normal orientation of N-C bond of the amine adlayers may result from the Coulombic interactions between charged species (CO_2^- vs. NH_3^+, CO_2^- vs. CO_2^-, and NH_3^+ vs NH_3^+) that requires minimization of the total energy potential within the bilayer assembly causing the orientation of N-C bonds to be normal to the surface.

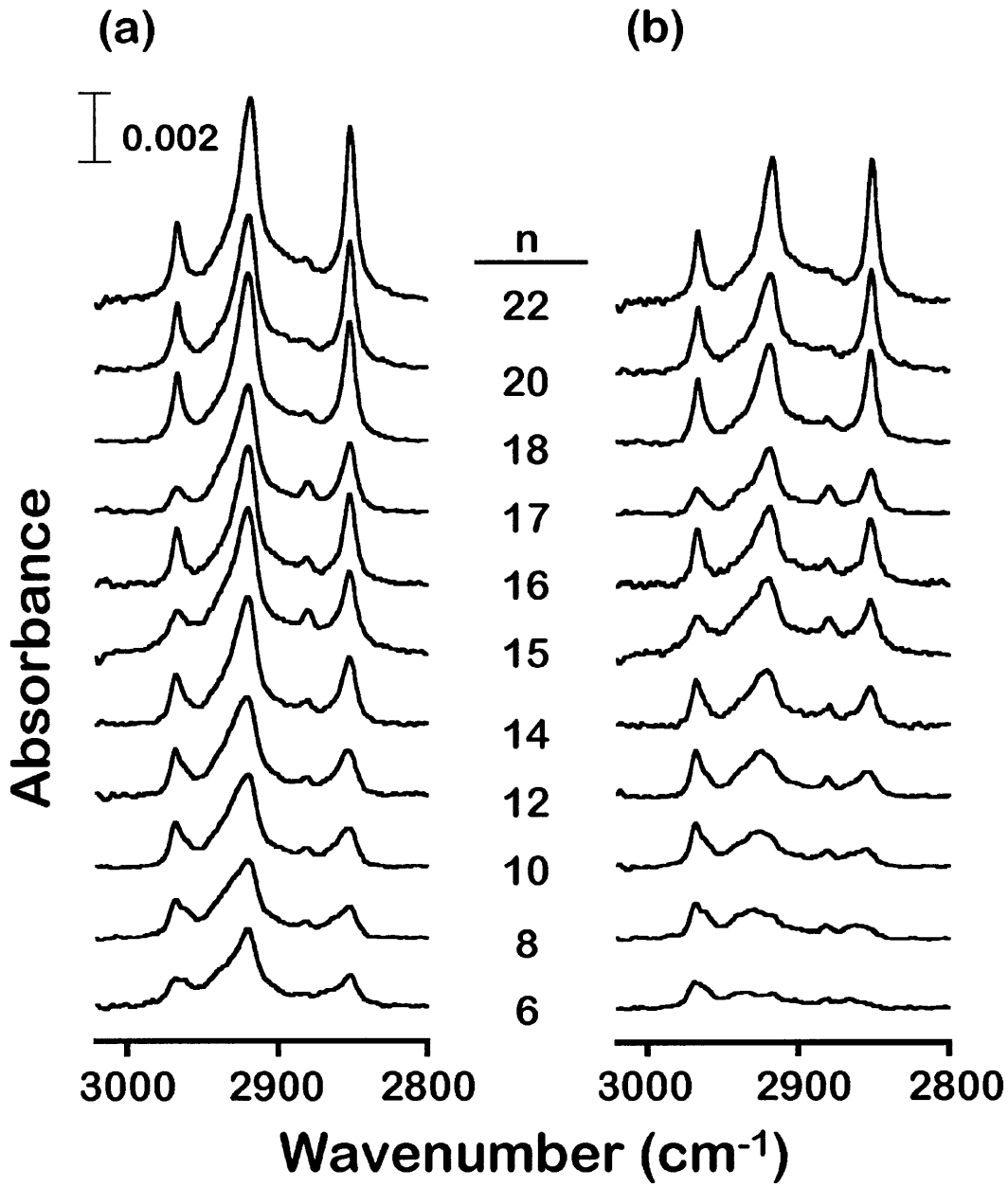

Figure 3-5. RAIRS spectra of bilayer assemblies formed on $Au/S(CH_2)_{15}CO_2H$. (a) Spectra of the bilayers, $Au/S(CH_2)_{15}CO_2H/H_2N(CH_2)_{n-1}CH_3$. (b) Spectra of the alkylamine component of the bilayers obtained by referencing spectra for the bilayers to those for $Au/S(CH_2)_{15}CO_2H$

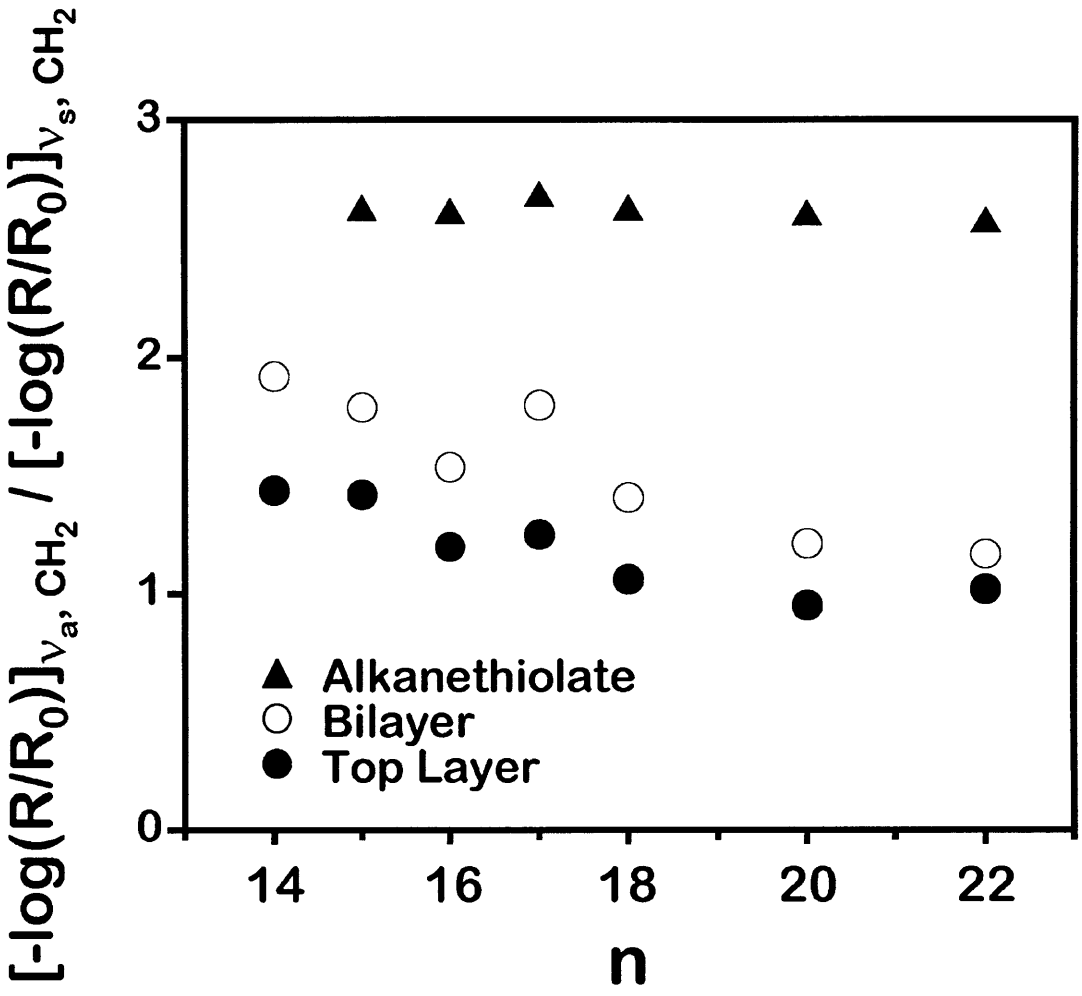

Figure 3-6. Dichroic ratios between the asymmetric and symmetric methylene peak intensities for $Au/S(CH_2)_{n-1}CH_3$ (▲), $Au/S(CH_2)_{15}CO_2H/H_2N(CH_2)_{n-1}CH_3$ (○), and the absorbed n-alkylamine component of the $Au/S(CH_2)_{15}CO_2H/H_2N(CH_2)_{n-1}CH_3$ (●). The alkylamine values were obtained from difference spectra.

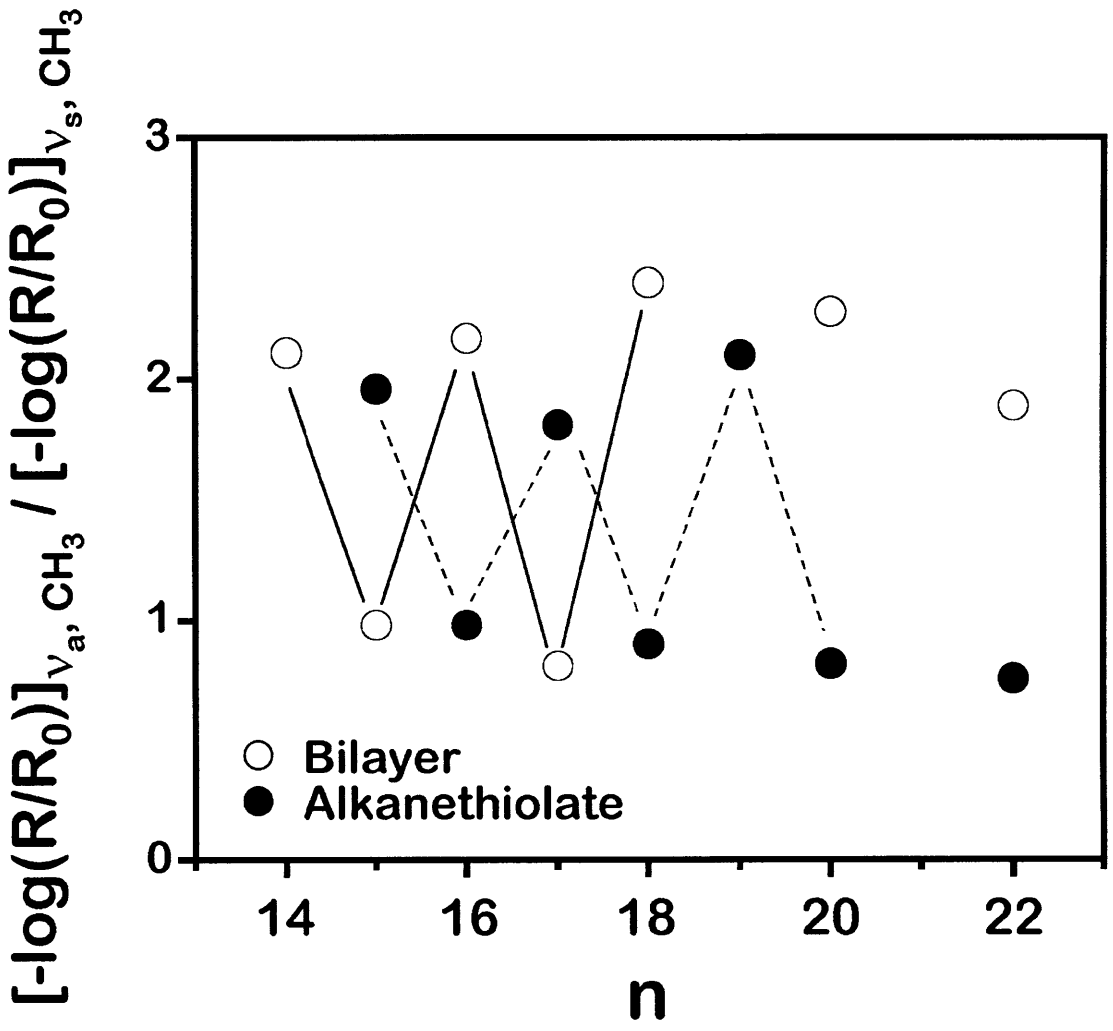

Figure 3-7. Dichroic ratios between the asymmetric and symmetric methyl peak intensities for $Au/S(CH_2)_{15}CO_2H/H_2N(CH_2)_{n-1}CH_3$ (open symbols) and $Au/S(CH_2)_{n-1}CH_3$ (filled symbols).

3.2.5. IR Spectra of the Bilayer Assemblies on Silver

Alkanethiolate SAMs formed on Ag differ in structure from those on Au, and their hydrocarbon chains are less tilted from the surface normal.[15,16] On Ag(111), the thiolates achieve a packing density that is approximately equal to the cross sectional area of the polymethylene chain (18.4 $Å^2$): for $CH_3(CH_2)_{17}S/Ag$, the nearest neighbor distance is 4.7 Å (19.1

Å^2/thiolate), shorter than that on Au (5.0 Å, 21.4 Å^2/thiolate). As a result, the hydrocarbon chains of n-alkanethiolate SAMs on silver can be less tilted from the surface normal than those of SAMs on gold. Therefore, we investigated the bilayers on Ag to see the effect of a different packing density onto the properties and structure of bilayers. The wetting behavior on the Ag-based bilayer assemblies were similar to that on the Au-based counterparts, and this observation parallels previous the study by Laibinis et al.[15] reporting macroscopic wetting properties by water and HD on alkanethiolate SAMs that assembled on Au and Ag. The broad peaks for asymmetric and symmetric CH_2 stretching modes in the spectra of CO_2H-terminated SAMs on Ag appear at ~2928 and 2854 cm^{-1}, respectively. These high wavenumbers of Ag samples are possibly due to the size of terminal CO_2H groups that are apparently bigger than methyl groups or due to the formation of a laterally hydrogen-bonded network that can disrupt the dense packing of hydrocarbon chains. However, the strong peak for C=O stretching mode appears at ~1718 cm^{-1} indicating that most of terminal carboxylic acids are laterally hydrogen-bonded at a high level.

Figure 3-8 shows the IR spectra of the bilayer assemblies (Figure 3-8a) in the CH stretching region for n = 12, 14-18 and their corresponding difference spectra. The positions and shapes of the bands show close similarity to those for Au systems; however, the peak intensities of the CH_2 stretching modes for the adsorbed layers at ~2919 cm^{-1} and ~2851 cm^{-1} (Figure 3-8b) are weaker than those for Au systems (Figure 3-5b), which indicates that polymethylene chains on silver are oriented more normal to the surface.[15] Figure 3-9 shows the methylene dichroic ratios of bilayer assemblies and alkanethiolate SAMs on Ag as functions of n and the ratios for the adlayers (~1.5) are lower than those for alkanethiolates on Ag (~2.0).

The odd-even variation of methyl dichroic ratios for the adlayers on Ag is similar to that for the adsorbed layers on Au, while no significant variation is evident for alkanethiolate SAMs on Ag (Figure 3-10). The range of the variation is slightly smaller than that for the adsorbed layers on

Au. For alkanethiolate SAMs, Laibinis et al. observed no significant modulation in the methyl stretching modes (r^+ and r_a^-) for Ag samples, while they observed a strong modulation for Au samples.[15] They explained the difference between the spectra obtained on Ag and on Au with a difference in structures of monolayers on these substrates. In other words, small or little modulation of the methyl stretching modes or CH_3 dichroic ratios for Ag samples indicate that the projection of the terminal C-CH_3 bond on the normal to the surface is invariant with chain length. Therefore, it is somewhat surprising that the modulation of the CH_3 dichroic ratios for the adlayers on Ag was significantly different from that for alkanethiolates on Ag and similar to that for the adsorbed layers on Au. Therefore, this observation leads us to infer that the hydrocarbon chains in the adsorbed layers are tilted more from the surface normal than those in alkanethiolates on Ag. The similar modulations in CH_3 dichroic ratio do not necessarily mean that they both have similar orientations of hydrocarbon chains, since the CH_2 dichroic ratios (closely related to the twist of hydrocarbon chains) of the adlayers on Ag and Au are different. In addition, since the terminal CH_3 groups of the adlayers can adopt both trans and gauche conformations at room temperature,[17] the intensities of methyl stretching modes should serve as a complementary probe to examine the film structure.

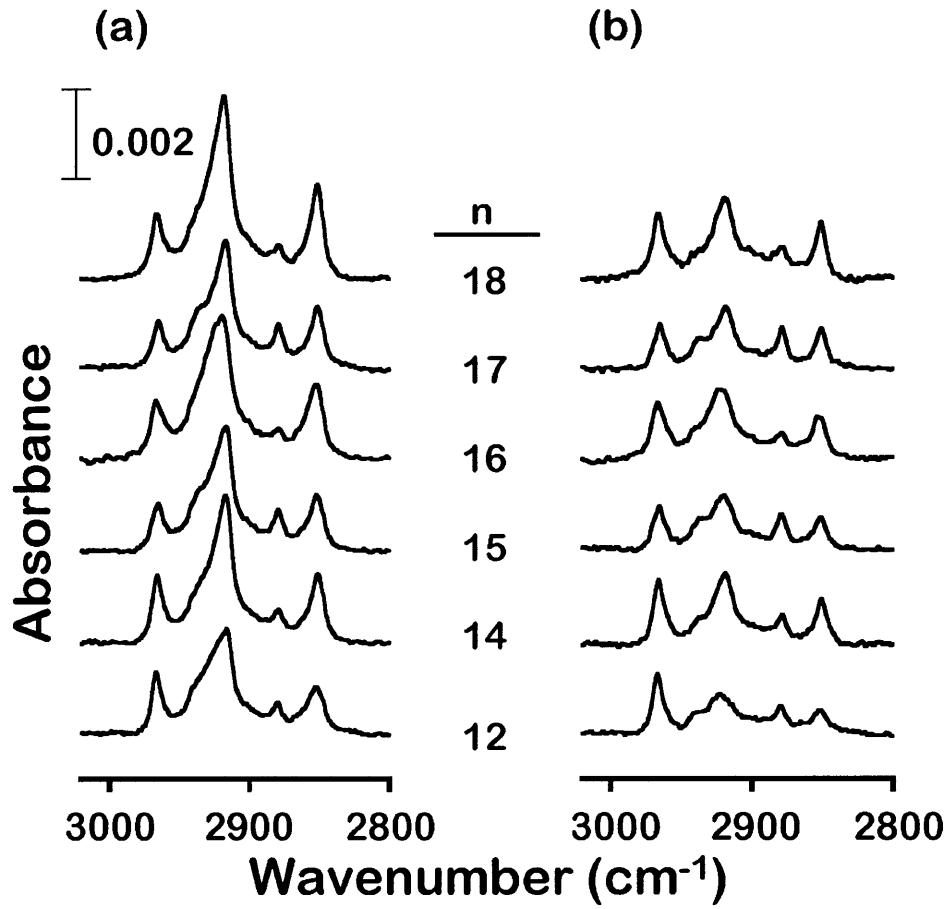

Figure 3-8. RAIRS spectra of bilayer assemblies formed on $Ag/S(CH_2)_{15}CO_2H$. (a) Spectra of the bilayers ($Ag/S(CH_2)_{15}CO_2H/NH_2(CH_2)_{n-1}CH_3$). (b) Spectra of the alkylamine component of the bilayers obtained by referencing spectra for the bilayers to those for $Ag/S(CH_2)_{15}CO_2H$

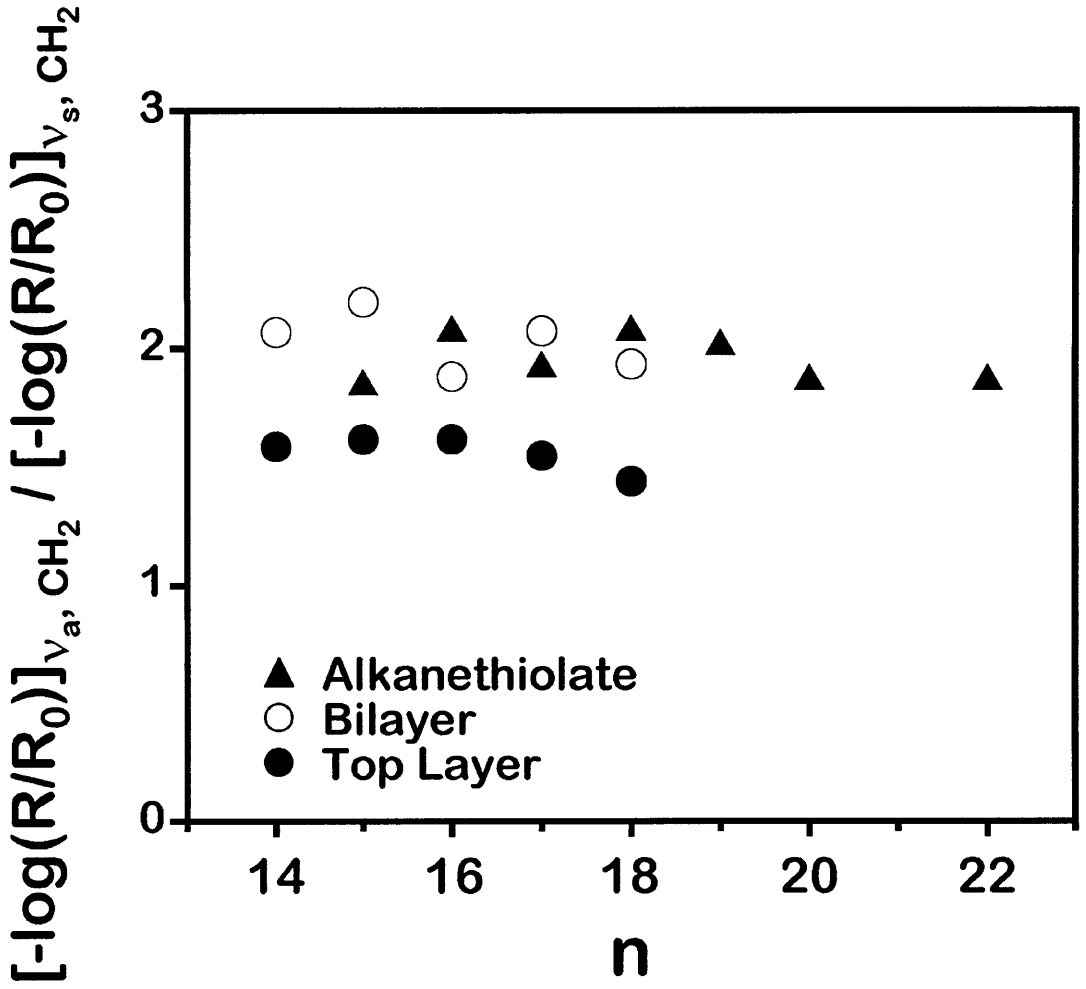

Figure 3-9. Dichroic ratios between the asymmetric and symmetric methylene peak intensities for $Ag/S(CH_2)_{n-1}CH_3$ (▲), $Ag/S(CH_2)_{15}CO_2H/H_2N(CH_2)_{n-1}CH_3$ (○), and the absorbed n-alkylamine component of the $Ag/S(CH_2)_{15}CO_2H/H_2N(CH_2)_{n-1}CH_3$ (●). The alkylamine values were obtained from difference spectra.

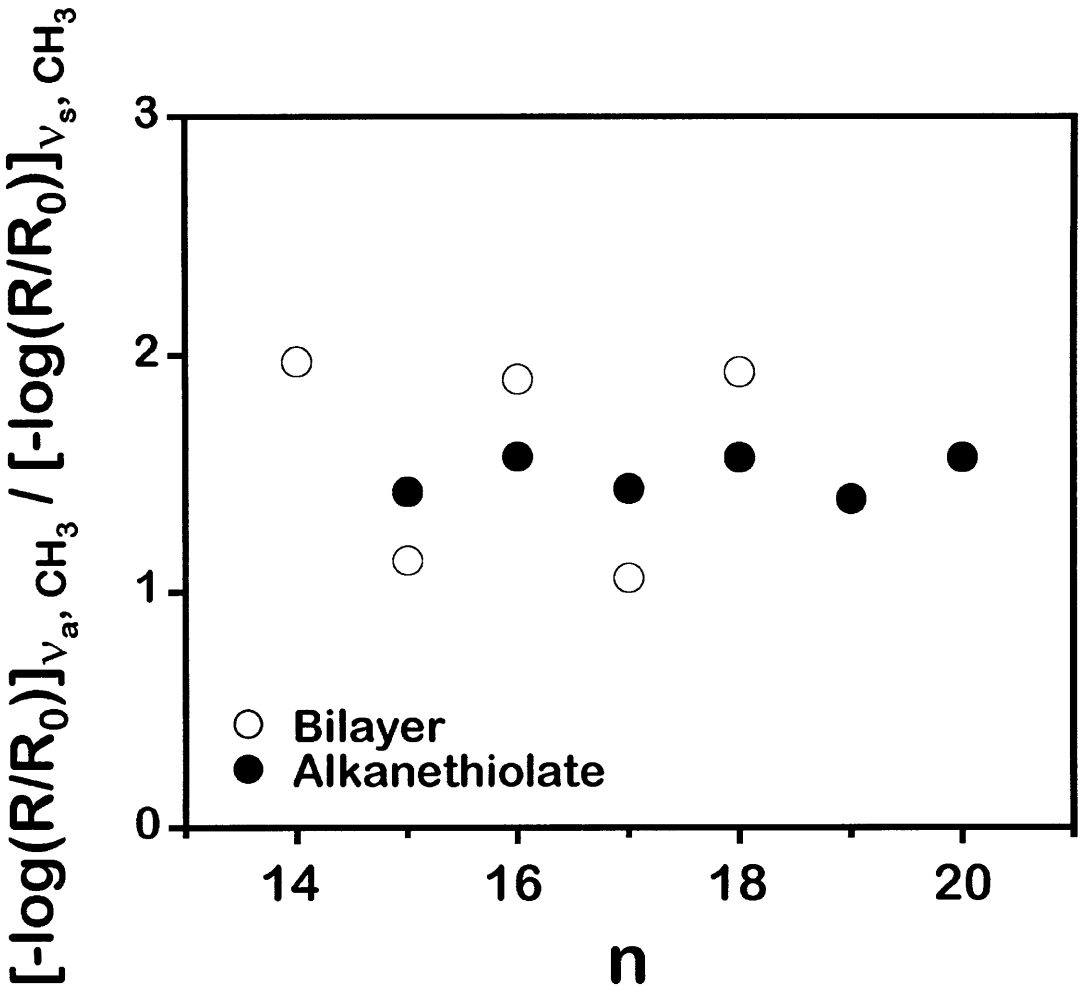

Figure 3-10. Dichroic ratios between the asymmetric and symmetric methyl peak intensities for $Ag/S(CH_2)_{15}CO_2H/H_2N(CH_2)_{n-1}CH_3$ (open symbols) and $Ag/S(CH_2)_{n-1}CH_3$ (filled symbols).

3.2.6. Orientation of Hydrocarbon Chains

Infrared spectroscopy has been an invaluable technique for characterizing the structure of SAMs.[5,12,15,16] For this investigation, the technique provides a probe of the average orientation of the hydrocarbon chains in these assemblies, their level of conformational disorder, and the changes in the chemical states of the tail groups for both the SAMs and adlayers. The spectral

intensity (I) of each mode in a RAIRS spectrum is related to its orientation. Specifically, the intensity of a mode is proportional to the square of the average projection of its corresponding transition dipole moment (μ_z) along the surface normal.[18] This specific relationship allows a quantitative analysis of the average orientation of alkyl chains within SAMs.[12,14,15,19-21]

The difference spectra were used to probe the structure of the alkylamine adlayers (Figures 3-5b and 3-8b). The use of the difference spectra assumes that the formation of the adlayers does not alter the structure of their underlying CO_2H-terminated SAMs. To check the validity of our approach, we formed a bilayer assembly using n-tetradecylamine-d_{29} ($CD_3(CD_2)_{13}NH_2$; Cambridge Isotope Laboratories, Andover, MA) as an adsorbate onto a CO_2H-terminated SAM. Since the band from C-D stretching vibrations (2260-2040 cm^{-1}) does not overlap with the C-H stretching bands (3000-2840 cm^{-1}), we could directly monitor any change that occurred in the structure of underlying SAMs from IR spectra. We observed no change in the C-H stretching band after adsorption of n-tetradecylamine-d_{29} and this result supports our approach to analyzing the structure of adlayers with the difference spectra.

Their structure can be simply described in terms of a tilt angle (α) and a twist angle (β) for the alkyl chains within the SAM.[15,21] For these systems, α and β can be obtained using the peak intensities of the C-H stretching modes. Notably, the intensity ratio between the asymmetric and symmetric methylene modes, I (d^-, CH_2)/I (d^+, CH_2), changes upon the formation of the adlayer on a SAM on gold (Figure 3-6). This observation suggests that the adlayers may possess different structures from those of their underlying SAMs. These ratios can be related to twist angles (β) by the expression:[20,21]

$$\tan\beta = \tan\beta_0 \left[\left(\frac{I(d^-, CH_2)}{I(d^+, CH_2)} \right) \Big/ \left(\frac{I_0(d^-, CH_2)}{I_0(d^+, CH_2)} \right) \right]^{1/2} \quad (3\text{-}1)$$

where the subscript 0 denotes a "reference SAM" (formed from an alkanethiol that contains the same number of methylene units as the adsorbate that forms an adlayer). To calculate β for the adlayers (C_nNH_2; n ≥ 14), we used the spectra of SAMs derived from C_nSH on gold and silver as references and values for β_0 of ~52° (gold) and ~49° (silver) as reported in preceding studies.[12,15] We obtained spectra for the adlayers by subtracting the spectra of the underlying SAMs from those of the bilayers (Figures 3-5b and 3-8b) and calculated twist angles by eq 3-1 of ~44° (gold) and ~46° (silver) for the $C_{18}NH_2$ adlayers. The origin of the difference is not clear; however, it is likely due to the preferred geometries for the interactions between X and Y that then modulate the chain structure.

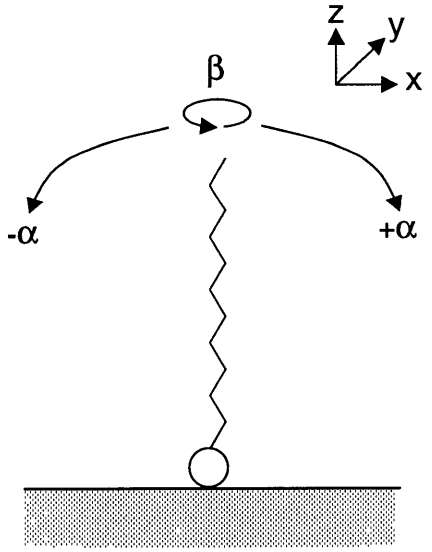

Figure 3-11. Schematic illustration of an all-trans chain of an adsorbed layer on a SAM. The cant angle α and the chain twist β are shown along with their relationship to the surface coordinate.

We also estimated the cant angles (α) for the hydrocarbon chains in these adlayers by comparing the methylene mode intensities of the adlayers with those of reference alkanethiolate SAMs using our calculated values of β and reported values of α_0 (= ~26° and ~13° for gold and silver, respectively) and β_0.[12,15] The calculated value of α for the adlayers on gold was ~30°, which is similar to those for their underlying SAMs. This result suggests that the adlayers and the underlying SAMs have similar packing densities. By ellipsometry, the thicknesses of the adlayers were similar to those of alkanethiolate SAMs on gold with common chain lengths, thus supporting common values of α and similar packing densities for both layers. For the adlayers on Ag substrates, we obtained an average tilt of ~20°. The cant of the adlayers is higher than that for alkanethiolate SAMs on Ag (~13°). We infer that the higher contact angles by ~7° possibly come from the different packing density of hydrocarbon chains of CO_2H-terminated SAMs from that of methyl-terminated SAMs, as discussed in the previous section.

3.3. Conclusions

The results from ellipsometry, contact angle measurements, and IR spectroscopy demonstrated that n-alkylamines adsorb onto carboxylic acid-terminated SAMs and produce oriented monomolecular films. Their IR spectra suggest that the amines can form densely-packed monolayers on the SAMs and the acid-base interactions between CO_2H and NH_2 occur during the adsorption process. The RAIRS results on the effects of chain length showed that the films possess a defined structure. The infrared data also allowed us to infer that the hydrocarbon chains of the adlayers are tilted approximately the same as those of their underlying SAMs possibly due to the complete reaction of terminal carboxylic acids with amines leading to a similar packing density to that of underlying SAMs. We didn't observe any significant influence of Ag substrates, which

usually induced a more dense packing of hydrocarbon chains, on the physical properties of adlayers.

3.4. Experimental

Mercaptoalkanoic acids ($HS(CH_2)_nCO_2H$; n = 10, 11, 15), pentadecylamine, hexadecylamine, heptadecylamine and docodecylamine were synthesized according to literature procedures.[6,22] The other alkylamines were obtained from Aldrich (Milwaukee, WI) and n-tetradecylamine-d_{29} ($CD_3(CD_2)_{13}NH_2$) was obtained Cambridge Isotope Laboratories (Andover, MA) and used without further purification. n-Alkanethiols were available from other studies.[23] SAMs and adlayers were prepared and characterized as noted in Chapter 2.

3.5. References

(1) Ulman, A. *An Introduction to Ultrathin Organic Films: From Langmuir-Blodgett to Self-Assembly*; Academic Press: Boston, 1991.

(2) Bigelow, W. C.; Pickett, D. L.; Zisman, W. A. *J. Colloid Sci.* **1946**, *1*, 513-538.

(3) Allara, D. L.; Nuzzo, R. G. *Langmuir* **1985**, *1*, 45-52.

(4) Zhu, J.; Mirkin, C. A.; Braun, R. M.; Winograd, N. *J. Am. Chem. Soc.* **1998**, *120*, 5126-5127.

(5) Porter, M. D.; Bright, T. B.; Allara, D. L.; Chidsey, C. E. D. *J. Am. Chem. Soc.* **1987**, *109*, 3559-3568.

(6) Bain, C. D.; Troughton, E. B.; Tao, Y.-T.; Evall, J.; Whitesides, G. M.; Nuzzo, R. G. *J. Am. Chem. Soc.* **1989**, *111*, 321-335.

(7) Bewig, K. W.; Zisman, W. A. *J. Phys. Chem.* **1963**, *67*, 130-135.

(8) Allara, D. L.; Swalen, J. D. *J. Phys. Chem.* **1992**, *86*, 2700-2704.

(9) Rabolt, J. F.; Burns, F. C.; Schlotter, N. E. *J. Chem. Phys.* **1983**, *78*, 946-952.

(10) Snyder, R. G.; Hsu, S. L.; Krimm, S. *Spectrochimica Acta* **1978**, *34A*, 395-406.

(11) Chidsey, C. E. D.; Loiacono, D. N. *Langmuir* **1990**, *6*, 682-691.

(12) Nuzzo, R. G.; Dubois, L. H.; Allara, D. L. *J. Am. Chem. Soc.* **1990**, *112*, 558-569.

(13) Sukhorukov, G. B.; Feign, L. A.; Montrel, M. M.; Sukhorukov, B. I. *Thin Solid Films* **1995**, *259*, 79-84.

(14) Allara, D. L.; Nuzzo, R. G. *Langmuir* **1985**, *1*, 52-66.

(15) Laibinis, P. E.; Whitesides, G. M.; Allara, D. L.; Tao, Y.-T.; Parikh, A. N.; Nuzzo, R. G. *J. Am. Chem. Soc.* **1991**, *113*, 7152-7167.

(16) Walzcak, M. M.; Chung, C.; Stole, S. M.; Widrig, C. A.; Porter, M. D. *J. Am. Chem. Soc.* **1991**, *113*, 2370-2378.

(17) Nuzzo, R. G.; Korenic, E. M.; Dubois, L. H. *J. Chem. Phys.* **1990**, *93*, 767-773.

(18) Greenler, R. G. *J. Phys. Chem.* **1966**, *44*, 310-315.

(19) Dubois, L. H.; Nuzzo, R. G. *Annu. Rev. Phys. Chem.* **1992**, *43*, 437-463.

(20) Sinniah, K.; Cheng, J.; Terrettaz, S.; Reutt-Robey, J. E.; Miller, C. J. *J. Phys. Chem.* **1995**, *99*, 14500-14505.

(21) Hou, Z.; Abbott, N. L.; Stroeve, P. *Langmuir* **1998**, *14*, 3287-3297.

(22) Gibson, M. S.; Bradshaw, R. W. *Angew. Chem. Int. Ed. Engl.* **1968**, *7*, 919-930.

(23) Jennings, G. K.; Laibinis, P. E. *J. Am. Chem. Soc.* **1997**, *119*, 5208-5214.

Chapter 4

Spontaneous Formation of Monolayers on Chemically-Defined Surfaces Using Hydrogen Bonding

4.1. Introduction

The previous chapter discussed the formation of densely packed monolayers of primary, aliphatic amines onto CO_2H-terminated SAMs using acid-base ionic interactions. The present chapter uses different adsorption chemistry, hydrogen bonding, to assemble bilayers. Hydrogen bonding is reported to be relatively weaker than ionic interactions in interaction strength. Thomas et al. reported studies on the adhesive forces between thiol-derivatized Au probes and Au substrates using interfacial force microscope (IFM).[1] Their experimental results demonstrated that the work of adhesion for $-CO_2H$ and $-CO_2H$ interactions was approximately three times less than that for the ionic interactions between $-NH_2$ and $-CO_2H$. Interestingly, they found that the calculated work of adhesion for $-CO_2H$ and $-CO_2H$ interactions work of adhesion was smaller than that obtained from gas-phase experiments and attributed this difference to the environment for terminal CO_2H groups, where head-to-head hydrogen bonding with adsorbing CO_2H groups is in competition with intramonolayer lateral hydrogen bonding within SAMs.[2-4]

Formation of adlayers based on hydrogen bonding-based adsorption has been reported in the literature mostly based on CO_2H-CO_2H interactions.[3,5] Sun et al. formed a monomolecular-level layer of *n*-tetradecanoic acid ($CH_3(CH_2)_{12}COOH$) by exposing a CO_2H-terminated SAM on gold ($Au/S(CH_2)_2CO_2H$) to a vapor of $CH_3(CH_2)_{12}CO_2H$. They monitored formation of an adlayer with infrared spectroscopy, which showed the shift of a peak assigned for C=O stretching vibration mode; however, their experimental results indicate that the adlayers possess a disordered structure on the SAM. Green et al. also reported formation of adlayers using the acid-acid hydrogen bonding (SAM from 16-mercaptohexadecanoic acid and stearic acid).[5] They also confirmed formation of assemblies using infrared spectroscopy; however, their frictional force microscopy (FFM) images showed topological irregularities suggesting incomplete coverage.

The adsorption of long-chained amides onto surfaces has not received much attention since Zisman's seminal work in 1946.[6] It is possibly due to the poor ability of amide groups to coordinate with inorganic substrates. Their ability to form a strong hydrogen bond,[7] however, can be utilized if the inorganic substrates are derivatized with organic films exposing functional groups that can form hydrogen bonds. For example, in chapter 2, we demonstrated that the adsorption of alkyl amides was preferred over alkylamines and alkanoic acids when the surface was covered with amide groups and the resulting adlayers of alkyl amides were as organized as other adlayer systems that we examined. This chapter, therefore, reports detailed studies on the bilayer assemblies that uses amide-amide interactions.

4.2. Results and Discussion

4.2.1. Preparation of Monolayers and Bilayers

SAMs were prepared by exposing freshly evaporated gold-coated silicon wafers to ~1 mM ethanolic solutions of amide-terminated thiols ($HS(CH_2)_mCONH_2$; n = 10 and 11) for 6-24 h at room temperature. The resulting films were wetted by water and hexadecane (HD) indicating formation of high energy surfaces.[8] Bilayers were prepared by exposing the $CONH_2$-terminated SAMs to supersaturated decahydronaphthalene (DHN) solutions of the alkyl amides ($CH_3(CH_2)_nCONH_2$) for more than 6 h to insure complete formation of the assemblies. The primary, aliphatic amides were much less soluble in DHN than the *n*-alkylamines discussed in the previous chapter, and we observed increase in solubility by substituting toluene for DHN. For example, hexanoamide, $CH_3(CH_2)_4CONH_2$, is soluble in toluene at more than 10 mM, while it is soluble at less than 1 mM in DHN; however, the wetting properties and film thicknesses of assembled films from toluene solutions were similar to those from DHN solutions.

4.2.2. Wetting Properties and Film Thickness

The ellipsometric thicknesses of bilayers are shown in Figure 4-1a. The measured values were typically scattered in ± 2.0 Å about the averaged in the figure. The measured thicknesses of the $CONH_2$-terminated SAMs ($Au/S(CH_2)_mCONH_2$) are scattered about 14 and 15 Å for m = 10 and 11, respectively, and these measured values were close to the intercepts of the fitted lines. The slopes of the lines were approximately 1.5 Å/-CH_2-, also similar to those of amine adlayers of Chapter 3 and the previous studies on alkanethiolate SAMs on gold.[9,10] The values for advancing contact angles of water and hexadecane on $CONH_2$-terminated SAMs on gold

($Au/S(CH_2)_mCONH_2$; m = 10 and 11) were < 15° as reported in literature.[8] The $CONH_2$-surfaces displayed oleophobicity after exposure to the DHN solutions of the alkyl amides and this observation visually indicated the formation of methyl-terminated bilayer assemblies. The dependence of wetting properties on the chain length of adsorbates ($CH_3(CH_2)_nCONH_2$) exhibited a trend similar to the results of the previous chapter on amine adlayers (Figure 4-1b). No significant difference in contact angle was observed when n ≥ 10 and this observation agrees with the previous studies on the organized films of a monomolecular level.[9-12] These results from wetting measurements and ellipsometry suggest formation of organized monolayers onto $CONH_2$-surfaces.

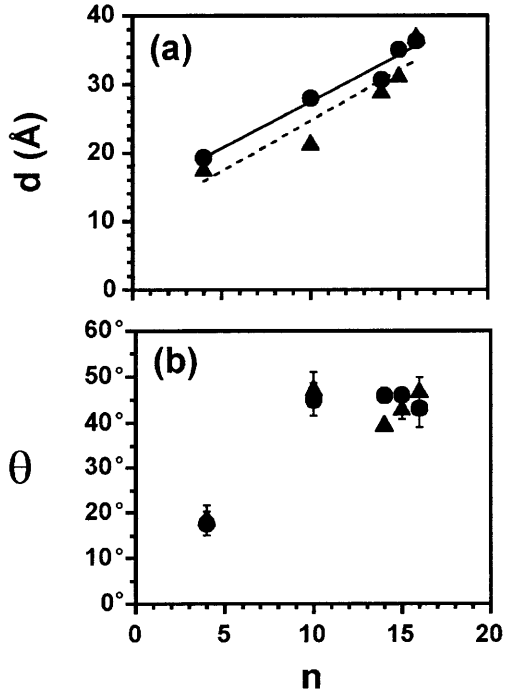

Figure 4-1. Ellipsometric thicknesses and wetting properties of bilayers formed by self-assembly of long-chained amides ($CH_3(CH_2)_nCONH_2$) onto amide-terminated SAMs on gold ($Au/S(CH_2)_mCONH_2$) when m = 10 (▲) and m = 11 (●). (a) Ellipsometric thicknesses of the bilayers. The lines are least-squares fits to the data. (b) Contact angles of decahydronaphthalene on the bilayers. Each point represents the average value obtained on a slide.

4.2.3. IR Spectra of the Amide-terminated SAMs and Bilayers

Figures 4-2 and 4-3 show the spectra of amide-terminated SAMs ($Au/S(CH_2)_mCONH_2$; m =10, 11) before and after exposure to a stearamide ($CH_3(CH2)_{16}CONH_2$) solution in DHN. The spectra of $CONH_2$-terminated monolayers were in agreement with the literature (lower spectra in each panel of Fig 4-2 and Fig 4-3)[4] and the assignments of the peaks on the spectra are shown in Table 4-1. The asymmetric and symmetric CH_2 C-H stretching vibrations (d^- and d^+) of the SAMs are averaged at ~2919 and ~2851 cm^{-1}, respectively, indicating that the hydrocarbon chains in the films are highly organized and mostly trans-zig-zag extended.[13] The intensities of both CH_2 C–H stretching bands at m = 11 are approximately 10 percent stronger than those at m = 10, which parallels one methylene difference between two systems. The dichroic ratios (d^-/d^+ in intensities), related to the twist of hydrocarbon chains within a monolayer,[14] of both systems are the same. These observations, therefore, suggest that hydrocarbon chains within both $CONH_2$-terminated SAMs have the same orientations. A noticeable feature in the IR spectra of the SAMs is the N-H stretching mode that displays a different pattern in the spectra of the KBr matrices.[4] Two broad bands at ~3400 and ~3200 cm^{-1} appear in the spectra obtained from the KBr matrix samples, while the $CONH_2$-terminated SAMs show only a sharp band at ~3500 cm^{-1}. The two broad bands at ~3400 and 3200 cm^{-1} are ascribed to the asymmetric and symmetric N-H stretching modes resulting from the formation of amide-to-amide hydrogen bonding. The sharp peak at ~3500 cm^{-1} in the spectra of $CONH_2$-terminated SAMs is assigned as probably the antisymmetric stretching mode of the N-H stretching of the free NH_2.[4,15] The spectral intensity of the free N-H stretching band is 1.4 times stronger when m = 11 than that when m = 10 suggesting that the collective orientation of free N-H bonds of terminal amides is more normal to the surface when m = 11.[16] In contrast, the band assigned for the C=O stretching mode that

centered at ~1667 cm^{-1} was approximately 10 percent stronger when m = 10 than when m = 11. These differences in spectral intensities of N-H stretching and C=O stretching modes may result from the different orientations of terminal $CONH_2$ groups since the fixed Au-S-CH_2 valence angle forces the chains into the same absolute orientation under assumption that the hydrocarbon chains within the films are crystalline leading the orientation of terminal $CONH_2$ groups to modulate with m;[17] however, no significant influence of this modulation on their macroscopic wetting properties was observed as discussed. After formation of bilayers, the intensities of two CH_2 C–H stretching bands (d^+ and d^-) at ~2919 and ~2851 cm^{-1} increased with the appearances of two peaks at 2965 and 2879 cm^{-1} attributed to the asymmetric and symmetric CH_3 C–H stretching modes (Figure 4-2). The intensity of CH_2 C-H scissors deformation band at ~1470 cm^{-1} also increased after the immersion (Figure 4-3). The intensity of two CH_2 C–H stretching modes increased as the chain length of adsorbing amides increased. The IR spectra of bilayers exhibit other notable features that provide information for the adsorption chemistry. For example, after the formation of an adsorbed monolayer from stearamide, the band at ~3498 cm^{-1} assigned as a free N-H stretching disappeared and two bands at ~3400 and ~3200 cm^{-1}, assigned as asymmetric and symmetric hydrogen-boned N-H stretching vibrations, appeared.[15] This result strongly suggests that the formation of bilayers involves head-to-head hydrogen bonding between the terminal amides of adsorbates and SAMs, not physisorption of long-chained amides onto the SAM surface. The C=O stretching band at ~1667 cm^{-1} and N-H deformation band at 1610 cm^{-1} shifted to ~1659 and 1626 cm^{-1}, respectively, after the formation of an adlayer. These shifted positions are close to the values for the solid-state hydrogen-bonded *n*-alkylamide.[15]

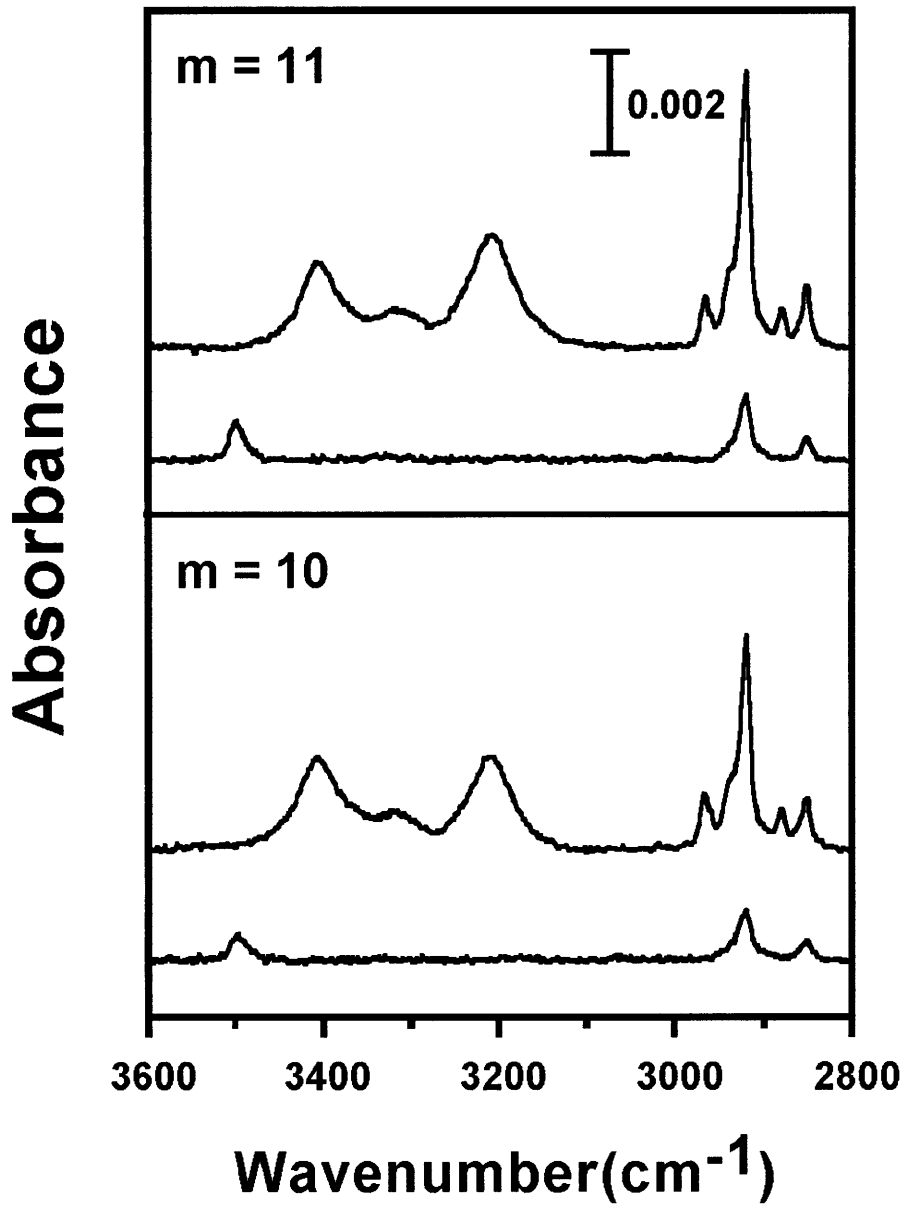

Figure 4-2. RAIRS spectra in the high frequency region for amide-terminated SAMs ($Au/S(CH_2)_mCONH_2$) before (bottom spectra in each panel) and after (top spectra in each panel) exposure to a dilute DHN solution of stearamide ($CH_3(CH_2)_{16}CONH_2$).

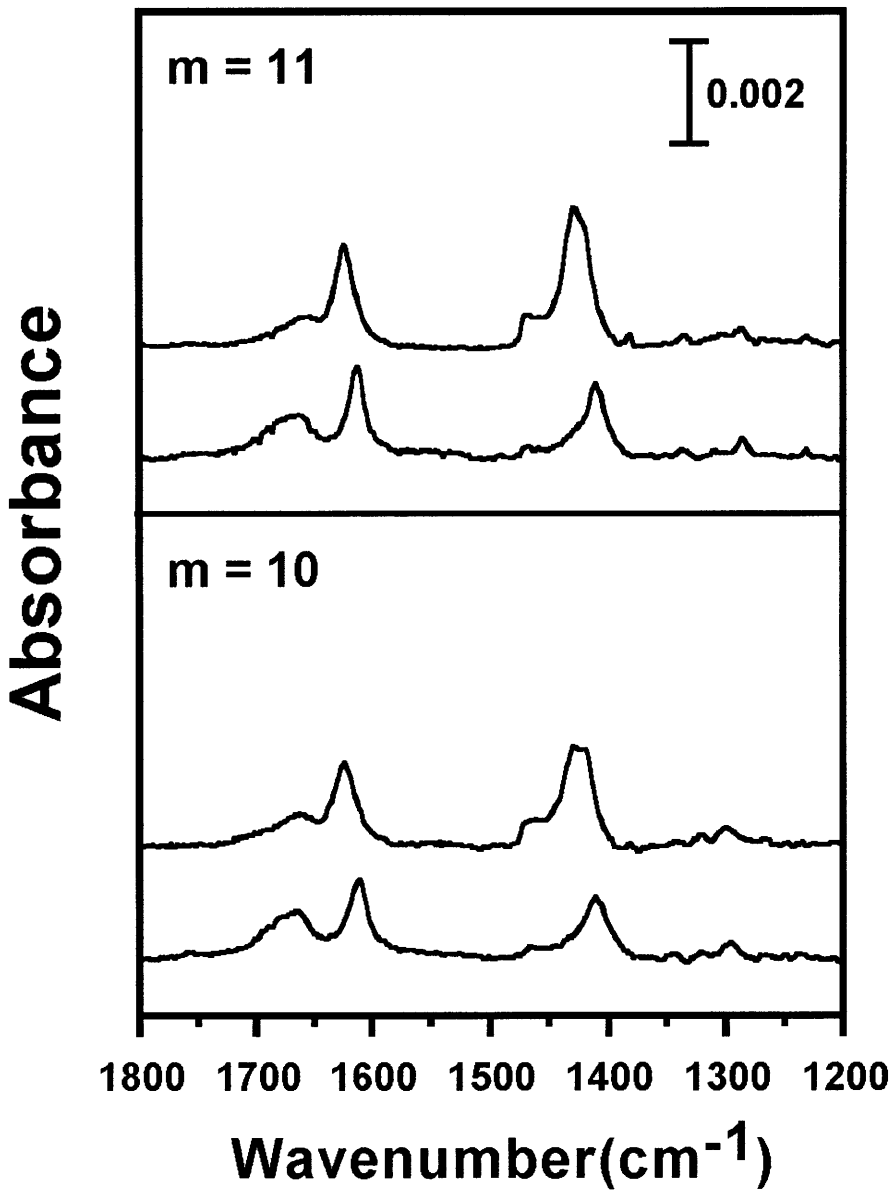

Figure 4-3. RAIRS spectra in the low frequency region for amide-terminated SAMs ($Au/S(CH_2)_mCONH_2$) before (bottom spectra in each panel) and after (top spectra in each panel) exposure to a dilute DHN solution of stearamide ($CH_3(CH_2)_{16}CONH_2$).

Table 4-1. Spectral mode assignments and peak positions (cm^{-1}) for amide-substituted SAMs ($Au/S(CH_2)_mCONH_2$) before and after exposure to a dilute DHN solution of stearamide.

Mode Assignment	Before	After
N-H str (free) [a]	~3499	
N-H str (H-bonded, asym) [b]		~3401
N-H str (H-bonded, sym) [b]		~3205
C-H str (CH_3, asym), r^- [c]		~2965
C-H str (CH_2, asym), d^- [c]	~2919	~2919
C-H str (CH_3, asym), r^+ [c]		~2879
C-H str (CH_2, asym), d^+ [c]	~2851	~2851
C=O str [d]	~1667	~1659
NH_2 def [d]	~1610	~1626

[a] This peak may come from the N-H stretch of the free NH_2 group (refs 4,15,18).
[b] These frequencies fit the general pattern for alkylamides in the solid state (ref 15).
[c] Ref. 13.
[d] These bands correspond to the amide I band (C=O str) and the amide II band (NH_2 bend) (see ref 15).

4.2.4. Structure of Adlayers

The structure of the adlayers was investigated using the RAIRS spectra and the methodology to calculate cant (α) and twist (β) for the adlayers is described in detail in the previous chapter. To examine their structure, the difference spectra that only contain the spectral information of the adlayers were obtained by subtracting the spectra of the underlying amide-terminated SAMs from those of bilayers (Figure 4-4). When $n \geq 10$, the d^- and d^+ CH_2 C–H stretching modes appear at ~2919 and ~2851 cm^{-1}, respectively, indicating all-trans conformation for the alkyl chains and presence of few gauche defects within the SAMs,[16] while the r^- and r^+ CH_3 C-H stretching modes appear at ~2965 and ~2879 cm^{-1}, respectively. As noted in the previous chapter, the intensity ratio between the asymmetric and symmetric methylene stretching modes, I (d^-, CH_2)/I (d^+, CH_2), upon the formation of the adlayer on a SAM. The ratio for the $CONH_2$-terminated SAMs was ~2.5. In contrast, the ratio increased to ~7.5 upon adsorption of amides onto $CONH_2$-terminated SAMs. We calculated twist angles (β) = ~66° for the adlayers by relating these ratios to twist angles (β) with eq 3-1 and obtained cant angles (α) = ~30° using the procedure described in section 3.3.6. Notably, the cant angles for the adlayers is similar to those

for their underlying SAMs[4] and this result suggests that the adlayers and their underlying SAMs have similar packing densities possibly due to the complete one-to-one hydrogen bonding between amide groups of adlayers and underlying SAMs.

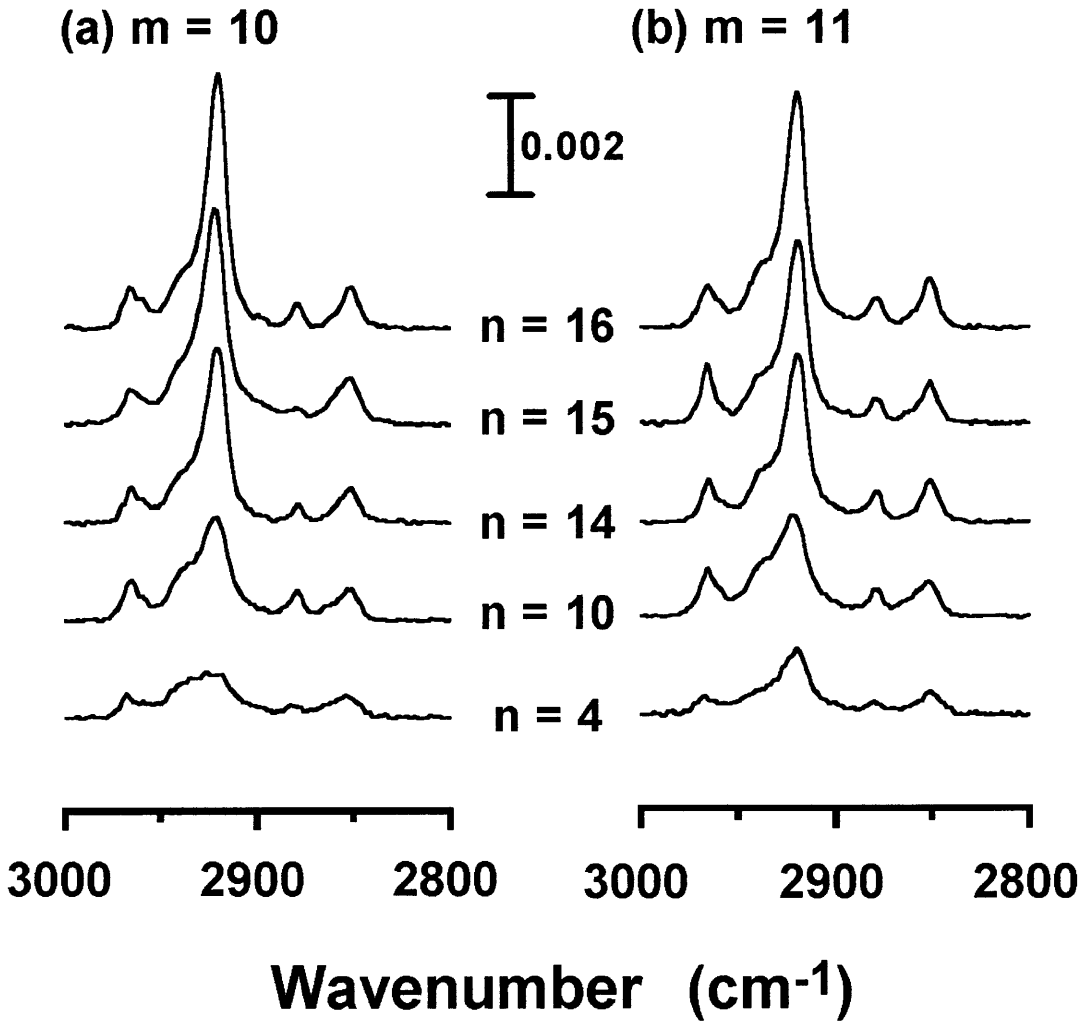

Figure 4-4. Difference infrared spectra for adlayers of n-alkyl amides ($CH_3(CH_2)_nCONH_2$) formed on amide-terminated SAMs ($Au/S(CH_2)_mCONH_2$). Spectra were obtained by referencing spectra for the bilayers to those for $Au/S(CH_2)_mCONH_2$.

Figure 4-4 shows the two sets of difference spectra for m = 10 and 11 and they exhibited similar patterns. The peak intensities of CH_2 C–H stretching modes (d^+ and d^-), which reflect the orientation of hydrocarbon chains within the adlayers,[16] did not show any significant effects from odd-even variations (10 and 11) of m and this observation parallels the similar wetting properties of both systems. The spectra of CH_3 C–H stretching modes (r^- and r^+) for both odd and even values of n do not differ significantly in comparison to those of amine adlayers in Chapter 3. This observation is especially notable considering that the hydrocarbon chains within the films possess the same orientations.[17] It can be inferred that the result originates from a significant degree of reorganization of the methyl surface. Chapman and Tabor investigated the self-assembled films of long-chain amines and acids using electron diffraction methods.[19] They discovered that the chain-to-chain distance within films is larger in acid adlayers than in amine adlayers and they ascribed the difference to the different sizes of adsorbing moieties (acid vs. amine). Since the adsorption chemistry in these amide adlayers relies on head-to-head hydrogen bonding, the size of amide groups is even larger than the adsorbed acids onto glass surfaces in Chapman and Tabor's work. Therefore, the resulting larger distance between alkyl chains seems to provide an opportunity for the reorganization of the methyl surface, which induced the similar patterns of methyl stretching bands.

4.3. Conclusions

This chapter demonstrated formation of the monolayers of *n*-alkyl amides on amide-terminated SAMs. The experimental results indicate that the formation of assemblies is driven by head-to-head hydrogen bonding interactions and the assemblies have highly organized structures as densely packed as alkanethiolate SAMs on gold. No significant effects of the odd-even

variation of chain length of the amide-terminated SAMs on the macroscopic properties and structure of the amide adlayers was observed possibly due to the formation of laterally hydrogen-bonded networks of terminal amides.

4.4. Experimental

Hexanoamide and octadecanamide were obtained from Aldrich (Milwaukee, WI) and Fluka (Ronkonkoma, NY), respectively, and used without further purification unless otherwise specified. Mercaptoalkanamides ($HS(CH_2)_mCONH_2$; m = 10 and 11), dodecanamide, hexadecanamide, and heptadecanamide were synthesized according to literature procedures.[5,12] The preparation of SAMs and adlayers on the SAMs and their characterization by infrared spectroscopy, ellipsometry, and wetting were detailed in Chapter 2 and will not be repeated here.

4.5. References

(1) Thomas, R. C.; Houston, J. E.; Crooks, R. M.; Kim, T.; Michalske, T. A. *J. Am. Chem. Soc.* **1995**, *117*, 3830-3834.

(2) Smith, E. L.; Alves, C. A.; Anderegg, J. W.; Porter, M. D.; Siperko, L. M. *Langmuir* **1992**, *8*, 2707.

(3) Sun, L.; Kepley, L. J.; Crooks, R. M. *Langmiur* **1992**, *8*, 2101-2103.

(4) Nuzzo, R. G.; Dubois, L. H.; Allara, D. L. *J. Am. Chem. Soc.* **1990**, *112*, 558-569.

(5) Green, J.-B. D.; Mcdermott, M. T.; Porter, M. D.; Siperko, L. M. *J. Phys. Chem.* **1995**, *99*, 10960-10965.

(6) Bigelow, W. C.; Pickett, D. L.; Zisman, W. A. *J. Colloid Sci.* **1946**, *1*, 513-538.

(7) Vinogradov, S. N.; Linnell, R. H. *Hydrogen Bonding*; Van Nostrand Reinhold Company: New York, 1971.

(8) Laibinis, P. E.; Whitesides, G. M. *J. Am. Chem. Soc.* **1992**, *114*, 1990-1995.

(9) Porter, M. D.; Bright, T. B.; Allara, D. L.; Chidsey, C. E. D. *J. Am. Chem. Soc.* **1987**, *109*, 3559-3568.

(10) Bain, C. D.; Troughton, E. B.; Tao, Y.-T.; Evall, J.; Whitesides, G. M.; Nuzzo, R. G. *J. Am. Chem. Soc.* **1989**, *111*, 321-335.

(11) Bewig, K. W.; Zisman, W. A. *J. Phys. Chem.* **1963**, *67*, 130-135.

(12) Allara, D. L.; Nuzzo, R. G. *Langmuir* **1985**, *1*, 45-52.

(13) Snyder, R. G.; Hsu, S. L.; Krimm, S. *Spectrochimica Acta* **1978**, *34A*, 395-406.

(14) Sinniah, K.; Cheng, J.; Terrettaz, S.; Reutt-Robey, J. E.; Miller, C. J. *J. Phys. Chem.* **1995**, *99*, 14500-14505.

(15) Bellamy, L. J. *The Infrared Spectra of Complex Molecules*; 3rd ed.; Chapman & Hall: London, 1975.

(16) Allara, D. L.; Nuzzo, R. G. *Langmuir* **1985**, *1*, 52-66.

(17) Laibinis, P. E.; Whitesides, G. M.; Allara, D. L.; Tao, Y.-T.; Parikh, A. N.; Nuzzo, R. G. *J. Am. Chem. Soc.* **1991**, *113*, 7152-7167.

(18) Carson, G. A.; Granick, S. *J. Mater. Res.* **1990**, *5*, 1745-1751.

(19) Chapman, J. A.; Tabor, D. *Proc. Roy. Soc. A* **1957**, *242*, 96-107.

Chapter 5

Directed Movement of Liquids on Patterned Surfaces Using Non-Covalent Molecular Adsorption

5.1. Introduction

Pressure gradients provided by pumps or external forces govern the flow characteristics of fluids within many pipes and other conduits.[1] For microfluidic systems, the description of liquid flows becomes complicated due to the presence of capillary forces that can affect the controlled delivery of small volumes of liquids within microelectromechanical systems (MEMS) or to different unit operations within a microreactor network.[2] As an alternative to the use of macroscale methods for delivering liquids within microscale systems, the transport of liquids can be driven on surfaces by a gradient in wettability, even against the force of gravity.[3-5] These gradients can be generated passively using surfaces with spatial variations in free energy or actively using surfactant-like agents that adsorb on one side of a drop and produce a less-wettable or lower energy surface that induces a localized dewetting by the liquid (Figure 5-1). This latter topic has been the subject of recent theoretical studies;[6-9] however, complementary experimental studies are lacking due to difficulties in controlling the direction of drop movement and modulating the responsible surface interactions. Previous examples of adsorption-driven drop movement include

those based on the irreversible attachment of adsorbates to a substrate.[10] Such systems are single-use and unable to transport more than one drop on their surface as the reacted surface does not allow further adsorption by a subsequent adsorbate. Surfaces with fixed spatial gradients in wettability offer an alternative for directing liquid movement. These systems are reusable but are limited by hysteresis effects to the delivery of liquids over short distances. The procedure detailed here overcomes the limitations of the present systems and provides a new direction for both fundamental and practical studies of surface-mediated drop movement.

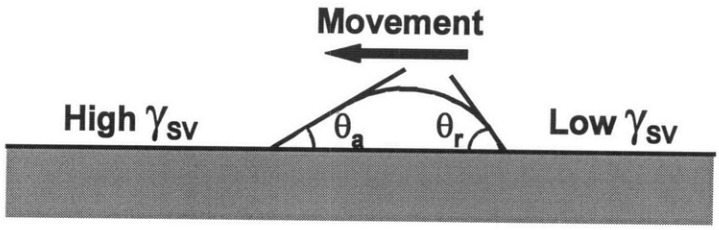

Figure 5-1. Schematic cross-sectional view of a moving drop. The drop moves due to the asymmetric adsorption of a surfactant-like adsorbate at one side of the droplet to produce a less wettable surface.

5.2. Results and Discussion

5.2.1. Preparation of Samples

The adsorption of alkylamine onto a high energy CO_2H-surface produced the energetic driving force for drop movement. To direct the liquid movement using the change in surface energy, we employed microcontact printing (μCP) to pattern solid substrates with two different self-assembled monolayers (SAMs):[11] CO_2H-terminated SAM to define the path of movement and a CH_3-terminated SAM to define the boundaries of the path. Figure 5-2 illustrates the procedure used to generate the patterned surfaces. The stamp was fabricated by casting

poly(dimethylsiloxane) (PDMS) on a photolithographically-prepared master with the desired features (2 × 60 mm^2 rectangular tracks). The PDMS stamp was "inked" with a 5 mM ethanolic solution of octadecanethiol ($CH_3(CH_2)_{17}SH$), and the thiol was transferred to specified areas of the gold surface by contacting the stamp with the gold surface. The remaining areas of the surface were derivatized by immersing the slide in a 5 mM ethanolic solution of 16-mercaptohexadecanoic acid ($HS(CH_2)_{15}CO_2H$) to complete formation of 2 × 60 mm^2 CO_2H-terminated tracks surrounded by a low energy CH_3-terminated surface.

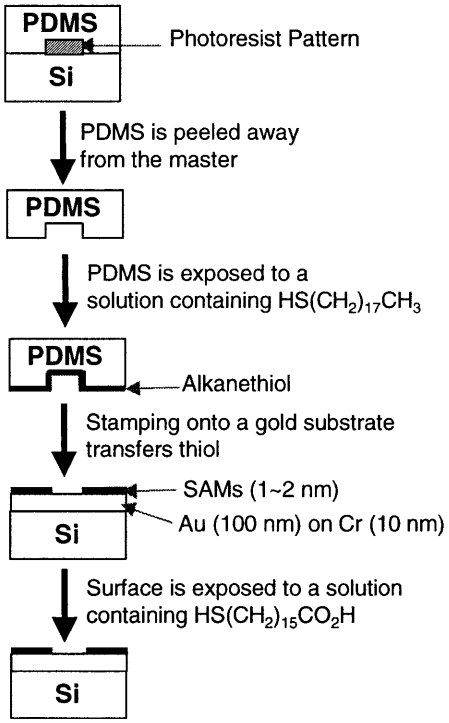

Figure 5-2. Procedure for preparing the patterned elastomeric stamp and patterned surface.

5.2.2. Surface Energy Effect

When a 1 μL drop of decahydronaphthalene (DHN) containing 1 mM of n-alkylamine ($CH_3(CH_2)_{n-1}NH_2$ or C_nNH_2) was applied to a track terminus at the boundary of the CO_2H and

CH_3 regions, the DHN drop spontaneously moved along the length of the track as a discrete object (Figure 5-3) and left behind an oriented monolayer of the alkylamine. Complementary experiments using reflectance infrared spectroscopy indicated that the adsorption of the amine layer onto the CO_2H-surface results from acid-base interactions and forms a densely-packed molecular film that exposes methyl groups at its surface.* The adsorption process responsible for drop movement worked best with nonpolar liquids, and the dewetting process that drives the drop movement required that the surface tension of the liquid be greater than ~ 30 mN/m.

DHN drops containing longer-chained alkylamines moved at faster velocities on the CO_2H-surfaces than those containing shorter-chained alkylamines (Figure 5-3). The resulting non-covalently adsorbed amine layers produced by self-assembly could be removed simply by rinsing the substrate with a polar solvent such as ethanol or water. This process could regenerate the original patterned CO_2H/CH_3 surfaces and allowed the delivery of additional drops. The non-covalent nature of the interaction between the adsorbed alkylamines and the CO_2H surface also allowed a deposited amine adlayer to be replaced by simply exposing it to a solution of a second longer-chained alkylamine. For example, when an adlayer on a CO_2H surface derived from C_6NH_2 was immersed into a 1 mM DHN solution of $C_{18}NH_2$, the ellipsometric thickness, wetting properties, and infrared spectra of the resulting film were the same as for the direct assembly of a layer of $C_{18}NH_2$ on a CO_2H surface. The replacement of the adsorbed amines occurred within seconds of contact with the $C_{18}NH_2$ solution and produced a lower energy, more oleophobic surface. The concurrent changes in surface energy provided the basis for achieving a previously unrealized ability to sequentially deliver two and more drops across a surface. For example, on the patterned substrate, the placement of a drop of 1 mM C_6NH_2 in DHN at one end of a track

* We note that non-covalent interactions between other functional group pairs such as $CONH_2$-$CONH_2$ and CO_2H-$CONH_2$ also produce drop movement.

resulted in its movement over the track and the deposition of a C_6NH_2 layer as in Figure 5-3. Placement of a $C_{18}NH_2$ drop at one end of this C_6NH_2-derivatized track resulted in the movement of this second drop along the same path as the C_6NH_2 drop and the deposition of an oriented film of $C_{18}NH_2$ in place of the C_6NH_2 adlayer (Figure 5-4). The ability to replace the C_6NH_2 layer and further reduce the surface energy of the track by the adsorption of $C_{18}NH_2$ provided the energetic requirements for this sequential delivery of drops to proceed on the surface. We note that the $C_{18}NH_2$ drop in this two-drop experiment moved with roughly half the velocity of a $C_{18}NH_2$ drop deposited on a bare CO_2H surface.

In these various experiments, the dominant force responsible for the drop movement is the unbalanced Young force, F_Y,[3,12] that results from the difference in wettability or surface energy between the front and back sides of the drop (Figure 5-1):

$$F_Y = \gamma_{LV} (\cos \theta_a - \cos \theta_r) \qquad (6\text{-}1)$$

where γ_{LV} is the surface tension of the liquid,** and θ_a and θ_r are the advancing and receding contact angles for the drop, respectively. As DHN wets CO_2H surfaces, $\theta_a \cong 0°$; therefore, the exerted F_Y directly depends on θ_r when a monomolecular film of the alkylamine is deposited on a bare CO_2H surface. With increasing chain lengths of the alkylamine, θ_r increases in value and effects a greater F_Y on the drop as manifested by an increase in drop velocity with increasing chain length (Figures 5-3 and 5-5). When an amine adlayer replaces another, both θ_a and θ_r must be considered. For example, for the DHN drop containing $C_{18}NH_2$ on the C_6NH_2-derivatized track,

** Dilute concentrations of the alkylamines at ~1 mM do not alter the surface tension of DHN.

$\theta_a \cong 32°$. As a result, F_Y is reduced and the $C_{18}NH_2$-containing drop moves with a lower velocity than when deposited on a bare CO_2H surface (Figure 5-5). Figure 5-5 plots the steady-state velocities for various alkylamine-containing drops of DHN on the CO_2H surface with respect to their values of the quantity, $\cos\theta_a - \cos\theta_r$ (i.e. F_Y/γ_{LV}).

As indicated by the line in Figure 5-5, the velocity appears to be proportional to the difference between $\cos\theta_a$ and $\cos\theta_r$. This observation can be explained by equating the unbalanced Young force of the surface with the drag force on the moving drop:

$$W\gamma_{LV}(\cos\theta_a - \cos\theta_r) = A\mu\frac{v}{h} \tag{5-2}$$

where μ is the viscosity of the liquid, W is the length of contact lines at the front and rear of the drop and is roughly the width of track, A is the contact area between the drop and substrate, and h is a characteristic length that approximates the mean height of the drop as averaged over the drop/substrate contact area with respect to the local drag force. The proportionality constant, $(Wh\gamma_{LV})/(A\mu)$, obtained from Figure 5-5 is ~3 cm/sec, with the value of h being roughly a micrometer suggesting that the drag force is localized primarily near the contact lines.[13,14]

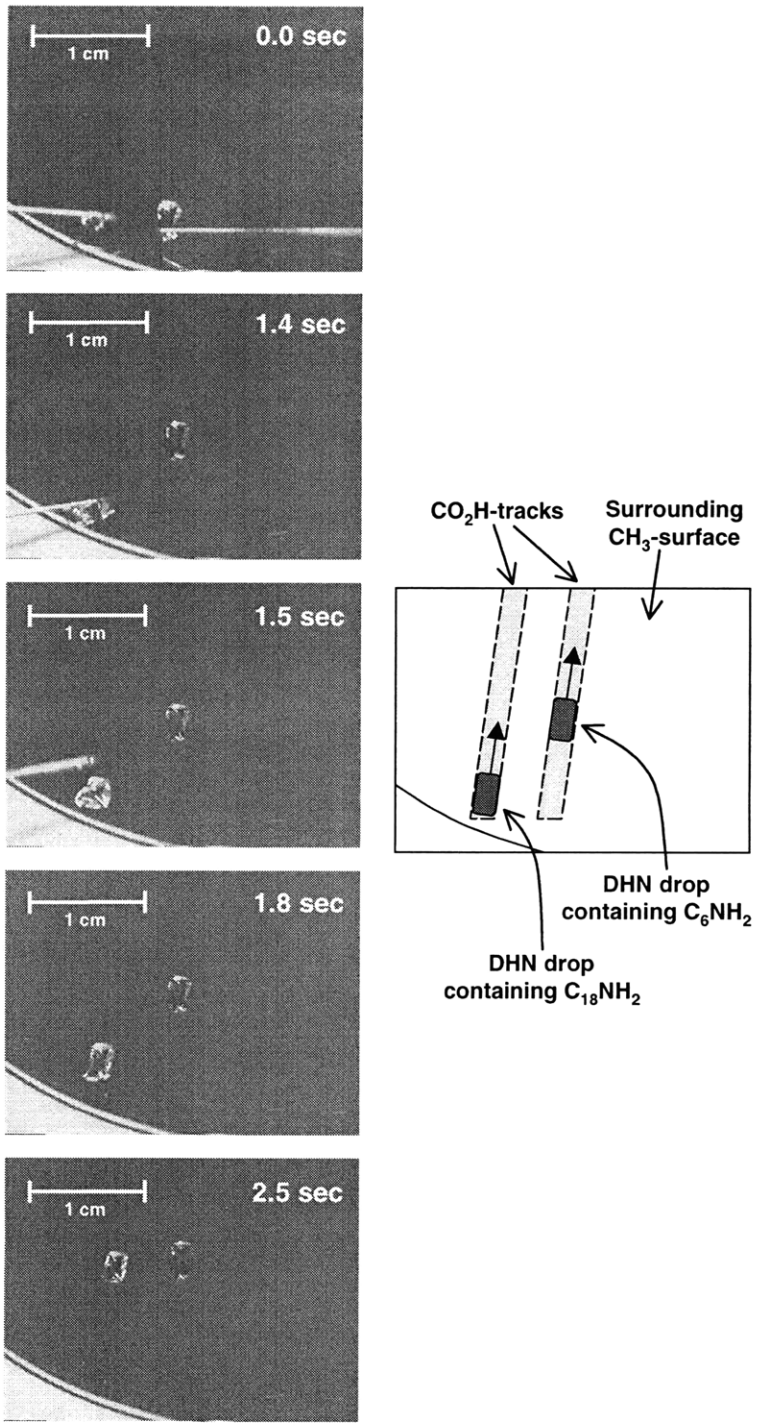

Figure 5-3. Movement of amine-containing DHN drops on a patterned gold surface produced by microcontact printing. The drops containing 1 mM C_6NH_2 (right) and 1 mM $C_{18}NH_2$ (left) were applied on different tracks (2 mm wide and 60 mm long) each expressing CO_2H groups. CH_3-terminated domains surround the tracks and restrict the movement of each drop to a specified path. The $C_{18}NH_2$-containing drop was deposited on the end of the left track ~1.5 s after the C_6NH_2-containing drop began to move. The $C_{18}NH_2$ drop caught up to the slower C_6NH_2-containing drop within ~1.5 s and later passed it.

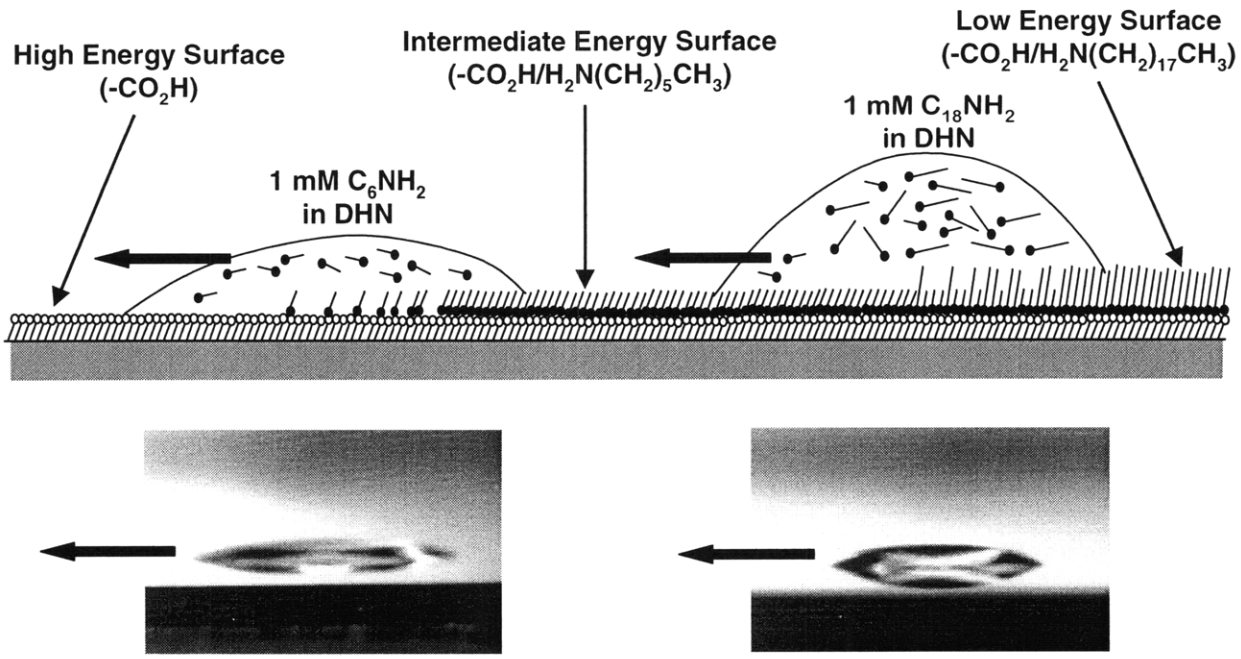

Figure 5-4. Schematic cross-sectional view of the adsorption process that allows sequential movement of Schematic cross-sectional view of the adsorption process that allows sequential movement of decahydronaphthalene (DHN) drops containing 1 mM C_6NH_2 and 1 mM $C_{18}NH_2$, and their corresponding images obtained by a CCD camera. The $C_{18}NH_2$-containing drop moves due to replacement of C_6NH_2 by $C_{18}NH_2$ to produce a lower energy surface. The images contain a reflection due to the gold substrate, and the arrows indicate the direction of motion. The differences in the wetting properties of the two drops are clearly visible in the CCD images.

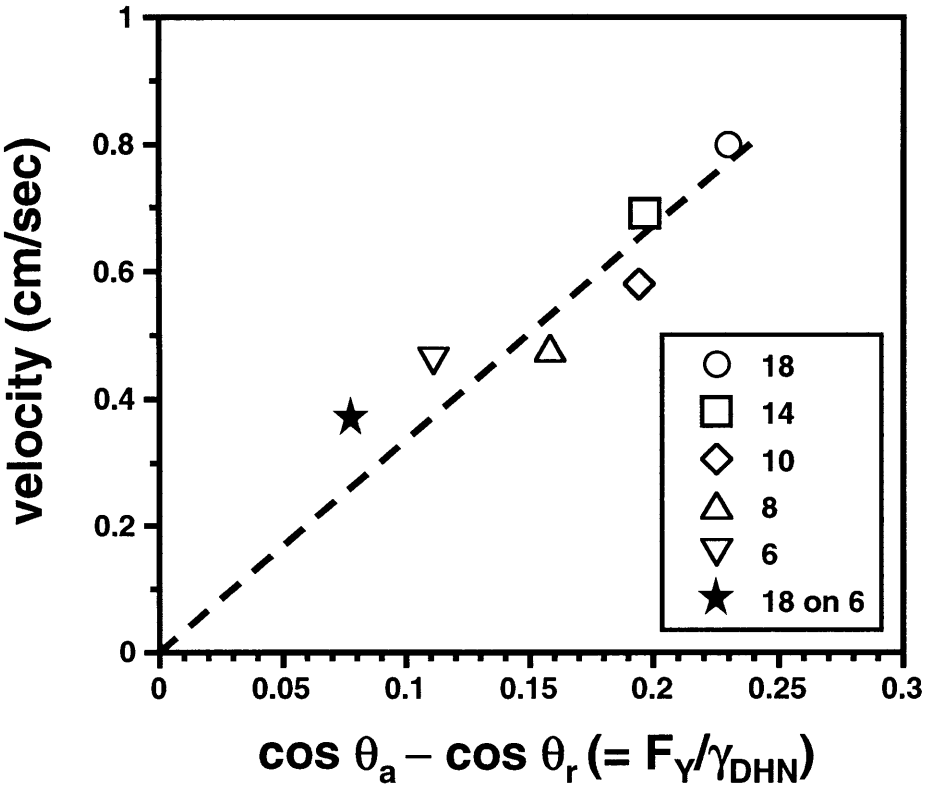

Figure 5-5. The velocity of DHN drops containing various alkylamines (C_nNH_2) on bare CO_2H surfaces (open symbols) and an adsorbed film derived from C_6NH_2 on a CO_2H surface (filled symbol) with respect to ($\cos \theta_a - \cos \theta_r$). The dashed line is a linear fit to the data.

5.2.3. Concentration Effect

In Figure 5-6, the velocities of ~1 microliter moving drops of DHN are plotted against the concentration of octadecylamine within the drops. The velocities exhibit roughly linear increase rapidly with concentration to 0.5 mM and have roughly a constant value at concentration greater than ~2 mM. This dependence of the moving drop velocity against concentration can be the results of different equilibrium adsorptions with assumption that the system reaches equilibrium

very rapidly. This velocity and concentration can be bridged by incorporating an adsorption isotherm into the eq 5-2. First, we rearrange the eq 5-1:

$$v = \frac{W\gamma_{LV}h}{A\mu}(\cos\theta_a - \cos\theta_r) = K_1(\cos\theta_a - \cos\theta_r) = K_1(1 - \cos\theta_r) \tag{5-3}$$

where $K_1 = (Wh\gamma_{LV})/(A\mu)$ and $\theta_a \cong 0°$. The simplified form of the eq 5-3 suggests that the concentration of amines within the moving drop relies mostly on θ_r that can vary with respect to the surface coverage of adsorbed amines in the rear side of the drop. The θ_r is assumed to follow a Cassie–type behavior that describes the contact angle of DHN on the solid substrates consisting of multiple-domains:

$$\cos\theta_r = \sum_i x_i \cos\theta_i = x\cos\theta_{100} + (1-x)\cos\theta_0 = 1 - (1 - \cos\theta_{100})x \tag{5-4}$$

where x is the fractional composition of adsorbed amines, and θ_{100} and θ_0 is the corresponding receding contact angles for full adlayers and bare CO_2H surfaces, respectively. Since DHN wets the CO_2H-surface, θ_0 can be approximated to equal ~0°.

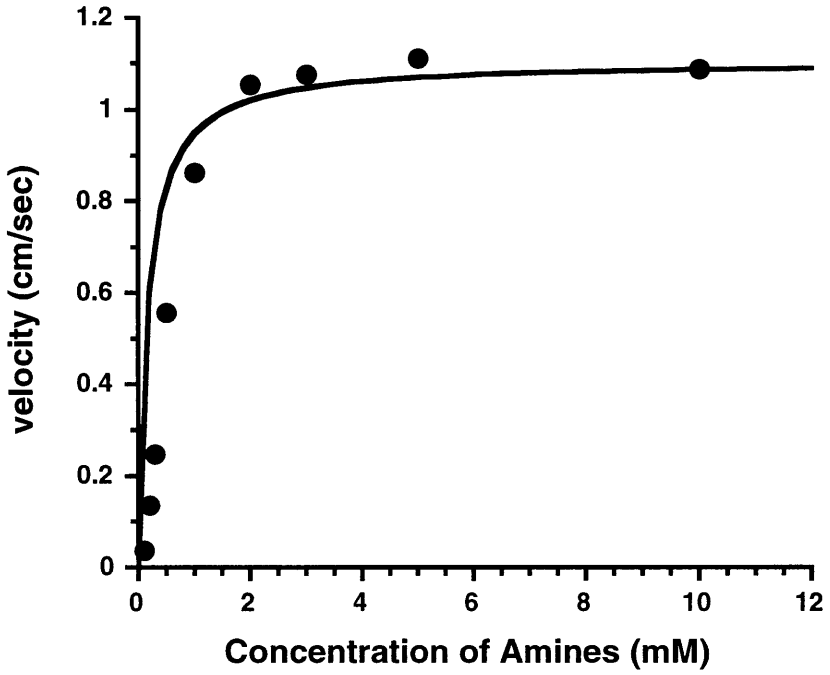

Figure 5-6. Velocity of DHN drops containing various concentrations of octadecylamine ($C_{18}NH_2$) on a CO_2H surface.

Substitution of eq 5-4 into eq 5-3 yields:

$$v = K_1(1 - \cos\theta_{100})x \tag{5-5}$$

The fractional composition in eq 5-5 can be related to the concentration of amine in the drop by an appropriate adsorption isotherm. We employed a Langmuir adsorption isotherm not only because of its simplicity but also because of its applicability to this system considering its assumptions. The model assumes that adsorption is restricted to monolayer coverage (alkylamines form a monomolecular film on a SAM surface, as shown in Chapter 3), that specific adsorption

sites exist and interactions are between the site and a specific adsorbate (as noted in Chapter 3, the adsorption process relies on the specific acid-base interactions between CO_2H and NH_2), and that the heat of adsorption is independent of the amount of material adsorbed. The last assumption strictly may not apply to this system; however, it can be tolerated with a hypothesis that the head group interaction is a dominant factor in the adsorption process, as shown in Chapter 2 that demonstrated the influence of head group combinations on the formation of adlayers. The Langmuir approach is based on a molecular kinetic model where the rates of adsorption and desorption will be equal at equilibrium:

$$x = \frac{Kc}{1+Kc} \tag{5-6}$$

where K is the adsorption coefficient or equilibrium constant (the ratio of the adsorption and desorption rate constants) and c is the concentration of alkylamines in the contacting DHN drop. Combining eqs 5-5 and 5-6 yields:

$$v = K_1(1-\cos\theta_{100})\frac{Kc}{1+Kc} \tag{5-7}$$

Eq 5-7 gives the limiting velocity at high concentrations of the amine as $K_1(1-\cos\theta_{100})$. If we insert the numbers for K_1 (= ~3 cm/sec) and θ_{100} (= ~41°) in $K_1(1-\cos\theta_{100})$, the calculated limiting velocity becomes roughly 1 cm/sec, which is close to the velocity we observed as shown in Figure 5-6. The curve fit with the data yields ~6 mM^{-1} for K.

5.2.4. Drop Length Effect

Figure 5-7 shows the velocity of various moving drops containing octadecylamine ($C_{18}NH_2$) against their length. The drop length was proportional to the volume of the deposited drops in the range of our study. We observed that the velocity of the drop exhibits a decrease as its length increases. This observation can be also explained with the idea behind eq 5-2. As drop length increases, the contact area at a drop/substrate interface increases and causes an increased drag force on the drop. In contrast, the driving force (unbalanced Young force) remains constant due to the unchanged length of the contact lines at the front and back sides of the drop.

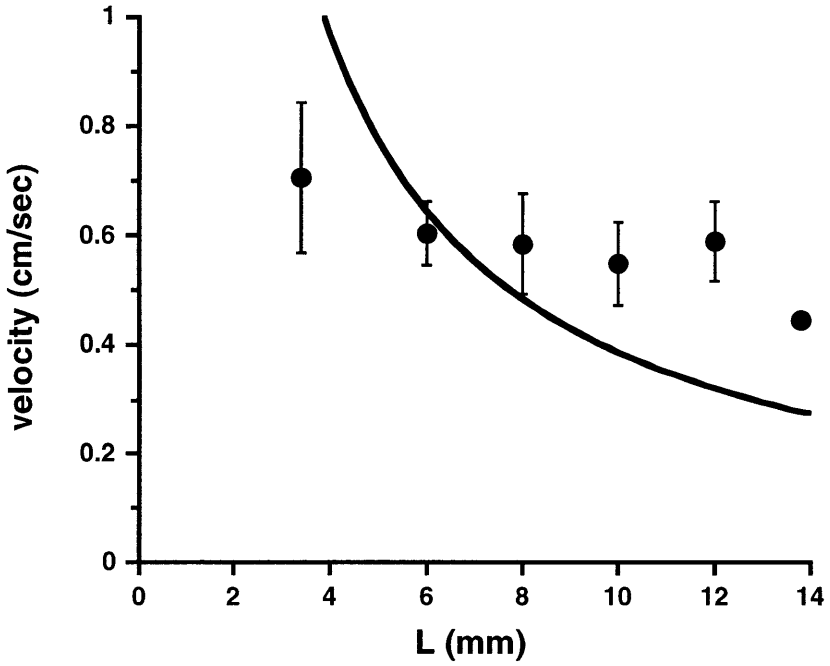

Figure 5-7. Velocity of DHN drops containing 1 mM octadecylamine as a function of drop length. The solid curve is a fit to the data using eq 5-8.

If the length of the contact lines at the front and rear sides of the drop is approximated to roughly equal the track width, eq 5-1 can be simplified:

$$v = \frac{W\gamma_{LV}h}{A\mu}(\cos\theta_a - \cos\theta_r) = \frac{\gamma_{LV}h}{\mu}(\cos\theta_a - \cos\theta_r)\frac{1}{L} \tag{5-8}$$

where L is the length of drops. Eq 5-8 suggests an inverse relationship of velocity and length of drops. Using the value of h that was determined using eq 5-2, the constant (= L × v) was calculated to be ~35 mm^2/sec that roughly equals the curve-fit value (~39 mm^2/sec), though the model (eq 5-8) does not match the data well. However, it is worth noting that this model provides a prediction of the trend in velocity with respect to the geometry of drops.

5.3. Conclusions

The present work demonstrates that liquid drops can be delivered laterally along specified paths using solid substrates with patterned surfaces and a driving force for motion based on molecular adsorption. The velocity of the drops on these surfaces can be manipulated by selection of the molecular structure of the incorporated adsorbate. A particular feature of the detailed adsorption chemistry is its reliance on a non-covalent adlayer that can allow the sequential transport of two drops along a common specified path and the ability to regenerate the active surface for further use. Using the system, the effects of adsorbate chain length, adsorbate concentration, and drop length were examined and the appropriate models were presented to explain our observations. The strategies used here should be amenable to the design of three-dimensional systems, where adsorption processes onto the functionalized walls of a channel would

cause spontaneous liquid movement. Such systems would offer a new strategy for the design of microdevices that must deliver small volumes of chemical reagents or analytes within their channeled networks.

5.4. Experimental

5.4.1. Materials

Silicon wafers were test grade and obtained from Silicon Sense (Nashua, NH). Gold shot (99.99 %) and chromium-coated tungsten filaments were obtained from Americana Precious Metals (East Rutherford, NJ) and R. D. Mathis Co. (Long Beach, CA), respectively. Stamps were made of poly(dimethylsiloxane) (PDMS) sold by Dow-Corning (Midland, MI) as SYLGARD Silicon Elastomer-184. Decahydronaphthalene (anhydrous, mixture of cis and trans) and alkylamines were obtained from Aldrich Chemical Co. (Milwaukee, WI). Ethanol (190 proof) was obtained from Pharmco (Weston, MO). Octadecanethiol ($CH_3(CH_2)_{17}SH$) was available from other studies.[15] 16-Mercaptohexadecanoic acid ($HS(CH_2)_{15}CO_2H$) was synthesized according to literature procedures.[16]

5.4.2. Preparation of Substrates

Gold films (~1000 Å) were deposited by thermal evaporation on silicon wafers that had been primed with chromium (~100 Å) to promote adhesion between silicon oxide and gold.

5.4.3. Preparation of Stamps and Formation of Monolayers

Masters for fabrication of the stamps were prepared using conventional photolithography as described elsewhere.[11] The masters with the desired features (negative 2 × 60 mm^2 rectangular

tracks) were placed in a plastic or glass petri dish, and a 10:1 ratio (w:w) mixture of SYLGARD silicone elastomer 184 and SYLGARD silicone elastomer 184 curing agent was poured over them to a thickness of the mixture is 5-10 mm. The mixture was allowed to cure overnight at room temperature or was placed in an oven (~65 °C, 1-3 h) after setting at room temperature for approximately 1 h. After removal from the oven, the cured polymer was allowed to cool to room temperature. Sections of the polymer were cut with a razor blade and then peeled from the master. The peeled sections were washed several times with ethanol and dried with a stream of nitrogen before use as stamps. The PDMS stamp was inked with a 5 mM ethanolic solution of octadecanethiol by directly pouring the solution onto the stamp. After inking, the stamp was placed gently on the gold substrate and removed after approximately 3-5 min. The remaining surface (2 × 60 mm^2 tracks) was derivatized by immersion of the slide in a 5 mM ethanolic solution of 16-mercaptohexadecanoic acid ($HS(CH_2)_{15}CO_2H$) leading to the formation of 2 × 60 mm^2 CO_2H-terminated tracks surrounded by a low energy CH_3-terminated surface. Samples were rinsed with ethanol and deionized water, and blown dry with N_2 before use.

5.4.4. Moving Drop Experiments

Moving drop experiments were performed at atmospheric conditions. Drops were deposited at one end of a track using a microliter syringe. Images of the moving drops were taken using a CCD camera (60 video fields per second) with a microscopic lens, synchronized strobe illumination, and SVHS recorder.

5.5. References

(1) Bird, R. B.; Stewart, W. E.; Lightfoot, E. N. *Transport Phenomena*; John Wiley & Sons: New York, 1960.

(2) Adamson, A. W.; Gast, A. P. *Physical Chemistry of Surfaces, 6th Ed.*; John Wiley & Sons, Inc.: New York, 1997.

(3) Chaudhury, M. K.; Whitesides, G. M. *Science* **1992**, *256*, 1539-1541.

(4) Bain, C. D.; Burnett-Hall, G. D.; Montgomerie, R. R. *Nature* **1994**, *372*, 414-415.

(5) Gallardo, B. S.; Gupta, V. K.; Eagerton, F. D.; Jong, L. I.; Craig, V. S.; Shah, R. R.; Abbott, N. L. *Science* **1999**, *283*, 57-60.

(6) Brochard-Wyart, F.; de Gennes, P.-G. *C. R. Acad. Sci. (Paris) II B* **1995**, *321*, 285-288.

(7) Shanahan, M. E. R.; de Gennes, P.-G. *C. R. Acad. Sci. (Paris) II B* **1997**, *324*, 261-268.

(8) De Gennes, P.-G. *Europhys. Lett.* **1997**, *39*, 407-412.

(9) De Gennes, P.-G. *PHYSICA A* **1998**, *249*, 196-205.

(10) Dos Santos, F. D.; Ondarçuhu, T. *Phys. Rev. Lett.* **1995**, *75*, 2972-2975.

(11) Xia, Y.; Whitesides, G. M. *Annu. Rev. Mater. Sci.* **1998**, *28*, 153-184.

(12) Haidara, H.; Vonna, L.; Schultz, J. *J. Chem. Phys.* **1997**, *107*, 630-637.

(13) Brochard-Wyart, F.; de Gennes, P.-G. *Adv. Colloid Interface Sci.* **1992**, *39*, 1-11.

(14) Schiaffino, S.; Sonin, A. A. *Phys. Fluids* **1997**, *9*, 2227-2233.

(15) Jennings, G. K.; Laibinis, P. E. *J. Am. Chem. Soc.* **1997**, *119*, 5208-5214.

(16) Bain, C. D.; Troughton, E. B.; Tao, Y.-T.; Evall, J.; Whitesides, G. M.; Nuzzo, R. G. *J. Am. Chem. Soc.* **1989**, *111*, 321-335.

Chapter 6

Protein Resistant Coatings for Glass and Metal Oxide Surfaces Derived from Oligo(ethylene glycol)-terminated Alkyltrichlorosilanes

6.1. Introduction

The non-specific adsorption of proteins and other biomolecules onto surfaces is a problem common to biomedical devices, biochemical processing, and biodiagnostics.[1,2] This problem is particularly acute for objects made of metal or glass as proteins and other species will often adsorb in multilayer quantities onto their corresponding metal oxide surfaces by electrostatic attraction.[3] Common methods to retard the adsorption include the use of alkyltrichlorosilanes (typically *n*-$C_{18}H_{37}SiCl_3$) to passivate the glass or metal oxide surface with a covalent hydrocarbon film[4] or the attachment or grafting of poly(ethylene glycol) to the surface.[5-7] In the former approach, molecular films from the silane are prepared on the high-energy oxide surface to produce a low energy, hydrophobic surface.[8-10] The attached hydrocarbon chains reduce the non-specific adsorption of proteins by screening the electrostatic attraction between the underlying material and charged biomolecules such as proteins; however, the hydrophobic surface—by nature of

having a relatively high interfacial free energy ($\gamma_{SL} \approx 50$ mN/m) when contacted with water—will routinely adsorb roughly a monolayer of protein.

Surface-bound poly(ethylene glycol) (PEG) is a common strategy for retarding the non-specific adsorption of proteins and other biological species.[11] Methods for covalently attaching PEG to surfaces include the incorporation of PEG monomers into polymer networks by graft polymerization[12-18] and the direct attachment of PEG chains to surfaces by various coupling reactions.[11] In graft polymerization, the PEG chains are incorporated as segments of a polymer backbone, and the incorporated PEGs can have limited effect on non-specific adsorption depending on the surface density of the PEG chains.[19,20] The direct attachment of PEG chains to the surface provides a superior method for manipulating surface properties; however, multiple processing steps are often required for coupling the PEG molecules to the substrate.[21,22] For inorganic substrates, silane reagents are often used to present reactive organic moieties (amines, epoxides, isocyanates, etc.) that provide sites for the covalent attachment of PEG chains. In these procedures, the molecules used for attaching PEG chains to these sites frequently include a variety of specialty PEG derivatives[23]—PEG-monoacrylates, PEG-NH_2, PEG-CHO, CH_3O-PEG, PEG epoxides, star-PEGs, etc.—whose availability and cost can limit the utility of this approach. For these procedures, the effectiveness of the resulting coated surface is related to the surface density of PEG chains as uncoated regions that expose the underlying material often provide sites that undergo non-specific protein adsorption.[24] Objects with complex morphologies offer particular challenges for this method of surface modification due to difficulties in producing uniform, defect-free coatings of PEG. Molecular precursors, such as analogs of $CH_3(CH_2)_{17}SiCl_3$ that produce densely packed

films spontaneously onto surfaces from solution with high uniformity of coverage,[10] could offer distinct advantages over present methods if they exposed a PEG-type surface that retarded the non-specific adsorption of proteins.

To address this problem of surface modification, two new reagents were developed that combine the protocol of use of the trichlorosilane-based adsorbates with the generation of oligo(ethylene glycol)-based surfaces to generate robust coatings for glass and metal oxide substrates that are resistant against the non-specific adsorption of various proteins. These reagents are based on the results of Prime and Whitesides who demonstrated the effectiveness of films formed by the adsorption of $HS(CH_2)_{11}(OCH_2CH_2)_nOR$ (R = H and n = 0, 1, 2, 4, and 6; R = CH_3 and n = 6) onto gold to retard the non-specific adsorption of proteins.[25] Alkanethiols, $HS(CH_2)_mX$, spontaneously assemble onto gold surfaces via sulfur-gold interactions and form oriented, densely packed molecular coatings ("self-assembled monolayers" = SAMs), where the surface properties of the resulting films are controlled by selection of tail group (X).[26] Their observation that only a few ethylene glycol units were required in these densely packed, oriented assemblies to retard protein adsorption and that methyl-terminated ethylene glycol units were also effective provided the basis for our exploration of thiol compounds that combine these two factors and our development of the oligo(ethylene glycol)-terminated silane reagents. The methyl cap is needed on the ethylene glycol group for generation of a silane-based reagent that could be used on glass and metal oxide substrates as the hydroxyl group of an ethylene glycol cannot be accommodated within a molecule bearing a trichlorosilyl group due to their cross reactivity. In general, trichlorosilane reagents are useful for functionalizing a broader class of substrates (metal oxides)[26] than the thiols (coinage metals such as gold, silver, and copper),[27] and they are

widely used in practical applications as they exhibit dramatically superior levels of stability.[4,26]

This chapter demonstrates the effectiveness of methyl-capped di- and triethylene glycol-terminated silane reagents, $CH_3O(CH_2CH_2O)_{2,3}(CH_2)_{11}SiCl_3$, for producing robust molecular films that inhibit the non-specific adsorption of proteins. In particular, proteins with molecular weights from 10,000 to 400,000 Da (insulin, lysozyme, albumin, hexokinase, and fibrinogen) were examined. The reagents contained a methyl cap and either two or three ethylene glycol units as their tail group, where these functionalities become localized after assembly of the coating at the outer surface. Our investigation with these two compounds allowed examination of the effects of oligo-ethylene glycol length and their thickness on the properties of the coating; in this study, the thickness of the ethylene glycol portion of the coating was ~10 to 15 Å. The ethylene glycol-terminated alkyltrichlorosilane reagents adsorb onto the surface of an oxide spontaneously from solution and form a coating by methods (Figure 6-1) that are directly analogous to those commonly used to hydrophobize glass with unsubstituted alkyltrichlorosilanes ($CH_3(CH_2)_mSiCl_3$). This chapter compares the adsorptive properties of the hydrocarbon and ethylene glycol-terminated silane-based coatings with various proteins and examines the abilities of films prepared from the ethylene glycol-terminated silane reagents to maintain their non-adsorptive properties toward proteins after exposure to conditions of elevated temperatures and humidity.

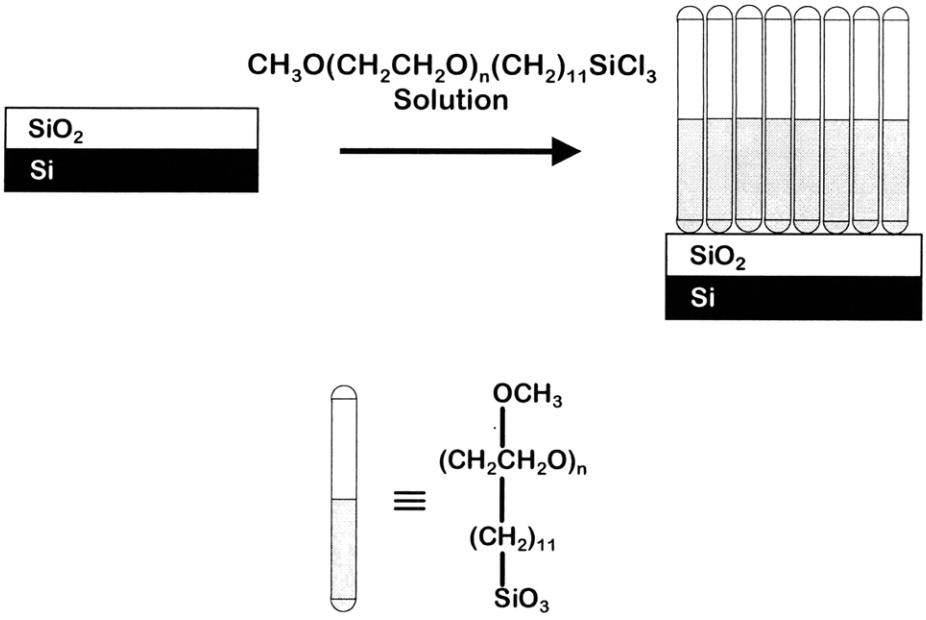

Figure 6-1. Schematic illustration of the formation of the oligo (ethylene oxide)-terminated SAMs

6.2. Results and Discussion

6.2.1. Synthesis of Silane Reagents

The oligo(ethylene glycol)-terminated alkyltrichlorosilanes were synthesized via a two-step synthesis from commercially available compounds (Figure 6-2). The monomethyl ether of an oligo(ethylene glycol) was reacted under basic conditions with 11-bromo-undec-1-ene in dimethylformamide (DMF) to yield an 11-oligo(ethylene glycol)-undec-1-ene methyl ether in high yield. Separation of the product from excess reagents was easily performed by extraction. The transformation of the resulting olefin to a trichlorosilane by photochemical addition of trichlorosilane ($HSiCl_3$) proceeded quantitatively. In this reaction, excess $HSiCl_3$ served as the solvent and was removed under reduced pressure to yield the product silane in sufficient purity to produce protein

resistant coatings although distillation under reduced pressure was used to produce the target silanes as purified compounds. The process for synthesizing the silane reagents (Figure 6-2) is amenable to scale-up as each reaction could be performed quantitatively and excess reagents were easily separated from the products by extraction and distillation procedures.

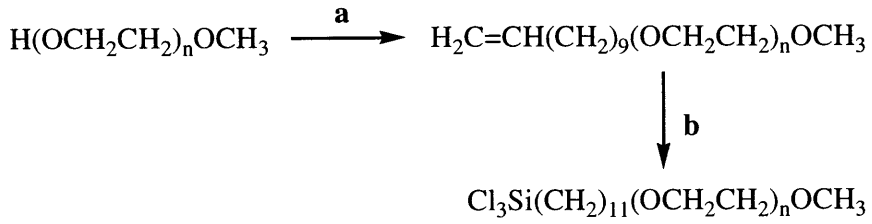

Key: (a) CH_2=CH$(CH_2)_9$Br, NaH, THF, reflux, 24 h (80%) ; (b) $HSiCl_3$, AIBN, hν, 6 h (90%)

Figure 6-2. Synthesis of ω–trichlorosilyl-oligo(ethylene glycol) derivatives, $CH_3O(CH_2CH_2O)_n(CH_2)_{11}SiCl_3$ (n = 2 or 3)

6.2.2. Preparation of Films

Siloxane films were prepared by a straightforward solution-phase adsorption process onto silicon wafers that exposed a hydrated oxide surface (Figure 6-1).[26] Silicon was used as a substrate in these studies as its oxide surface is similar to glass in reactivity and its reflective properties allowed measurement of adsorbed protein films by ellipsometry. The semiconducting properties of silicon additionally allowed direct analysis of the surface by x-ray photoelectron spectroscopy to verify formation of the coating and examine the levels of protein adsorption.

To prepare the siloxane coatings, the silicon substrates were immersed into unstirred solutions of the silanes in anhydrous toluene for 6-24 h at room temperature.

The silane solutions were handled and stored under a dry N_2 atmosphere and yielded reproducible formation of films over several weeks of use. Similar results may be obtained with trichlorosilane-based reagents when the adsorbate solutions are used under ambient laboratory conditions when the relative humidity is less than 40%;[10] however, the compounds exhibit a cumulative sensitivity toward moisture and produce insoluble polymerized aggregates that degrade the properties of the coatings. This problem is common to all trichlorosilane-based reagents (including alkyltrichlorosilanes, $CH_3(CH_2)_mSiCl_3$, used for hydrophobizing glass) due to the hydrolytic instability of the $SiCl_3$ group that is required for film formation. To avoid the possibility of solution-phase hydrolysis and aggregate formation from the silane reagents, we formed the siloxane coatings under a dry atmosphere of nitrogen.

As a comparison to the trichlorosilane-based films, oligo(ethylene glycol)-terminated monolayers on gold were prepared by contacting gold-coated silicon wafers with 2 mM solutions of $HS(CH_2)_{11}(OCH_2CH_2)_nOCH_3$ (n = 0, 2-4) in ethanol for 6-24 h at room temperature. As the assembly of thiols onto gold is not sensitive to humidity, we performed the assembly of these films in the laboratory ambient.

6.2.3. Characterization of Monolayer Films

Table 7-1 displays the wetting properties for films formed upon adsorption of various *n*-alkanethiols and *n*-alkyltrichlorosilanes onto Au and Si/SiO_2 surfaces, respectively. The wetting properties are compatible with the formation of oriented monolayer films that expose the tail group at the surface, with the thiol and silane-derived films exhibiting similar wetting properties for a common tail group. The formation of monolayer films was confirmed using ellipsometry where thicknesses for the various

ethylene glycol-terminated thiols (n = 2-4) ranged from 18 to 22 Å and those derived from the methyl-capped di- and triethylene glycol-terminated silanes were 18 and 20 Å, respectively. On gold, we observed that the difference in wettability between the hydroxyl- and methyl-capped ethylene glycol surfaces was ~30° and was much less than the difference for similar substitutions on a purely hydrocarbon chain (~100°). This difference in behavior probably reflects interaction by water with the ethylene glycol framework that moderates the effect of the terminal group. For both systems, water wets the methyl-capped ethylene glycol-terminated films ($\theta_a(H_2O)$ = 62-72°) better than for the methyl-capped alkyl films ($\theta_a(H_2O)$ = 110-115°). This greater wettability by the former surfaces implies a lower interfacial energy (γ_{SL}) between the film and water.

Table 6-1. Contact angles measured on films of $HS(CH_2)_{11}R$ on gold and of $Cl_3Si(CH_2)_{11}R$ on silicon [a]

Substrate	R[b]	$\theta_a(H_2O)$	$\theta_r(H_2O)$
Gold	CH_3	110	99
	$(CH_2)_6CH_3$	115	99
	OH	10	<10
	$(EG)_3OH$[c]	34	23
	$(EG)_4OH$[c]	38	24
	OCH_3	81	68
	$(EG)_2OCH_3$	68	59
	$(EG)_3OCH_3$	62	52
	$(EG)_4OCH_3$	62	52
Silicon	$(CH_2)_6CH_3$	115	98
	$(EG)_2OCH_3$	72	55
	$(EG)_3OCH_3$	67	49

[a]Advancing (θ_a) and receding (θ_r) static contact angles of water.
[b]EG = $-OCH_2CH_2-$
[c]Reference 28.

6.2.4. Protein Repellency of Films

The adsorption properties of the methyl-capped oligo(ethylene glycol)-terminated films on Au and Si/SiO_2 were examined by immersing them into various protein-containing solutions at a concentration of 0.25 mg/mL for 24 h at room temperature. Concurrent experiments in these solutions using surfaces coated with octadecyl chains were performed to allow direct comparisons of the performance of these films with available systems. The amount of adsorbed protein was determined optically ex situ using ellipsometry. Techniques such as x-ray photoelectron spectroscopy (for siloxane and thiolate SAMs) and polarized infrared external reflectance spectroscopy (for thiolate SAMs) were also used to determine the amount of adsorbed proteins. These techniques are superior to ellipsometry because of their detection of specific chemical signals—nitrogen composition or amide content—resulting from the protein; however, they require much longer times for characterizing each sample. In general, the thickness data from ellipsometry agreed with results from these other methods, and this technique was used as our primary characterization method.

Figure 6-3 summarizes the protein adsorption results for both substrates. On gold, the five proteins adsorbed onto the hydrophobic surfaces prepared from octadecanethiol, with the higher molecular weight proteins forming thicker adsorbed films. These thicknesses correspond to roughly a monolayer of adsorbed protein suggesting that the proteins adsorb to lower the interfacial energy between the hydrocarbon coating and water and that the resulting protein surface does not promote further adsorption. A surface expressing a methoxy group ($-OCH_3$) exhibits a lower interfacial energy with water than the purely alkyl surface (as evidenced by its lower contact angle by water, Table 7-1); however, this difference did not have a large effect on protein adsorption. This

observation suggests that the interfacial free energy for this surface when contacted with water is sufficient to drive adsorption of a layer of protein. Again, roughly a monolayer of protein appears to adsorb suggesting that the protein surface does not promote further protein adsorption.

The incorporation of two and four oligo(ethylene glycol) units as linkers between the methoxy terminus and the alkyl chain resulted in a reduction in the amount of protein adsorption on the gold surface (Figure 6-3). For insulin, lysozyme, albumin, and hexokinase, the SAMs resisted protein adsorption within the experimental errors of ellipsometry. Complete resistance against the adsorption of fibrinogen was not possible with the $EG_{2,4}$-CH_3 surface; however, the SAM reduced the adsorbed amount to roughly 10% of a monolayer. The difference in the adsorption characteristics of the purely alkyl CH_3O-capped monolayer and the CH_3-capped EG-containing film can be explained partially by the lower interfacial energy of the latter system with water. Entropic effects may also be operative for the oligo(ethylene glycol) system.[1,24]

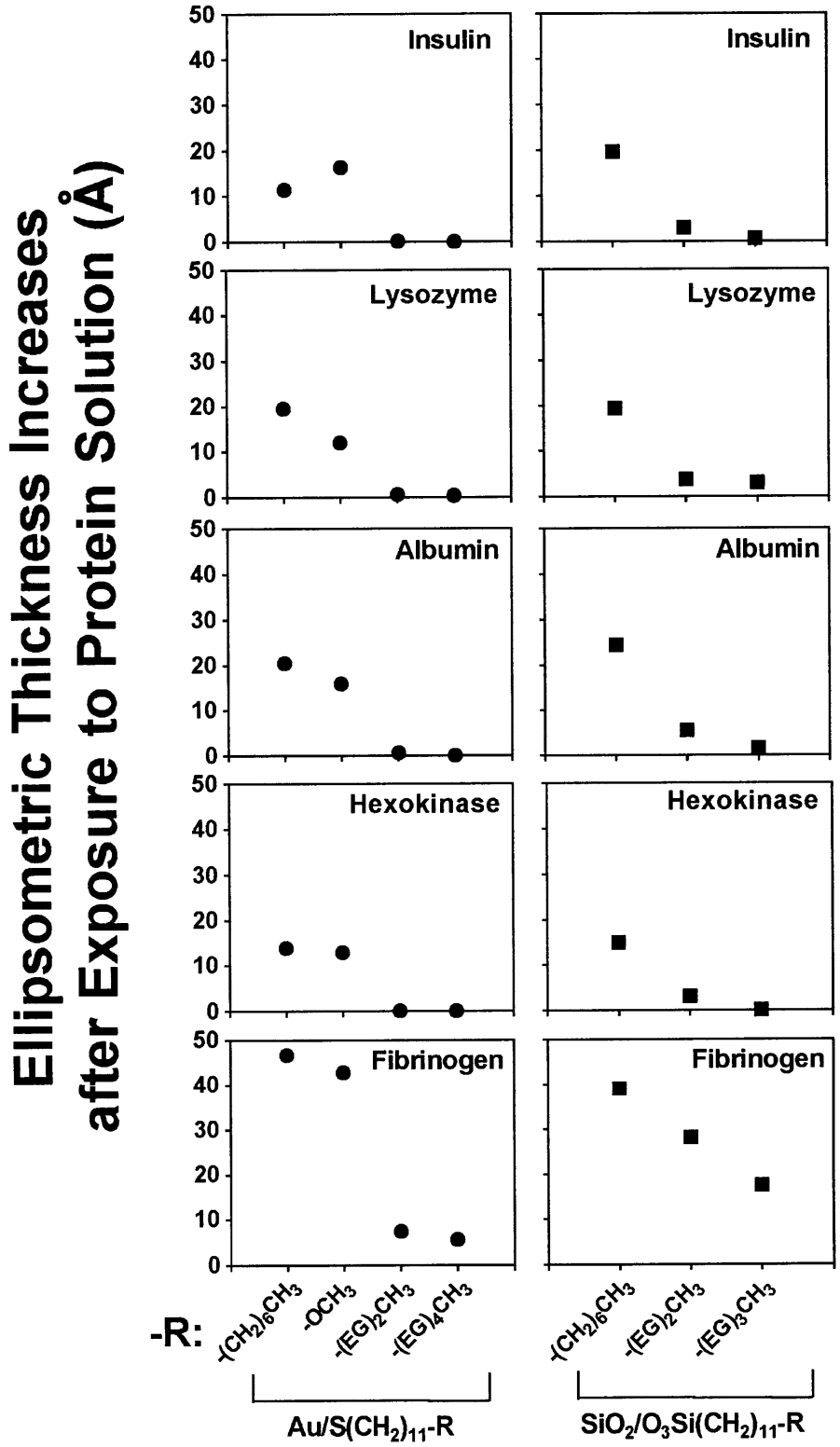

Figure 6-3. Ellipsometric thickness increase on various SAMs after exposure to protein solutions.

With the silane reagents, the results mirrored those on the gold substrates where the CH_3-capped oligo(ethylene glycol) monolayers adsorbed less protein than did the purely alkyl film. Films derived from octadecyltrichlorosilane adsorbed roughly a monolayer of protein. The CH_3-capped di- and tri-(ethylene glycol) films exhibited a resistance against adsorption by insulin, lysozyme, albumin, and hexokinase, with the tri-(ethylene glycol) films offering superior properties and being resistant against adsorption for these proteins within the error of ellipsometry. As for gold, the CH_3-capped oligo-(ethylene glycol) films adsorbed fibrinogen, with the adsorbed amounts being greater for the silane-based films than for the thiols on gold. The superior properties on gold may reflect the greater ease for forming oriented, well-defined, self-assembled, thiol-based monolayer films as silane reagents can form polymeric aggregates that can diminish the surface properties of the film.[26] The presence of such aggregates could provide local hydrophobic sites for the adsorption of proteins and make the surface less homogeneous, which could lead to the larger contact angle hysteresis ($\Delta\theta = \theta_a - \theta_r$) presented in Table 7-1. As we assembled the silane films under an inert atmosphere and used physical methods to displace any physisorbed materials from the surface, the amount of physisorbed material on our surfaces should be low. Structural differences in the molecular conformation of the CH_3-capped tri(ethylene glycol) layer—crystalline vs. amorphous—have been reported to affect the protein resistance of such surfaces toward fibrinogen and such differences may be operative here.[29]

In addition to the ellipsometric results, the wetting properties of the surfaces provided a macroscopic (albeit qualitative) indicator of protein adsorption. The initially prepared surfaces were hydrophobic and emerged dry when rinsed with water. After exposure to the protein solutions, the purely alkyl systems became less hydrophobic, while

the methyl-capped oligo(ethylene glycol) surfaces maintained their hydrophobicity. In particular, the receding contact angle of water on surfaces with an adsorbed layer of protein was ~25° and was sufficiently low to provide a visual indication of protein adsorption.

6.2.5. Stability of Films

The practical utility of a coating is based on both its performance and its ability to maintain its useful properties. The stability of the siloxane films was examined by exposing them to various conditions including boiling water, hot hydrocarbon solutions, oven drying, and autoclaving. The films retained their protein resistant properties after immersion in boiling water at 100 °C or decahydronaphthalene (DHN) at 90 °C for 1 h and drying in an oven at 120 °C for 1 h; however, they exhibited significant deterioration after drying in an oven at 200 °C for 1 h. These observations are compatible with the literature regarding the thermal stabilities of siloxane monolayer films as such films are reported to exhibit no detectable changes in structure and wetting properties when heated to ~140 °C and subsequently characterized at room temperature.[9,30] For our reagents and coatings, the presence of the CH_3-capped oligo(ethylene glycol) tail does not appear to negatively impact the thermal stability of an alkylsiloxane monolayer. For use in applications that require sterilized glassware, we note the silane-based coatings maintained their integrity and properties after an extended sterilization cycle (1 h) in an autoclave at ~120 °C (pressure = 20 psi). This ability may make these films suitable for numerous applications where sterile conditions are required and there is a need to limit the non-specific adsorption of proteins.

The thermal stabilities of the siloxane monolayers contrasts with the rapid desorption under these conditions for their thiol counterparts on gold. For comparison, ~30% of a thiol-based oligo(ethylene glycol)-terminated monolayer desorbed within 5 min in boiling water and within 1 min in DHN at 90 °C and lost their abilities to resist the non-specific adsorption of proteins, while the siloxane films were stable for at least an hour under these conditions. The robust behavior of the siloxane monolayers offers the needed stabilities required for practical application, with the developed CH_3-capped oligo-(ethylene glycol)-terminated silane reagents providing easy access to robust, protein resistant molecular coatings for glass and metal oxide surfaces.

6.3. Conclusions

Molecular coatings that exhibit a resistance against the non-specific adsorption of proteins such as insulin, lysozyme, albumin, and hexokinase can be readily prepared on metal oxide surfaces using a CH_3-capped oligo-(ethylene glycol)-terminated silane reagent, $CH_3[OCH_2CH_2]_{2,3}O(CH_2)_{11}SiCl_3$. These compounds are synthesized by a straightforward two-step reaction sequence using commercially available precursors. Solution-phase contact between a metal oxide surface and the silane reagent results in the spontaneous formation of a densely packed, oriented siloxane coating that expresses the oligo(ethylene glycol) groups at its surface. These moderately hydrophilic surfaces exhibit superior protein resistant properties than the more hydrophobic surfaces prepared from the adsorption of octadecyltrichlorosilane onto glass. The oligo-(ethylene glycol)-terminated films maintain their integrity and protein resistant properties after exposure to temperatures of ~100 °C (including sterilization procedures in an autoclave), suggesting that the parent reagents could be suitable for producing coatings on various glassware and

another implements that contact protein-containing media and may be exposed to the conditions used in sterilization procedures.

6.4. Experimental

6.4.1. Materials

Reagents were obtained from Aldrich and used as received unless specified otherwise. Octadecyltrichlorosilane was distilled under reduced pressure before use. 10-Undecylenic-1-bromide was obtained from Pfaltz and Bauer (Waterbury, CT). Lysozyme (chicken egg white, grade III), albumin (human, fraction V), fibrinogen (bovine, type I-S), hexokinase (bakers yeast) and insulin (bovine pancreas, type III) were obtained from Sigma (St. Louis, MO) and used as received. Silicon wafers were test grade and obtained from Silicon Sense (Nashua, NH). Gold shot (99.99 %) and chromium-coated tungsten filaments were obtained from Americana Precious Metals (East Rutherford, NJ) and R. D. Mathis Co. (Long Beach, CA), respectively. Oligo(ethylene glycol)-undecenes and undecanethiols were synthesized by reported procedures;[25,28] methyl-capped derivatives were synthesized by direct modifications to these procedures. ^{1}H NMR spectra were obtained on a Bruker 250 MHz spectrometer in $CDCl_3$ and referenced to residual $CHCl_3$ at 7.24 ppm.

Syntheses of Methyl [(1-trichlorosilyl)undec-11-yl] oligo(ethylene glycol)s. Methyl (undec-10-en-1-yl) oligo(ethylene glycol) [**1**, CH_2=$CH(CH_2)_9(OCH_2CH_2)_nOCH_3$; n = 2 and 3][25] (9.5 mmol), $HSiCl_3$ (28.5 mmol), and t-butyl peroxide (0.14 mmol) were combined under a dry N_2 atmosphere in a glove box. The reaction mixture was stirred for 7 h under UV irradiation by a medium pressure Hg lamp[31] and concentrated under reduced pressure

to remove excess $HSiCl_3$. The NMR spectrum of the reaction mixture showed quantitative conversion of the olefin to the trichlorosilane. Further purification was performed by vacuum distillation. Methyl [(1-trichlorosilyl)undec-11-yl] di(ethylene glycol): ^1H NMR (250 MHz, $CDCl_3$) δ 1.2-1.5 (m, 16 H), 1.56 (m, 4 H), 3.38 (s, 3 H), 3.45 (t, 2 H), 3.5-3.75 (m, 8 H). Methyl [(1-trichlorosilyl)undec-11-yl] tri(ethylene glycol) was prepared by a similar procedure. ^1H NMR (250 MHz, $CDCl_3$) δ 1.2-1.5 (m, 16 H), 1.56 (m, 4 H), 3.38 (s, 3 H), 3.45 (t, 2 H), 3.5-3.75 (m, 12 H).

6.4.2. Preparation of Silicon Substrates

Si(100) test wafers were cut into strips of ~1 × 3 cm^2 that were subsequently cleaned by immersion in freshly prepared "piranha" solution of 70 % conc. H_2SO_4(aq)/30 % H_2O_2(aq) (v/v) for 0.5 to 1 h at 70 °C (CAUTION: "piranha" solution reacts violently with many organic materials and should be handled with care). The substrates were immediately rinsed with distilled water, dried in a stream of N_2, and used within 1 h of cleaning. This process produces a highly wettable, hydrated oxide surface on silicon with similar properties to that for glass.[32] Optical constants were measured on the bare substrates by ellipsometry for use in determining thicknesses subsequently of the adsorbed silane films and protein layers. The piranha-cleaned substrates were typically exposed to the air for no more than 15 min before immersion in the silane solution.

6.4.3. Formation of Assemblies on SiO_2 and Au

The piranha-cleaned silicon substrates were functionalized by immersion in a 2 mM solution of the trichlorosilane in anhydrous toluene. The solutions were prepared and kept in a dry nitrogen atmosphere (glove box). After 6 to 24 h, the substrates were

removed from solution and rinsed in 20 mL of CH_2Cl_2. The substrates were removed from the glove box, rinsed sequentially with $CHCl_3$ and ethanol to remove any residual organic contaminants, and dried in a stream of N_2.

Gold substrates were prepared by the sequential evaporation of Cr (100 Å) and Au (1000 Å) onto Si(100) wafers at pressures of ~10^{-6} torr. The wafers were cut into ~1 x 3 cm^2 strips and immersed into ~2 mM solutions of the thiols in absolute ethanol for 24 h at room temperature. These samples were rinsed with ethanol and blown dry with N_2 before use.

6.4.4. Protein Adsorption Experiments

The proteins were dissolved at a concentration of 0.25 mg/mL in phosphate buffer saline (PBS) solution (10 mM phosphate buffer, 2.7 mM KCl, and 137 mM NaCl) that was adjusted to pH 7.4 and contained sodium azide (0.2 mg/mL) as a bacteriostat. The coated substrates were immersed in the PBS solutions for 24 h at 20-25 °C, rinsed with deionized water (Milli-Q), and dried in a stream of N_2. The amount of protein that remained on each substrate after this procedure was determined by ellipsometry. Experiments were also conducted using adsorption times of 3 to 6 h and yielded similar thicknesses as those performed using adsorption times of 24 h. Adsorption times were standardized to 24 h for consistency.

6.4.5. Contact Angle Measurements

Contact angles were measured on a Ramé-Hart goniometer (Ramé-Hart Inc., Mountain Lakes, NJ) equipped with a video-imaging system. Drops were placed on at least three locations on the surface in the ambient environment and measured on both

sides of the drops. Contacting liquid drops were advanced and retreated with an Electrapipette (Matrix Technologies, Lowell, MA) at approximately 1 μL/s. Angles were measured to ~±1° and were reproducible from sample to sample within ±2°.

6.4.6. Ellipsometric Film-Thickness Measurements

The thicknesses of the films were determined with a Gaertner L116A ellipsometer (Gaertner Scientific Corporation, Chicago, IL). For each substrate, measurements were made before and after derivatization with the trichlorosilanes, and after protein adsorption. The thicknesses of the films were determined using a three-phase model and a refractive index of 1.45[33] and have an error of ±2Å. The use of this value allows direct comparison with data obtained by other groups[25,28,29] and provides an accurate relative measure of the amounts of materials adsorbed on the various coatings.

6.5. References

(1) Norde, W. *Adv. Colloid Interface Sci.* **1986**, *25*, 267-340.

(2) Andrade, J. D.; Hlady, V. *Adv. Polym. Sci.* **1986**, *79*, 1-63.

(3) Vroman, L. ; Natural History Press, 1966.

(4) Plueddemann, E. P. *Silane Coupling Agents*; Plenum Press: New York, 1982.

(5) Nashabeh, W.; Elrassi, Z. *J. Chromatog.* **1991**, *559*, 367-383.

(6) Herren, B. J.; Shafer, S. G.; Van Alstine, J.; Harris, J. M.; Snyder, R. S. *J. Colloid Interface Sci.* **1987**, *115*, 46-55.

(7) Yang, Z.; Yu, H. *Adv. Mater.* **1997**, *9*, 426-429.

(8) Maoz, R.; Sagiv, J. *Journal of Colloid and Interface Science* **1984**, *100*, 465-496.

(9) Cohen, S. R.; Naaman, R.; Sagiv, J. *J. Phys. Chem.* **1986**, *90*, 3054-3056.

(10) Wasserman, S. R.; Tao, Y.-T.; Whitesides, G. M. *Langmuir* **1989**, *5*, 1074-1087.

(11) *Poly(Ethylene Glycol) Chemistry*; Harris, J. M., Ed.; Plenum Press: New York, 1992.

(12) Mori, Y.; Nagaoka, S.; Takuichi, T.; Kikuichi, T.; Noguchi, N.; Tanzawa, H.; Noishiki, Y. *Trans. Am. Soc. Artif. Intern. Org.* **1982**, *28*, 459-463.

(13) Merrill, E. W.; Salzman, E. W. *Am. Soc. Artif. Intern. Org. J.* **1983**, *6*, 60-64.

(14) Sun, Y. H.; Gomboltz, W. R.; Hoffman, A. S. *Compat. Polym.* **1986**, *1*, 316-334.

(15) Grasel, T. G.; Cooper, S. L. *Biomaterials* **1986**, *7*, 315-328.

(16) Su, Y. H.; S., H. A.; Gomboltz, W. R. *Polym. Prep.* **1987**, *28*, 292-294.

(17) Grainger, D. W.; Nojiri, C.; Okano, T.; Kim, S. W. *J. Biomed. Mater. Res.* **1988**, *22*, 231-249.

(18) Grainger, D. W.; Knutsen, K.; Okano, T.; Feijin, J. *J. Biomed. Mater. Res.* **1990**, *24*, 403-431.

(19) Jeon, S. I.; Lee, J. H.; Andrade, J. D.; De Gennes, P. G. *J. Colloid Interface Sci.* **1991**, *142*, 149-158.

(20) Jeon, S. I.; Andrade, J. D. *J. Colloid Interface Sci.* **1991**, *142*, 159-166.

(21) Lassen, B.; Gölander, C.-G.; Johansson, A.; Elwing, H. *Clinical Materials* **1992**, *11*, 99-103.

(22) Kiss, E.; Gölander, C.-G. *Colloids and Surfaces* **1990**, *49*, 335-342.

(23) Harris, J. M. *Rev. Macromol. Chem. Phys.* **1985**, *C25*, 325-373.

(24) Andrade, J. D.; Hlady, V.; Jeon, S.-I. In *Hydrophilic Polymers*; American Chemical Society:, 1996.

(25) Prime, K. L.; Whitesides, G. M. *J. Am. Chem. Soc.* **1993**, *115*, 10714-10721.

(26) Ulman, A. *An Introduction to Ultrathin Organic Films: From Langmuir-Blodgett to Self-Assembly*; Academic Press: Boston, 1991.

(27) Laibinis, P. E.; Whitesides, G. M. *J. Am. Chem. Soc.* **1992**, *114*, 1990-1995.

(28) Pale-Grosdemange, C.; Simon, E. S.; Prime, K. L.; Whitesides, G. M. *J. Am. Chem. Soc.* **1991**, *113*, 12-20.

(29) Harder, P.; Grunze, M.; Dahint, R.; Whitesides, G. M.; Laibinis, P. E. *J. Phys. Chem. B* **1998**, *102*, 426-436.

(30) Calistri-Yeh, M.; Kramer, E. J.; Sharma, R.; Zhao, W.; Rafailovich, M. H.; Sokolov, J.; Brock, J. D. *Langmuir* **1996**, *12*, 2747-2755.

(31) Eaborn, C.; Harrison, M. R.; Walton, M. R. *J. Organomet. Chem.* **1971**, *31*, 43-46.

(32) Pintchovski, F.; Price, J. B.; Tobin, P. J.; Peavey, J.; Kobold, K. *J. Electrochem. Soc.* **1979**, *126*, 1428-1430.

(33) Allara, D. L.; Nuzzo, R. G. *Langmuir* **1985**, *1*, 52-66.

Chapter 7

Development of a Hydroxyl-Terminated Oligo(ethylene glycol) Alkylsiloxane Coating for Targeted Binding of Proteins on Solid Substrates

7.1. Introduction

The development of hybrid molecular devices that incorporate biological species such as proteins and DNA within inorganic platforms has led to new paradigms for performing assays and other operations in biotechnology.[1,2] In general, the construction of such devices has employed a variety of functional biomolecules and coupling methods. For this purpose, it is necessary to develop a suitable method for immobilizing the biomolecules. Ideally, the method has to be capable of both orienting adsorbed biomolecules for the retention of their bioactivity at surface and inducing selective adsorption of desired biomolecules that is essential for the construction of biosensors. Most of the preceding studies focused on the adsorption of one individual biomolecule onto a desired surface using physical adsorption[3,4] or surface modification;[5-10] however, the development of an optimal system and its testing of the selective adsorption of a biomolecule against other biomolecules have not been approached much.

The fabrication of biosensing and bioelectronic devices requires methods for organizing biomolecules on the surface of a device in controlled ways. A recurring problem is the non-

specific adsorption of biomolecules (such as proteins) can cause defects on the patterned surfaces.[11] In addition, the non-specifically adsorbed proteins usually undergo conformational changes that lead to their denature and loss of their desired functions.[12] The attachment of poly or oligo(ethylene glycol) to surfaces has been a common strategy to lessen non-specific adsorption of proteins and other biomolecules to surfaces.[13,14] Chapter 6 showed that the incorporation of a short oligo(ethylene glycol) moiety into alkylsiloxane SAMs on glass or metal oxide surfaces can retard or prevent the non-specific adsorption of proteins.[15]

This chapter addresses a potential strategy for inducing the selective adsorption of proteins on solid substrates using a functionalized organic thin film. Si wafer surfaces were derivatized with an acetyl-terminated oligo(ethylene glycol) silane and converted the terminal acetate to a hydroxyl group by a surface reaction. The HO-termination of the resulting film provides sites for covalently grafting biomolecules to the surface, which is a reoccurring need in many areas of biotechnology. Among many specific interaction pairs, biotin-streptavidin[16-18] and mannose-Concanavalin-A (Con-A)[19-22] were selected for this work. Biotin or α-mannose moieties were attached by a series of surface reactions for the specific adsorption of streptavidin and Con-A, respectively. The protein-bound surface may be utilized for further attachment of biotin- or mannose-containing molecules to the surface.

7.2. Results and Discussion

7.2.1. Preparation of Films

The hydroxyl group was protected as an acetate to prevent reaction of free hydroxyl groups with chlorosilyl groups. The molecular precursor—acetyl [(1-trichlorosilyl)undec-11-yl]

oligo(ethylene glycol), $Cl_3Si(CH_2)_{11}(OCH_2CH_2)_nOCOCH_3$, **1**—was prepared by the three-step synthesis outlined in Figure 7-1. Monolayers were prepared by adsorption of **1** onto silicon wafers from a ~2 mM solution of **1** in anhydrous toluene (~5 mM). After 6 to 24 h, the substrates were removed from solution and rinsed in 20 mL of CH_2Cl_2. The substrates were removed from the glove box, rinsed sequentially with acetone and ethanol to remove any residual organic contaminants, and dried in a stream of N_2. The ellipsometric thickness of the film (n = 4) was 13 ± 2 Å. In Chapter 6, the thickness of films derived from various ethylene glycol-terminated thiols (n = 2-4) ranged from 18 to 22 Å; therefore, the thickness of the film was less than that (~22 Å) for a full siloxane monolayer, based on the results in Chapter 6. The films were formed by immersion in silane solutions of high concentrations at 10-20 mM but no increase in film thickness was observed. This coverage is possibly due to the bulky acetate-terminal group that can prevent close-packing structure.

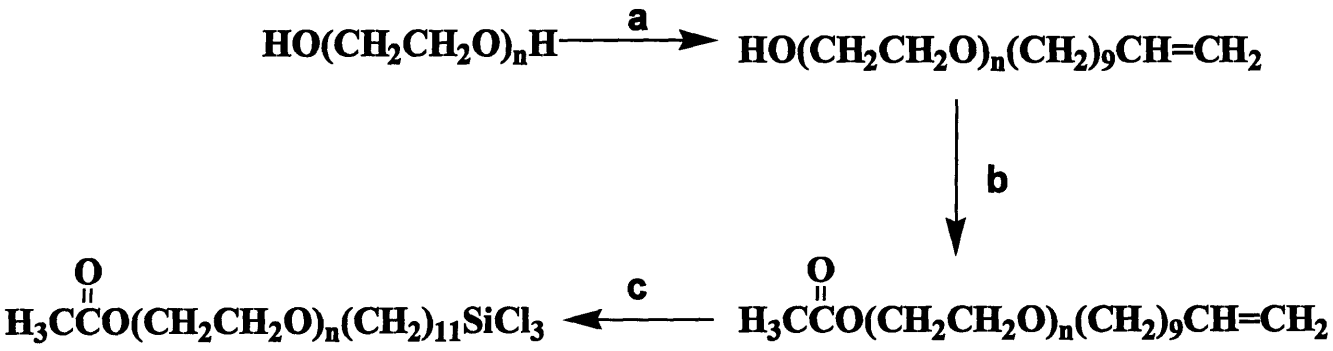

Key: (a) CH_2=$CH(CH_2)_9Br$, 50 % aqueous NaOH, 100 °C, 24 h (79 %); (b) CH_3COCl, $(CH_3CH_2)_3N$ in CH_2Cl_2, overnight, (75 %); (c) $HSiCl_3$, H_2PtCl_6 in THF (90 %)

Figure 7-1. Synthesis of acetyl [(1-trichlorosilyl)undec-11-yl] oligo(ethylene glycol), **1**.

7.2.2. Surface Reactions

Figure 7-2 outlines the surface reactions employed in this work. The hydrolysis reaction procedure was the same as that published by Wenzler and coworkers for a single acetate-terminated organosiloxane SAM.[23,24] The substrates derivatized with **1** were sonicated in 0.1 mM $LiAlH_4$ in anhydrous diethyl ether for 10 min to convert the terminal acetate groups to hydroxyl groups. The substrates were then washed sequentially with ~4% HCl, chloroform, acetone, and deionized water, and dried under a stream of N_2. The advancing and receding angles of water on the acetate-terminated monolayers derived from **1** were θ_a (H_2O) = ~64° and θ_r (H_2O) = ~52°, respectively. After deprotection of the acetate, θ_a (H_2O) and θ_r (H_2O) changed slightly to ~61° and ~47°, respectively. The reaction caused a ~1 Å decrease in the ellipsometric thickness of the monolayer. Based on bond lengths, the hydrolysis of the terminal acetate group should produce a decrease of 2.57 Å in the expected length of the molecule. For the density of adsorbates in the monolayers, the expected change is ~1.5 Å (60% of 2.57 Å) and agrees with the observed decrease.

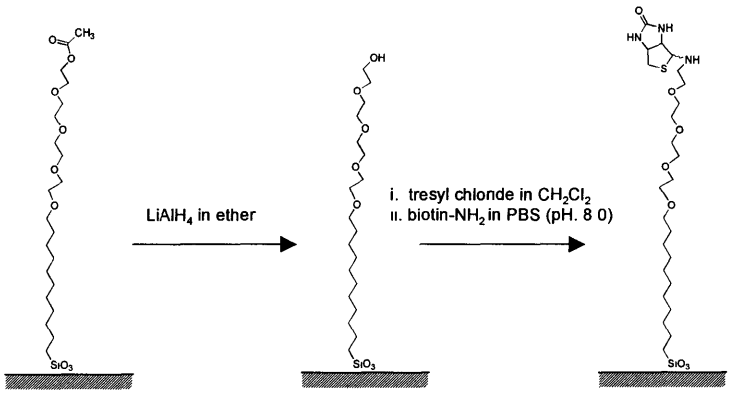

Figure 7-2. Reaction sequence to transform a SAM from **1** and to covalently attach biotin moieties to the substrate

The substrates were then tresylated by immersion in a 1.25 mg/mL tresyl chloride solution in anhydrous CH_2Cl_2 for 1 h at room temperature, rinsed with anhydrous methanol, and dried under a stream of N_2.[25] The tresylated samples were immersed immediately overnight into a phosphate buffer saline (PBS) solution (10 mM phosphate buffer, 2.7 mM KCl, and 137 mM NaCl) at pH 8.0 that contained 1 mg/mL biotin-terminated amine, **2** or a mannose-terminated amine, **3**.

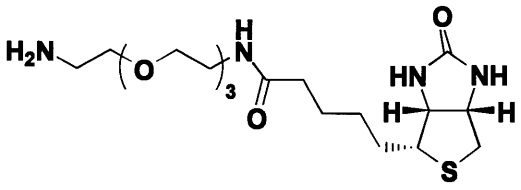

2

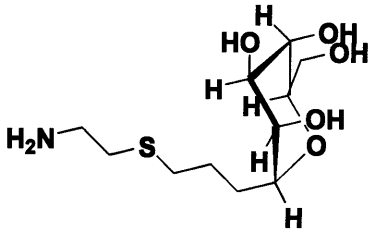

3

7.2.3. Characterization of Surfaces

XPS (X-ray photoelectron spectroscopy), also known as ESCA (Electron Spectroscopy for Chemical Analysis), was used as the primary characterization method in this study. XPS permits a non-destructive surface analysis of most solids including insulators, conductors, organic materials, and powders.[26] The photoelectrons generated from the surface of the sample contain a signature of both the elemental and chemical nature of the first few atomic layers of the sample and measurements of the relative areas of the photoelectron peaks allow determination of the chemical composition of the surface. The thickness of the surface layer analyzed by XPS is typically less than 5-10 nm.

The presence of the terminal acetate group in a monolayer from **1** and its reduction to a hydroxyl group on the surface were confirmed from the C 1s peak of XPS spectra. Figure 7-3 shows the spectra of the acetate-terminated monolayer before and after the hydrolysis of the

acetate group. Peak fitting for the acetate-terminated siloxane monolayer gives three carbon states corresponding to the methylene carbons (284.6 eV), the carbons attached by single bonds to oxygen (286.2 eV), and the carbonyl carbon (C=O) in the acetate group (288.9 eV). In the spectrum of acetate-terminated siloxane monolayers after reduction (Figure 7-3b), the peak corresponding to the carbonyl carbon (C=O) was not observed and the other two peaks at 284.6 and 286.2 eV remained, indicating a complete conversion of the terminal acetates to hydroxyl groups.

Covalent attachment of biotin or mannose to the surface was easily confirmed from the nitrogen 1s peak intensity in the XPS spectra (Figure 7-4) since the linkers contained nitrogen atoms. The samples were rinsed thoroughly with acetone, ethanol, and deionized water prior to characterization to remove any non-covalently-adsorbed materials. The N 1s peak area was compared to that for an amide-terminated thiolate SAMs on gold ($Au/S(CH_2)_{11}CONH_2$), where the latter system provided a reference signal for estimating coverage. In this manner, the surface densities of attached biotin and mannose units could be estimated and were determined to be roughly 10 to 20 % that for molecules in an alkanethiolate SAM (~5 thiolates per 100 $Å^2$). The advancing contact of water on the biotin and mannose-containing films were ~56° and ~58°, respectively, while their receding angles were ~35° and ~36°, respectively.

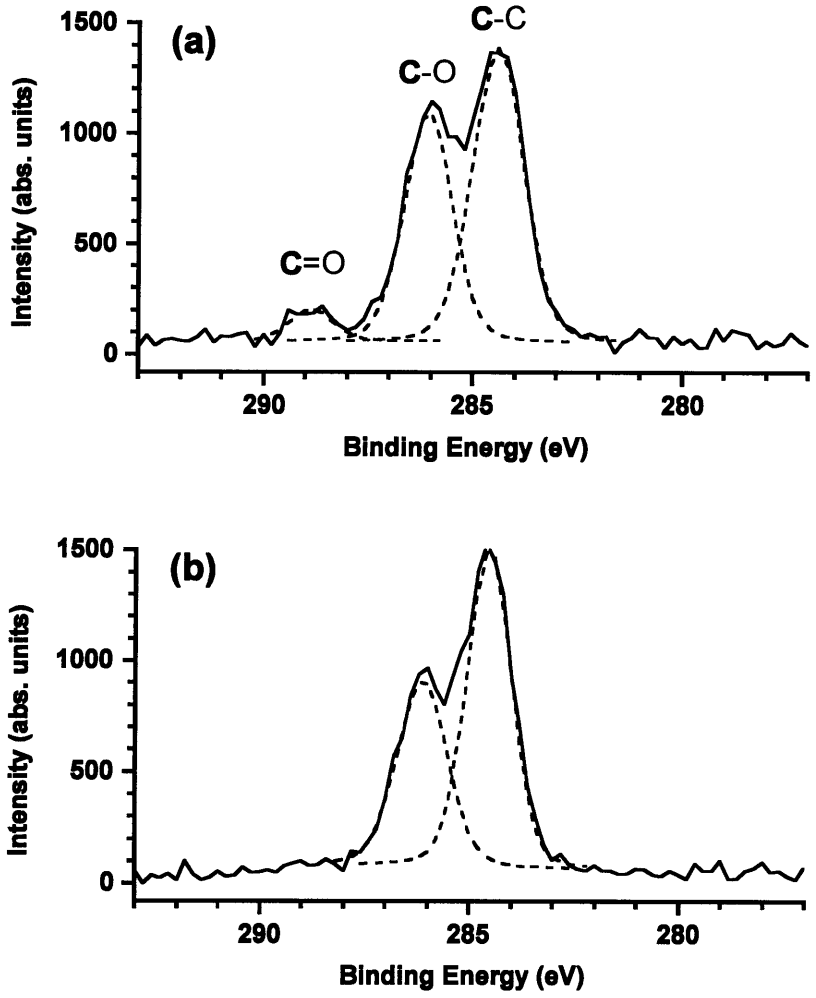

Figure 7-3. XPS spectra of acetate-terminated siloxane monolayers (a) before and (b) after reduction. Dashed peaks represent fits to the data using 80% Gaussian/20% Lorentzian profiles.

7.2.4. Protein Adsorption Experiments

The adsorption properties of the films were examined by immersing them into various protein solutions (pH = 7.4) at a concentration of 0.02 mg/mL at room temperature for 30 min,[27] followed by rinsing with deionized water. The amount of adsorbed proteins was measured by XPS using the intensity of the nitrogen 1s photoelectron signal. Hydrophobic, methyl-terminated monolayers formed from octadecyltrichlorosilane (OTS) were used as controls. Figure

7-4 shows a collection of nitrogen 1s spectra for methyl-, biotin-, and mannose surfaces before (top row) and after their exposure to a solution of insulin (second row), con-A (third row), or streptavidin (bottom row). As noted previously in this chapter, streptavidin and con-A selectively interact with biotin and mannose moieties, respectively. Insulin does not selectively interact with either of these recognition groups. For the parent SAMs, the methyl-terminated monolayer derived from OTS showed no N 1s signal, while the biotin- and mannose-terminated films exhibited weak N 1s signals from the nitrogen atoms within these films. Upon exposure of the OTS films to one of the protein solutions, the film exhibited an intense N 1s peak indicating their non-specific adsorption onto the surface. For the biotin- and mannose-terminated films, the adsorption of both con-A and streptavidin on these surfaces produced an increase in N 1s signal. In contrast, almost no adsorption of insulin was observed on these surfaces probably due to the presence of the protein-repellant oligo(ethylene glycol) moiety. The amount of adsorbed streptavidin and con-A varied with respect to the chemistry of surfaces as shown in Figure 7-4. On the biotin-containing films, the amount of adsorbed streptavidins was 40 % greater than on mannose-surfaces. In contrast, the amount of adsorbed con-A protein on the mannose-surfaces was 150% greater than on the biotin-surfaces. These observations show the influence of attached groups on the adsorption behavior of streptavidin and con-A, while reducing the non-specific adsorption of other proteins such as insulin by inclusion of oligo(ethylene glycol) groups. These results also indicate that this developed system can be applied to other specific interaction pairs of biological entities as far as we can anchor one of the pairs to the surface. However, in comparison to the adsorption of insulin (MW = ~20 kDa), the amount of adsorbed streptavidin (MW = ~60 kDa) and con-A (MW = ~26 kDa) onto the biotin and mannose-surfaces was significant. This result may be attributed to the loosely packed monolayer films leading the surface density of ethylene glycol to decrease, thereby diminishing their protein-repellent ability against these

proteins. For example, the amount of adsorbed streptavidin on the reduced-acetate (hydroxyl)-terminated EG monolayers was 47% of that on the films from OTS, supporting the preceding argument. However, the use of longer oligo (ethylene glycol) tails can provide a method to maintain the surface density of ethylene glycol as Jeon et al. suggested.[28]

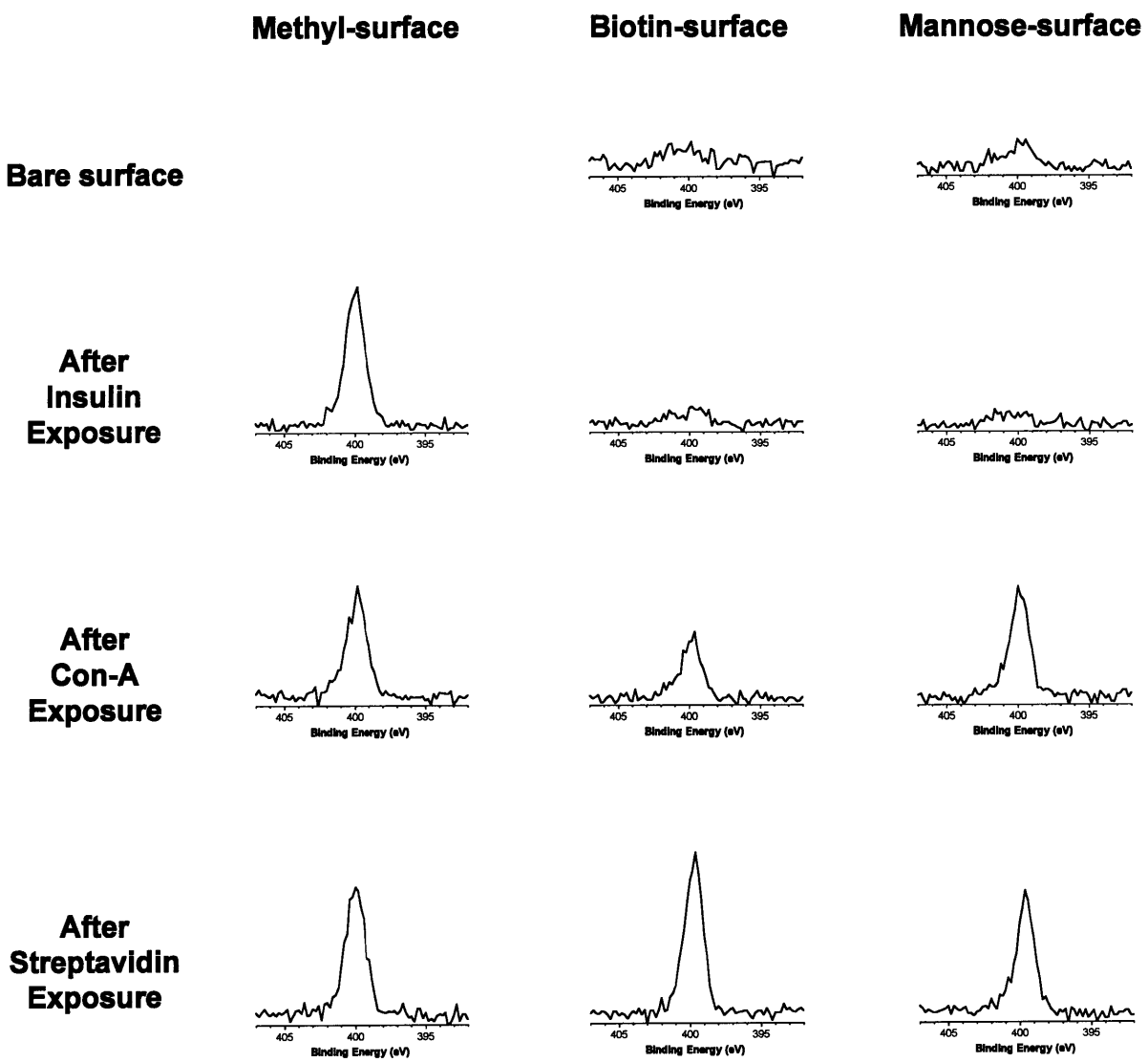

Figure 7-4. N 1s peaks of the XPS spectra of monolayers of octadecyltrichlorosilane (left column), biotin-attached monolayers (center column), and mannose-attached monolayers (right column) after exposure to various protein solutions. The first row shows spectra of biotin- and mannose-surfaces prior to exposure to the proteins.

7.3. Conclusions

This chapter demonstrated the development of alkylsiloxane films that could induce the adsorption of specific proteins onto a surface by incorporating a recognition group on their chain ends and also reduce the nonspecific nature of protein adsorption by including oligo(ethylene glycol) groups within the SAMs. Biotin and mannose were covalently attached to the surface by a series of surface reactions and the resulting films were exposed to various protein solutions. The resulting two surfaces were resistant against the adsorption of a protein, insulin, that does not bind to either of these recognition groups through specific interactions. In contrast, these surfaces attracted streptavidin and con-A differently with respect to their surface chemistry. These observations suggest that the developed protocol can be applied to modulate the adsorptive properties of other biological entities by tailoring available specific interactions at surfaces. However, additional efforts are required to reduce the non-specific adsorption of unwanted proteins on modified surfaces.

7.4. Experimental

7.4.1. Materials

Reagents were obtained from Aldrich and used as received unless specified otherwise. Octadecyltrichlorosilane was distilled under reduced pressure before use. 10-Undecylenic-1-bromide and EZ-Link™ Biotin-PEO-LC-Amine (**2**) were obtained from Pfaltz and Bauer (Waterbury, CT) and PIERCE (Rockford, IL), respectively. α-C-mannose-amine (**3**) was a gift from Insung Choi and Prof. George Whitesides at Harvard University. Silicon wafers were test grade and obtained from Silicon Sense (Nashua, NH). The synthesis of the methyl-capped

tri(ethylene glycol)-terminated undecyltrichlorosilane ($CH_3O(CH_2CH_2O)_3(CH_2)_{11}SiCl_3$) was detailed in Chapter 6. The acetate-capped tri(ethylene glycol)-terminated undecyltrichlorosilane was synthesized by the procedure outlined in Figure 7-1. ^1H NMR spectra were obtained on a Bruker 250 MHz spectrometer in $CDCl_3$ and referenced to residual $CHCl_3$ at 7.24 ppm.

Synthesis of Acetyl [(1-trichlorosilyl)undec-11-yl] tetra(ethylene glycol). The acetyl (undec-10-en-1-yl) tetra(ethylene glycol) precursor [**4**, $CH_2=CH(CH_2)_9(OCH_2CH_2)_4OCOCH_3$] was prepared by reported procedures[24,29] and hydrosilated to add a trichlorosilyl group.[30] The NMR spectrum of the reaction mixture showed the quantitative conversion of the olefin to the trichlorosilane. The excess $HSiCl_3$ was removed by vacuum distillation. Acetyl [(1-trichlorosilyl)undec-11-yl] tetra(ethylene glycol): ^1H NMR (250 MHz, $CDCl_3$, δ): 1.2 - 1.5 (m, 16 H), 1.55 (m, 4 H), 2.06 (s, 3 H), 3.43 (t, 2 H), 3.5-3.75 (m, 14 H), 4.20 (t, 2H)

7.4.2. Preparation of SiO_2 Substrates

Si(100) test wafers and glass slides were cut into strips of ~1 × 3 cm^2 that were subsequently cleaned by immersion in freshly prepared "piranha" solution of 70 % conc. H_2SO_4(aq)/30 % H_2O_2(aq) (v/v) for 0.5 to 1 h at 70 °C (CAUTION: "piranha" solution reacts violently with many organic materials and should be handled with care). The substrates were immediately rinsed with distilled water, dried in a stream of N_2, and used within 1 h of cleaning. This process produces a highly wettable, hydrated oxide surface on silicon with similar properties to that for glass.[31] The piranha-cleaned substrates were typically exposed to the air for no more than 15 min before immersion in the silane solution.

7.4.3. Formation of Siloxane Films on SiO_2

The piranha-cleaned silicon substrates were functionalized by immersion in a ~5 mM solution of the trichlorosilane in anhydrous toluene. The solutions were prepared and kept in a dry nitrogen atmosphere (glove box). After 6 to 24 h, the substrates were removed from solution and rinsed in 20 mL of CH_2Cl_2. The substrates were removed from the glove box, rinsed sequentially with acetone and ethanol to remove any residual organic contaminants, and dried in a flowing stream of N_2.

7.4.4. Covalent Attachment of Recognition Groups to SAMs

The silanated substrates were sonicated in 0.1 mM $LiAlH_4$ in anhydrous diethyl ether for 10 min to convert the terminal acetate groups to hydroxyl groups. The substrates were then washed sequentially in ~4% HCl, chloroform, acetone, and deionized water and dried under a stream of N_2. The substrates were then tresylated by immersion in a 1.25 mg/mL tresyl chloride solution in anhydrous CH_2Cl_2 for 1 hr at room temperature, rinsed with anhydrous methanol, and dried under a stream of N_2. The tresylated samples were then immediately transferred to a 1 mg/mL solution of EZ-Link™ Biotin-PEO-LC-Amine or α-C-mannose-amine in phosphate buffer saline (PBS) solution (10 mM phosphate buffer, 2.7 mM KCl, and 137 mM NaCl) that was adjusted to pH 8.0 and immersed overnight.

7.4.5. Contact Angle Measurements

Contact angles were measured on a Ramé-Hart goniometer (Ramé-Hart Inc., Mountain Lakes, NJ) equipped with a video-imaging system. Drops were placed on at least three locations on the surface in the ambient environment and measured on both sides of the drops. Contacting liquid drops were advanced and retreated with an Electrapipette (Matrix Technologies, Lowell,

MA) at approximately 1 μL/s. Angles were measured to ~±1° and were reproducible from sample to sample within ±2°.

7.4.6. Ellipsometric Film-Thickness Measurements

The thicknesses of the films were determined with a Gaertner L116A ellipsometer (Gaertner Scientific Corporation, Chicago, IL). For each substrate, measurements were made before and after derivatization with the trichlorosilanes, and after protein adsorption. The thicknesses of the films were determined using a three-phase model and a refractive index of 1.45 and have an error of ±2Å. The use of this value allows direct comparison with data obtained by other groups and provides an accurate relative measure of the amounts of materials adsorbed on the various coatings.

7.4.7. X-ray Photoelectron Spectroscopy (XPS)

The XPS spectra were obtained with a Surface Science Instrument Model X-100 spectrometer using a monochromatized Al Kα x-ray source (elliptical spot of 1.0 mm × 1. 7 mm) and a concentric hemispherical analyzer. The detector angle with respect to the surface parallel was 35°. Peak positions were referenced to C(1s) = 284.6 eV, and peaks were fit with 80% Gaussian/20% Lorentzian profiles and a Shirley background.

7.5. References

(1) Kossek, S.; Padeste, C.; Tiefenauer, L. X.; Siegenthaler, H. *Biosens. Bioelectron.* **1998**, *13*, 31-43.

(2) Hlady, V.; Buijs, J. *Curr. Opin. Biotech.* **1996**, *7*, 72-77.

(3) Caruso, F.; Rodda, E.; Furlong, D. N. *J. Colloid Interface Sci.* **1996**, *178*, 104-115.

(4) Sandwick, R.; Schray, K. J. *J. Colloid Interface Sci.* **1988**, *121*, 1-12.

(5) Tamiya, E.; Watanabe, N.; Matsuoka, H.; Karube, I. *Biosensors* **1987/88**, *3*, 139-146.

(6) Flounders, A. W.; Brandon, D. L.; Bates, A. H. *Appl. Biochem. Biotech.* **1995**, *50*, 265-284.

(7) Sigrist, H.; Collioud, A.; Clemence, J. F.; Gao, H.; Luginbuhl, R.; Sanger, M.; Sundarababu, G. *Opt. Eng.* **1995**, *34*, 2339-2348.

(8) Williams, R. A.; Blanch, H. W. *Biosens. Bioelectron.* **1994**, *9*, 159-167.

(9) Schlereth, D. D. *J. Electroanal. Chem.* **1997**, *425*, 77-85.

(10) Ito, T.; Namba, M.; Buhlmann, P.; Umezawa, Y. *Langmuir* **1997**, *13*, 4323-4332.

(11) Andrade, J. D.; Hlady, V.; Wei, A.-P.; Ho, C.-H.; Lea, A. S.; Jeon, S. I.; Lin, Y. S.; Stroup, E. *Clin. Mater.* **1992**, *11*, 67-84.

(12) Norde, W. *Adv. Colloid Interface Sci.* **1986**, *25*, 267-340.

(13) *Poly(Ethylene Glycol) Chemistry*; Harris, J. M., Ed.; Plenum Press: New York, 1992.

(14) Prime, K. L.; Whitesides, G. M. *Science* **1991**, *252*, 1164-1167.

(15) Lee, S.-W.; Laibinis, P. E. *Biomaterials* **1998**, *19*, 1669-1975.

(16) Jordan, C. E.; Frutos, A. G.; Thiel, A. J.; Corn, R. M. *Anal. Chem.* **1997**, *69*, 4939-4947.

(17) Paleos, C. M.; Tsiourvas, D. *Adv. Mater.* **1997**, *9*, 695-710.

(18) Ijiro, K.; Ringsdorf, H. *Langmuir* **1998**, *14*, 2796-2800.

(19) Varki, A. *Glycobiology* **1993**, *3*, 97-130.

(20) Ben-Bassat, H.; Goldbrum, N. *Proc. Natl. Acad. Sci. U.S.A.* **1975**, *72*, 1046-1049.

(21) Bittiger, H.; Schnebli, H. P. *Concanavalin A as a Tool*; John Wiley and Sons: New York, 1976.

(22) Brown, J. C.; Hunt, R. C. *Int. Rev. Cytol.* **1978**, *52*, 277-349.

(23) Wenzler, L. A.; Moyes, G. L.; Oslon, L. G.; Harris, J. M.; Beebe Jr., T. P. *Anal. Chem.* **1997**, *69*, 2855-2861.

(24) Wenzler, L. A.; Moyes, G. L.; Raikar, G. N.; Hansen, R. L.; Harris, J. M.; Beebe Jr., T. P. *Langmuir* **1997**, *13*, 3761-3768.

(25) Sofia, S. J.; Premnath, V.; Merrill, E. W. *Macromolecules* **1998**, *31*, 5059-5070.

(26) Briggs, D.; Seah, M. P. *Practical Surface Analysis: Auger amd X-Ray Photoelectron Spectroscopy, 2nd Ed.*; John Wiley & Sons: New York, 1996.

(27) Koyano, T.; Saito, M.; Miyamoto, Y.; Kaifu, K.; Kato, M. *Biotechnol. Prog.* **1996**, *12*, 141-144.

(28) Jeon, S. I.; Lee, J. H.; Andrade, J. D.; De Gennes, P. G. *J. Colloid Interface Sci.* **1991**, *142*, 149-158.

(29) Pale-Grosdemange, C.; Simon, E. S.; Prime, K. L.; Whitesides, G. M. *J. Am. Chem. Soc.* **1991**, *113*, 12-20.

(30) Balachander, N.; Sukenik, C. *Langmuir* **1990**, *6*, 1621-1627.

(31) Pintchovski, F.; Price, J. B.; Tobin, P. J.; Peavey, J.; Kobold, K. *J. Electrochem. Soc.* **1979**, *126*, 1428-1430.